

UNIVERSITY OF CALIFORNIA, SAN DIEGO

Cameleon Reveals a Physiologic Correlate for Alternative Behavioral States in  
*Caenorhabditis elegans* Egg-Laying

A dissertation submitted in partial satisfaction of the  
requirements for the degree Doctor of Philosophy  
in  
Neurosciences

By

Stanley I. Shyn

Committee in charge:

Professor William R. Schafer, Chair  
Professor Lawrence Goldstein  
Professor Michael Gribskov  
Professor Paul Slesinger  
Professor Roger Tsien

2003

UMI Number: 3094611

**UMI**<sup>®</sup>

---

UMI Microform 3094611

Copyright 2003 by ProQuest Information and Learning Company.

All rights reserved. This microform edition is protected against  
unauthorized copying under Title 17, United States Code.

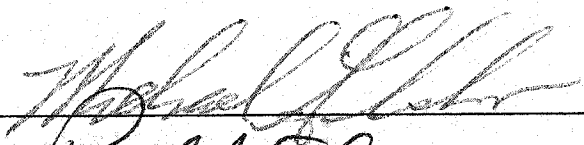
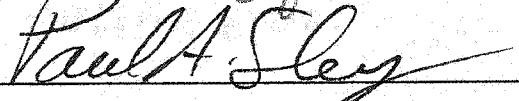


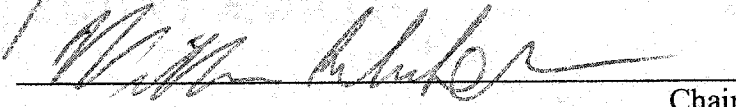
ProQuest Information and Learning Company  
300 North Zeeb Road  
P.O. Box 1346  
Ann Arbor, MI 48106-1346

Copyright

Stanley I. Shyn, 2003

All rights reserved.

The dissertation of Stanley I. Shyn is approved, and it  
is acceptable in quality and form for publication on  
microfilm:

  
\_\_\_\_\_  
  
\_\_\_\_\_  
  
\_\_\_\_\_  
  
\_\_\_\_\_  
  
\_\_\_\_\_ Chair

University of California, San Diego

2003.



## DEDICATION

This work is dedicated to my mother, whom I too often take for granted, but who is my inspiration and biggest cheerleader in life; to my father, for his moral support and witticisms (intentional and otherwise); and to Mr. Radke, my late 6<sup>th</sup> grade science teacher, who taught me the difference between matter babies and pink elephants—as well as how to smile, again.

## TABLE OF CONTENTS

Signature Page.....	iii
Dedication.....	iv
Table of Contents.....	v
List of Abbreviations.....	viii
List of Figures.....	x
List of Tables.....	xii
Acknowledgements.....	xiii
Vita and Publications.....	xiv
Abstract.....	xv
I. Introduction.....	1
A. The <i>C. elegans</i> nervous system.....	2
B. G-proteins in the worm.....	3
D. Locomotion and its modulation.....	4
E. Egg-laying.....	10
F. Advances in the analysis of <i>C. elegans</i> cellular physiology..	14
II. Serotonin and G <sub>o</sub> modulate functional states of neurons and muscles controlling <i>C. elegans</i> egg-laying behavior.....	21
A. Abstract.....	21
B. Introduction.....	22
C. Results.....	24

D. Discussion.....	31
E. Materials and Methods.....	33
F. Supplemental Materials and Methods.....	40
III. Characterization of the <i>ser-4(ok512)</i> serotonin receptor gene	
deletion mutant.....	47
A. Abstract.....	47
B. Introduction.....	47
C. Results.....	50
1. <i>ser-4</i> is expressed in the vm2 vulval muscles.....	50
2. <i>ser-4(ok512)</i> is an in-frame 1337 bp deletion.....	51
3. <i>ser-4(ok512)</i> does not have a discernible phenotype..	52
4. Overexpression constructs and the introduction of a putative gain-of-function mutation (W367R) do not produce hyperactive egg-laying.....	54
D. Discussion.....	56
E. Materials and Methods.....	59
Appendix A. Other calcium-imaging results.....	70
1. Other Ca <sup>2+</sup> channels.....	70
2. <i>egl-30</i> .....	70
3. Mini-genes.....	71
4. Vulval muscle-expression of pertussis toxin.....	72
5. Double-mutant combinations.....	73

6. Levamisole experiments.....	74
7. 5-carboxamidotryptamine (5-CT).....	75
8. Materials and Methods.....	75
Appendix B. Microarray studies of <i>mod-5(n3314)</i> and fluoxetine.....	83
1. Background.....	84
2. Choice of fluoxetine dose.....	86
3. Co-hybridizations.....	87
4. Results.....	87
5. Discussion & unfinished work.....	95
6. Materials and Methods.....	98
References.....	112

## LIST OF ABBREVIATIONS

5HT	5-hydroxytryptamine (serotonin)
aa	amino acid(s)
Ach	acetylcholine
bp	basepairs
CFP	cyan fluorescent protein
Egl	egg-laying defective
Egl-c	egg-laying constitutive
FaRPs	FMRFamide-related peptides
GPCR	G-protein-coupled receptor
HGM	high-growth medium
HSN	hermaphrodite specific neuron
Kb	kilobases / kilobasepairs
lev	levamisole (cholinergic agonist)
Mod	modulation (of locomotion) defective
nAChR	nicotinic acetylcholine receptor
N2	wild-type, Bristol
NGM	nematode growth medium
ORF	open-reading frame
R/G	red/green ratio
RT	room temperature

SEM	standard error of the mean
SERT	serotonin re-uptake transporter
Unc	uncoordinated
VC	VC ventral cord neuron
VDCC	voltage-dependent Ca <sup>2+</sup> channel
VGCC	voltage-gated Ca <sup>2+</sup> channel
vm	vulval muscle
Y/C	yellow/cyan ratio
YC	yellow cameleon
YFP	yellow fluorescent protein

## LIST OF FIGURES

### CHAPTER II

Figure 2-1. $\text{Ca}^{2+}$ -imaging of <i>C. elegans</i> vulval muscle with cameleon.....	36
Figure 2-2. Sample vulval muscle ratio traces & selected distributions of event frequency.....	37
Figure 2-3. HSN neuronal imaging with <i>cat-1::iY2C2.1</i> and neuronal silencing by serotonin.....	39
Supplemental Figure 2-1. VC neuronal imaging with <i>cat-1::iY2C2.1</i> .....	45
Supplemental Figure 2-2. Peak-detection.....	46

### CHAPTER III

Figure 3-1. Span of the <i>ok512</i> deletion and relation to SER-4 topology.....	63
Figure 3-2. Baseline egg-laying parameters for <i>ser-4(ok512)</i> do not reveal longer inactive phases.....	64
Figure 3-3. 5HT dose-response curves in M9 buffer.....	65
Figure 3-4. 5HT egg-laying responses on NGM + 7.5 mM 5HT plates.....	66
Figure 3-5. <i>ser-4(ok512)</i> vulval muscle $\text{Ca}^{2+}$ traces.....	67
Figure 3-6. Behavioral evaluation of <i>ser-4(ok512)</i> for “velocity spike” in locomotion before egg-laying events.....	68
Figure 3-7. <i>ser-4XS</i> and <i>ser-4(W367R)</i> do not respond to 5HT in an M9 behavioral assay.....	69

## APPENDIX A

Figure A-1. Sample levamisole and 5-CT Ca <sup>2+</sup> traces.....	82
---	----

## APPENDIX B

Figure B-1. April 2001 experiment grid.....	102
Figure B-2. Determination of appropriate fluoxetine dose.....	103
Figure B-3. Axes of statistical analysis of microarray data.....	105
Figure B-4. Calculation of “simple delta” for significance analysis along intra- experimental axis of microarray data.....	106
Figure B-5. Calculation of a “modified delta” by Significance Analysis of Microarrays (SAM).....	107
Figure B-6. Hierarchical clustering of genes with significant changes in expression across inter-experimental axis.....	108
Figure B-7. Correlation plots of called genes for drug target validation.....	111



## LIST OF TABLES

### CHAPTER II

Table 2-1. Muscle $\text{Ca}^{2+}$ events/min.....	35
Supplemental Table 2-1. Measures of inter-muscle correlation of activity.....	44

### CHAPTER III

Table 3-1. Frequency of vulval muscle $\text{Ca}^{2+}$ events (events/min) in <i>ser-4</i> deletion mutant and in lines expected to have enhanced SER-4 function.....	62
---	----

### APPENDIX A

Table A-1. Other vulval muscle $\text{Ca}^{2+}$ -imaging data.....	78
--	----

## ACKNOWLEDGEMENTS

I would like to thank my thesis advisor, William Schafer, for his unfailing patience and bottomless well of optimism. Bill is that rare combination of a great scientist who succeeds at being a terrific human being, too. And I would like to thank Rex Kerr, who has been our lab's "Scotty" and "Mr. Spock" all rolled into one. This work would not have been possible without Rex's pioneering vision (—and indispensable computer programming skills).

The text of Chapter II was adapted from an article submission which is presently under peer-review. It was reformatted to conform to the referencing style and format of this dissertation, though a supplemental section was retained as a separate body (just as in the article submission). The dissertation author was the primary researcher and author for this work, with Rex Kerr (second author) contributing computer and statistical expertise.

## VITA

- 1996 S.B., Biology, Massachusetts Institute of Technology  
Graduated Phi Beta Kappa
- 1996- M.D.-Ph.D. candidate, Medical Scientist Training Program  
University of California, San Diego
- 2000 Teaching assistant, Department of Biology, University of California,  
San Diego
- 2003 Ph.D., Neurosciences, University of California, San Diego

## PUBLICATIONS

Yoshikawa S, Bonkowsky JL, Kokel M, Shyn S, Thomas JB. 2001. The Derailed guidance receptor does not require kinase activity *in vivo*. *J Neurosci.* 21:RC119:1-4.

Solomon J, Su L, Shyn S, Grossman AD. 2003. Isolation and characterization of mutations in the oligopeptide permease of *Bacillus subtilis* that alter the specificity of oligopeptide transport. (*submitted*).

Shyn SI, Kerr R, Schafer WR. 2003. Serotonin and G<sub>o</sub> modulate functional states of neurons and muscles controlling *C. elegans* egg-laying behavior. (*submitted*).

ABSTRACT OF THE DISSERTATION

Cameleon Reveals a Physiologic Correlate for Alternative Behavioral States in  
*Caenorhabditis elegans* Egg-Laying

By

Stanley I. Shyn

Doctor of Philosophy in Neurosciences

University of California, San Diego, 2003

Professor William R. Schafer, Chair

I have studied the *Caenorhabditis elegans* egg-laying system using the genetically encodable calcium indicator, cameleon. Specifically, I sought to better understand the effects of the neuromodulator, serotonin, and the  $G_{\alpha}$  G-protein subunit, GOA-1, on the functional properties of individual neurons and muscle cells in the egg-laying neuromuscular junction. The work presented here demonstrates that calcium transients in wild-type vulval muscle cells are sporadic and clustered. Under serotonin treatment, calcium transient frequency increases and the baseline pattern is dramatically altered to one characterized by sustained trains of small rapid calcium events. This effect of serotonin is shown to be a direct action on vulval muscles, independent of the egg-laying motoneurons. Examination of the motoneurons

revealed, however, that these cells, too, undergo a serotonin-induced change. Specifically, serotonin silenced the spontaneous activity observed under drug-free conditions in one class of egg-laying motoneurons, the HSNs. Mutants in the *goa-1* gene also exhibited altered vulval muscle and egg-laying neuron activity: they had an increased frequency of muscle calcium transients suggesting a normally inhibitory role for GOA-1 in vulval muscle—and also, to our surprise, were resistant to HSN motoneuron silencing by serotonin. This latter finding provides a potential regulatory feedback mechanism which may contribute to serotonergic adaptation.

Next, I present work on *ser-4*, a gene encoding the only known candidate 5HT receptor expressed in *C. elegans* vulval muscle. I expand on previous information about *ser-4*'s expression pattern, characterize the 1.3 Kb deletion allele, *ser-4(ok512)*, and discuss possible reasons for its lack of a mutant phenotype. Preliminary data on *ser-4* overexpression and putative gain-of-function transgenic worms is also presented.

At the end of this dissertation are two appendices—one containing supplemental calcium-imaging data and, the other, a narrative of work I performed on an unfinished project to use DNA microarrays to compare and contrast global gene expression profiles produced by a genetic versus a pharmacologic ablation of the worm serotonin re-uptake transporter, MOD-5.

## CHAPTER I. INTRODUCTION

How do genes contribute to behavior? Today, 50 years after the discovery of the structure of DNA—and with the just recent completion of the monumental task of sequencing the human genome—we are still unable to completely answer this question, but can, at least, better recognize the complexity of the riddle: Only 30,000 genes give rise to a human being—yet endow an individual with  $10^{11}$  neurons and 1000x that number of synapses (Swanson et al, 1999). From this vast network of cells, its direction and coordination of the rest of the body in the dynamic interplay that occurs with an individual's environment—behavior somehow emerges.

As one can quickly appreciate, bridging the divide between genes and behavior is not trivial. The task of establishing fundamental biological principles can be made easier, however, by taking a reductionist approach. In 1965, Sydney Brenner selected the 1.5 mm-long soil nematode, *Caenorhabditis elegans*, to fulfill the role of a molecular biology primer to understanding development and behavior (Brenner, 1974). For four decades, *C. elegans* has flourished as a model system in biological studies through the ease of its laboratory cultivation and maintenance, the power of its genetics, and the talent and spirit of cooperation within its research community.

The body of work I describe in the following chapters was produced with the hope that I could add cellular and physiologic definition to past genetic and behavioral studies on the simple motor behavior of egg-laying in *C. elegans*. This Introduction is

intended to familiarize the reader with: the *C. elegans* nervous system and the advantages it affords for neurobiological studies; background on the diversity of G-proteins in the worm; a few key examples of worm behaviors and what is known about the neurotransmitter and G-protein signalling underlying their execution; and, finally, a brief treatment of methods developed only in the last few years to examine neurophysiology at a *cellular* level and truly begin to bridge the divide between genes and behavior.

### **THE *C. ELEGANS* NERVOUS SYSTEM**

The adult nervous system of the *C. elegans* hermaphrodite consists of exactly 302 neurons of known position, lineage, and synaptic connectivity—documented by a landmark serial electron microscopy study completed in the 1980s (White et al, 1986). There are approximately 5,000 chemical synapses in the worm, 2,000 neuromuscular junctions, and in excess of 700 gap junctions. The largest collection of neuronal cell bodies is located anteriorly, around the large pumping organ, the pharynx, which the worm uses during feeding; the toroidal bundle of neuronal processes surrounding the pharynx is commonly referred to as the “nerve ring.” The other major process bundles are the midline ventral cord (which houses the cell bodies of most of the worm’s motorneurons) and, connected to the ventral cord by circumferential commissures (mostly on the right side of the animal), a midline dorsal cord (axonal tracts only).

Chemical neurotransmission in *C. elegans* employs many of the same neurotransmitters utilized in higher organisms. These include: acetylcholine (the

major excitatory neurotransmitter at worm neuromuscular junctions—and, notably, the only neurotransmitter absolutely required by the worm for viability), GABA, glutamate, dopamine, octopamine, serotonin, as well as a plethora of neuropeptides (predominantly FaRPs, or FMRFamide-related peptides). As in other nervous systems, worm neurons respond to this array of neurotransmitters using both ionotropic and metabotropic receptors (Brownlee and Fairweather, 1999).

### **G-PROTEINS IN THE WORM**

The completion of the worm genome project in 1998 allowed an earlier accounting in *C. elegans* of the molecular ingredients needed for a functional nervous system (Bargmann, 1998). It was determined that the worm carries a complement of 20  $G\alpha$ , 2  $G\beta$ , and 2  $G\gamma$  G-protein subunit genes, and, within the next year, Jansen et al (1999) had systematically determined the expression patterns and generated mutants in most of the  $G\alpha$  subunits. Some of these had been previously characterized—particularly the worm homologues to the classical mammalian  $G\alpha$  classes of  $G_q$  (*egl-30*),  $G_s$  (*gsa-1* in the worm), and  $G_o$  (*goa-1*)—but the vast majority of  $G\alpha$  gene mutants Jansen et al described were new—and 14 of them appeared to be principally expressed in chemosensory neurons. This is likely a consequence of the fact that, unlike in mammalian systems, *C. elegans* chemosensory neurons are limited in number and, by necessity, one cell bears more than one odorant or gustatory receptor type. Null mutations in each of the  $G\alpha$  genes have been created, and developmental



lethality results in the cases of *egl-30*, *gsa-1*, and *gpa-16* (Brundage et al, 1996; Korswagen et al, 1997; Gotta et al, 2001).

The two *C. elegans* G $\beta$  genes, *gpb-1* and *gpb-2* serve functionally distinct roles. Both have similarly ubiquitous expression patterns, but where *gpb-1* is over 80% identical to mammalian G $\beta$ , *gpb-2* is much less conserved, and, indeed, is actually most similar to the divergent G $\beta$ 5 subunit in mammals (van der Linden et al, 2001; Chase et al, 2001; Robatzek et al, 2001). *gpb-1* mutants are not amenable to behavioral analysis because of an embryonic lethal phenotype characterized by random spindle orientations in early cell divisions (Zwaal et al, 1996).

Finally, *gpc-1* and *gpc-2* constitute the worm's complement of G $\gamma$  subunit genes. *gpc-1* expression is restricted to a set of about a dozen amphid and phasmid neurons and, thus, appears to have a specialized chemosensory role. *gpc-2*, on the other hand is found in all neurons and muscles, but suffers from a mitotic spindle defect identical to that of *gpb-1* (Gotta et al, 2001; Jansen et al, 2002).

## **LOCOMOTION AND ITS MODULATION**

Worms can respond to a wide range of environmental stimuli, including modalities mechanosensory (Driscoll and Kaplan, 1997), thermosensory, chemosensory, and osmosensory in nature (Bargmann and Mori, 1997). These inputs can then be processed to effect responses in motor behaviors such as locomotion, foraging, feeding, defecation, social behavior, mating, and egg-laying (Avery and Thomas, 1997; Rankin, 2002).

Locomotion is one of the most extensively studied behaviors in the worm. It is executed by the coordinated flexion of 95 adult body muscle cells arrayed across 4 quadrants of longitudinal muscle strips receiving their innervation from motoneurons in the ventral cord as well as (more anteriorly in the worm) from the nerve ring (White et al, 1986). *C. elegans* propagates alternating waves of dorsal and ventral muscle contractions to track sinusoidally through its laboratory environment of a bacterial lawn spotted on an agar plate. Locomotion studies have focused, in particular, on the opposing neuronal signal transduction networks of GOA-1 ( $G_o$ ) and EGL-30 ( $G_q$ ). *goa-1* hypomorphs (or *egl-30* gain-of-function worms) are hyperactive for locomotion, and produce sinusoidal tracks with deeper flexions than those of wild-type (N2) worms. Conversely, *egl-30* hypomorphs (or *goa-1* gain-of-function worms) are sluggish, and leave tracks that are comparatively flattened (Segalat et al, 1995; Mendel et al, 1995; Brundage et al, 1996).

The discovery that *egl-30* mutants are resistant to the acetylcholinesterase inhibitor aldicarb (Miller et al, 1996)—but still sensitive to the cholinergic agonist levamisole—suggested that *egl-30*'s sluggish locomotion might be due, in part, to impaired acetylcholine (ACh) release from motor nerve terminals, and provided a rough assay for identifying additional related signalling components. *egl-8* was isolated with such a screen, and encodes a phospholipase C $\beta$  (PLC $\beta$ ) homolog. Because a major action of  $G_q$  and PLC $\beta$  activation would be expected to be diacylglycerol (DAG) production (from hydrolysis of its precursor, phosphatidylinositol 4,5-bisphosphate or PIP $_2$ ), Lackner et al (1999) asked if

acetylcholine release (assayed by aldicarb sensitivity) could be restored in these mutants with phorbol esters (DAG analogs)—and found it could. They went on to demonstrate that one DAG target is the DAG-binding pre-synaptic protein, UNC-13, which would then represent one avenue for the facilitation of acetylcholine release. In opposition to these effects is GOA-1 action. *goa-1* mutants, in contrast to *egl-30*, are aldicarb-hypersensitive, indicating that with reduced GOA-1 function there is greater Ach release. Potential effectors for GOA-1 were found to include the RGS (regulator of G-protein signalling) protein, EAT-16 (inactivates EGL-30/G<sub>q</sub>), and the diacylglycerol kinase, DGK-1 (Hadju-Cronin et al, 1999; Lackner et al, 1999; Miller et al, 1999). The implication of DGK-1 would seem to suggest that DAG could be a point of convergence for the opposing GOA-1 and EGL-30 signalling networks. DAG can be thought of as the “currency” responsible for promoting motorneuron release of Ach, and where EGL-30 (via PLC $\beta$ ) increases its availability, GOA-1 might diminish its numbers via DGK-1 phosphorylation of DAG (and DAG’s subsequent conversion to phosphatidic acid). Finally, Nurrish et al (1999) reported that serotonin (5HT) inhibits motorneuron release of Ach and that GOA-1 and DGK-1 are molecular requirements for this inhibition.

This model of G<sub>o</sub>-G<sub>q</sub> antagonism and activation of G<sub>o</sub> by 5HT may represent a partial explanation for the observation that worm locomotion is depressed upon treatment with exogenous 5HT (Horvitz et al, 1982). It is important to note, however, certain caveats to this paradigm. *egl-30* mutants have more severe phenotypes than do *egl-8* worms, suggesting there are relevant additional EGL-30 effectors (Miller et al,

1999). DGK-1 is not necessarily established as a direct effector of GOA-1—and may, indeed, act in a parallel pathway. While 5HT inhibition of locomotion is rendered less effective in the absence of *goa-1*, the same can be said of inhibition of locomotion by other neurotransmitters such as the neuropeptide FLP-1 (Nelson et al, 1998). Finally, although reports of expression patterns in the studies above place EGL-30, GOA-1, EGL-8, EAT-16, and DGK-1 in the ventral cord motorneurons, the neurons and muscles which effect locomotion represent a very distributed system—and, beyond the use of the aldicarb assay, little has been done to more specifically identify critical cells and the loci of action at a finer resolution.

A separate body of worm locomotion studies focused on more subtle effects on behavior exerted by environment and experience. Sawin et al (2000) describe a “basal slowing response” in locomotion when worms continuously cultured on *Escherichia coli* are transferred to new plates, crawl, and re-encounter a bacterial lawn. Basal slowing is apparently dependent on intact dopamine signalling, as mutants defective in biosynthesis of this transmitter lose this behavioral response (but can be rescued with exogenous dopamine). Sawin et al observed some functional redundancy among the worm’s 3 classes of dopaminergic neurons (8 cells total)—and through exquisite manipulations demonstrated that these neurons promote basal slowing upon sensing the mechanosensory stimuli concomitant with entering the border of a bacterial lawn. A variation on this behavior which they termed “enhanced slowing response” was a further exaggerated slowing that could be elicited by starving worms for 30 minutes

before transferring them to a seeded plate and allowing them to crawl to a bacterial lawn—and this variation is dependent on serotonin signalling rather than on dopamine signalling. The critical source for the endogenous 5HT needed for enhanced slowing was traced to the large neuroendocrine NSM cells (dorsal to the pharynx) by laser ablation.

A genetic screen for mutants defective in enhanced slowing (*mod*, or modulation-defective, mutants) netted alleles in previously known genes such as *goa-1* and *dgk-1*—but also yielded new genes like *mod-1*. MOD-1 was eventually found to be an ionotropic 5HT receptor—but, unlike any other discovered to date, one that gates an inhibitory *chloride* current (Ranganathan et al, 2000). A *gfp* construct revealed *mod-1* expression in neurons in the head, ventral cord, and tail—but did not light-up muscle. A second *mod* mutant, *mod-5*, exhibits hyper-enhanced slowing (a phenotype opposite that of *mod-1*). *mod-5* encodes a worm serotonin re-uptake transporter (SERT)—a molecule which, in mammals, is responsible for terminating serotonergic neurotransmission by promoting the evacuation of synaptic 5HT through re-uptake at the nerve terminal (Deutch et al, 1999). Ranganathan et al created double mutant combinations of *mod-5* with *goa-1* and *mod-1*, separately, and discerned intermediate phenotypes in both genetic backgrounds. This implied residual 5HT signalling with the absence of *goa-1* or *mod-1* alone—and, indeed, it was only when the triple mutant was examined that enhanced slowing was almost completely eliminated. Ranganathan et al, therefore, concluded that two parallel 5HT pathways

mediate enhanced slowing and that GOA-1 and MOD-1 act on branches separate from each other.

Long-term (~6-hour) video- and position-tracking of worms by Hardaker et al (2001) uncovered yet another type of serotonergic modulation of locomotion—this time *stimulatory*. Sampling at 1-second intervals and then calculating running mean velocity in 10-second time windows, they observed that the direction and velocity of whole-worm movement fluctuated stochastically in wild-type worms. Animals alternated between periods of high and low locomotor activity—but without any periodicity. An interesting phenomenon occurred, however, around egg-laying events. Average velocity “spiked” over two-fold approximately 15-seconds before egg-laying events. This transient velocity increase was not 100% correlated with egg-laying (or vice-versa), but the probability of such a velocity spike was significantly enhanced in the period before egg-laying events. Serotonin was implicated in this positive modulation of velocity by several lines of evidence: First, the velocity spike was eliminated in animals lacking the serotonergic HSN egg-laying motoneurons. And second, it was also eliminated in *tph-1* (tryptophan hydroxylase) and *cat-4* (responsible for synthesizing a bipterin cofactor required by tryptophan hydroxylase) mutants, both of which lack serotonin biosynthesis. In addition to synapsing on vulval muscle to effect egg-laying, HSNs also synapse on interneurons known as the AVFs—whose synaptic output, in turn, is primarily to AVB, a command interneuron associated with inducing forward locomotion. Laser ablation of AVF also eliminated

the velocity spike prior to egg-laying—without affecting the incidence of egg-laying events themselves. While this more recently described action of 5HT on worm locomotion may seem at odds with the studies described above, the authors speculate that exogenous 5HT treatment hits multiple cellular targets simultaneously—and that the inhibitory effects may predominate because they are mediated at the more downstream site of the ventral cord motorneurons.

### **EGG-LAYING**

Another well studied behavior in *C. elegans* is egg-laying, and, unlike locomotion, egg-laying offers the advantage of a more compact nervous and muscular system. Eight vulval muscles are radially oriented around a ventral slit known as the vulva, and their contraction opens the vulva to allow the expulsion of eggs carried in the worm uterus. Half of these muscles are referred to as vm1's, and the other half as vm2's. Because of their two-fold radial symmetry, there is one vm1 pair and one vm2 pair for the right and left sides of the worm, each. From a lateral view, both vm1 and vm2 pairs to a particular side of the worm have diagonal "V" orientations, but, where a pair of anterior and posterior vm1's almost come to a point as they are followed ventrally, a pair of anterior and posterior vm2's diverge from each other (coming to a point, instead, as they are followed dorsally). Eight uterine muscles (circumferential bands encircling the roughly cylindrical or tube-shaped uterus) may also assist in egg-laying, though they are not strictly required for the behavior. All 16 hermaphrodite sex muscles are coupled by gap junctions (vm1R – vm1L; vm1 – vm2 for each side of

the worm; and the uterine muscles – vulval muscles via the vm2's; with no specific information available about possible anterior vm – posterior vm direct connections), and although at least 5 classes of motoneurons appear to synapse on the egg-laying muscle system, the most robust innervation is upon the vm2 muscles and originates from two classes of motoneurons—the HSNs (left and right) and ventral cord neurons VCs 4/5 (White et al, 1986).

Laser ablation studies have determined that only elimination of the vm2 muscle cells or the HSNs has adverse effects on the ability to execute egg-laying behavior (Trent et al, 1983). The former may be true because it is the primary target of motor innervation. As for the HSNs, these neurons are known to release a cocktail of neurotransmitters, including serotonin, acetylcholine, and FaRPs (Schinkmann et al, 1992; Rand and Nonet, 1997). Exogenous 5HT can rescue egg-laying in HSN<sup>-</sup> animals, suggesting an important role for this transmitter in stimulating egg-laying behavior (Trent et al, 1983). Interestingly, animals defective in 5HT or acetylcholine biosynthesis are not as severely egg-laying defective (Egl) as HSN<sup>-</sup> animals. These facts, combined with the observation that cholinergic stimulation of egg-laying is HSN-dependent (but not dependent on 5HT biosynthesis), suggest a third signal—possibly a neuropeptide—is also of importance (Lewis et al, 1980; Rand and Russell, 1984; Weinschenker et al, 1995). The VC neurons, when ablated on their own, do not produce a gross egg-laying phenotype (Garriga et al, 1993), but, combined with HSN ablation, egg-laying becomes 5HT-resistant. This defect is only overcome by the



simultaneous administration of exogenous 5HT and levamisole (a cholinergic agonist) (Waggoner et al, 1998).

A more detailed analysis in the last reference of the temporal pattern of egg-laying events (using video-tracking over 6-hour recordings) revealed that worms lay their eggs in clusters ('active phases')—separated by quiescent periods ('inactive phases'). The timing of both is aperiodic, but can be modeled well as linked Poisson processes, or random processes occurring with fixed probabilities. Waggoner et al found that N2 worms have a peak intra-cluster ('short') interval between events of about 20 seconds and a peak inter-cluster ('long') interval of about 20 minutes. Elimination of the HSNs or of 5HT biosynthesis primarily affected long intervals (decreasing the probability of the onset of an 'active phase') while perturbations of cholinergic signalling had a stronger association with changes in short intervals. Tracking on 5HT-containing plates induced what appeared to be a constitutive 'active phase'—and led to the conclusion that 5HT is important for inducing this "alternative behavioral state." In addition, two 5HT effectors were tentatively identified, based on their 5HT-resistance: EGL-19 (L-type voltage-gated  $\text{Ca}^{2+}$  channel,  $\alpha 1$  subunit) and TPA-1 (protein kinase C homolog). A 5HT receptor was never identified, but because of the *modulatory* nature of 5HT action on egg-laying (clustered egg-laying events still occurred without endogenous 5HT—inactive phases were simply longer), such a receptor was hypothesized to more likely be metabotropic than ionotropic.

Consistent with this, previous studies have demonstrated a significant role for G-protein signalling in egg-laying behavior. As with locomotion, the strongest

phenotypes known are associated with the paradigm of GOA-1 ( $G_o$ ) – EGL-30 ( $G_q$ ) antagonism. Reduced GOA-1 function (or excess EGL-30 function) results in hyperactive egg-laying while reduced EGL-30 function (or excess GOA-1 function) results in retention of eggs (Mendel et al, 1995; Segalat et al, 1995; Brundage et al, 1996). Determining the locus of these actions—and the exact relationship of 5HT to these G-proteins—has been problematic. Both Mendel et al and Segalat et al reported that *goa-1* is expressed in both neurons and muscles, but while the former used a GOA-1 GOF line (and pharmacologic manipulations) to argue that hyperactive egg-laying was a pre- and post-synaptic phenomenon, the latter genetically ablated the HSNs and argued that the *goa-1* phenotype was primarily a muscle phenomenon. A subsequent study examining this question (Waggoner et al, 2000b) used laser ablation of the HSNs and video-tracking to arrive at the conclusion that neuronal GOA-1 was important for maintaining the inactive phase of egg-laying behavior, but that muscle GOA-1 seemed to also inhibit egg-laying—perhaps by terminating existing active phases. In none of these three studies, however, could the specific cellular effects of genetic perturbations of *goa-1* be addressed to more thoroughly understand the basis of the final behavioral phenotypes.

Though Brundage et al (1996) reported a relatively straightforward 5HT-resistance phenotype in *egl-30* egg-laying, Lackner et al (1999) found no evidence for *egl-30::gfp* expression in the vulval muscles. (5HT-responsiveness is difficult to satisfactorily assay by behavior in *goa-1* mutants since their hyperactive egg-laying generally depletes worm uteruses of eggs.) Similarly unestablished is *egl-8* (encoding

PLC $\beta$ ) expression in the vulval muscles (Lackner et al, 1999; Miller et al, 1999)—though as the mutant name suggests, *egl-8* is egg-laying defective. *dgk-1* mutants, it should be noted, are, like *goa-1*, egg-laying-constitutive—though their expression pattern is neuronally-restricted (Nurrish et al, 1999).

In summary, though genetic and behavioral approaches have yielded a vast amount of information on G-protein signalling and its effects on behavior, there are limits inherent to these approaches because of an inability to examine the effects of genetic mutations on changes in physiology and function at the level of individual cells. An understanding of events at this level is critical, however, to accurately interpreting the basis of overall changes in behavior.

## **ADVANCES IN THE ANALYSIS OF *C. ELEGANS* CELLULAR PHYSIOLOGY**

For much of its history, *C. elegans* has not been fully tapped as a neurobiology resource. This is because, despite its smaller cell numbers and enviably well-defined neuroanatomy, it was not amenable to electrophysiologic study or to cell culture. A revolution began, however, in studies of the worm pharynx when Raizen et al (1995) successfully applied an extracellular recording technique known as the electropharyngeogram (EPG). In this method, a glass pipette is sealed onto the nose of the worm and pharyngeal muscle action potentials can be recorded with a patch-clamp amplifier. EPG deflections were then ascribed to specific neurons in the 20-neuron pharyngeal nervous system by an elegant laser ablation series. Sharp electrode

recordings have since been added to the arsenal of methods available for analysis of pharyngeal electrophysiology, enriching our understanding of the *in vivo* function of a  $\text{Na}^+/\text{K}^+$ -ATPase subunit (Davis et al, 1995) and a Kv-type potassium channel mutation's effect on feeding behavior (Davis et al, 1999)—and, more recently, implicating a voltage-gated  $\text{Na}^+$  current in pharyngeal pumping (Franks et al, 2002), putting into question long-held beliefs that the worm genome does not contain any voltage-gated  $\text{Na}^+$  channel genes.

The success of the EPG and sharp electrode techniques is not likely to be broadly applicable to other corners of the *C. elegans* nervous system, however, because the pharynx is an unusually large and accessible organ for the worm. Most *C. elegans* neurons, for example, are an order of magnitude smaller with an average diameter of 2-3  $\mu\text{m}$ . Another challenge in worm electrophysiology is the high internal hydrostatic pressure of the worm—normally contained by *C. elegans*' tough proteinaceous outer cuticle. Because accessing the internal contents of the worm requires piercing the cuticle, it is technically challenging to avoid incurring an explosion of worm tissue. A breakthrough was achieved by a combination of cell-selective *gfp* expression (to keep cells of interest clearly labeled) and the use of carefully placed incisions: the first *mid-body* to relieve some of the worm's internal pressure, and the second *at the site of interest* to produce a controlled 'flowering' (or 'bouquet') of neurons. When exposed, a *gfp*-expressing neuron of interest could then be patch-clamped (still quite challenging because of the diminutive scale of worm neurons). In this way, Goodman et al (1998) studied the sensory neuron ASER (as

well as other unidentified neurons) and were able to impressively characterize basic electrophysiologic properties of *C. elegans* neurons for the first time.

A ‘fillet’ preparation has also been described for which a longitudinal incision is made along the entire dorsum of the worm and splayed-open to allow recordings from body muscle. Using this technique, Richmond et al (1999) unambiguously established the presence of one GABA receptor and two acetylcholine receptor types in body muscle—a levamisole-sensitive and a (previously uncharacterized) levamisole-insensitive nicotinic receptor.

The number of patch-clamp recording studies in *C. elegans* is now steadily increasing—and has even expanded to studies of head interneurons. (For these and other related papers, the reader is encouraged to read the review by Francis et al, 2002.)

Christensen et al (2002) recently published a report detailing a method for successful large-scale primary culture of *C. elegans* cells. Where previous efforts had suffered from problems with cell viability, cell-substrate interactions, and reproducibility, this new attempt empowered worm researchers with a reliable technique for harvesting embryonic cells, allowing them to differentiate *in vitro* into neurons and muscles, and, augmented by *gfp* to readily identify cells of interest, obtaining patch-clamp recordings from cells. Significant drawbacks of the technique, however, are that postembryonically derived tissues are not found to appear (which would preclude studies of vulval muscle or VC neurons for analyses pertaining to egg-

laying), and, additionally, functional synaptic connectivity has not yet been found to develop by this culturing technique.

Patch clamp and cell culture techniques share a common liability in their invasiveness and disruption of the worm as an intact, functioning organism. And it was with considerations like these in mind that Kerr et al (2000) sought to employ cameleon in studies of worm cellular and physiologic function. Cameleon is a GFP-based calcium ( $\text{Ca}^{2+}$ ) indicator which utilizes fluorescence resonance energy transfer (FRET) to measure changes in intracellular  $\text{Ca}^{2+}$  as a function of time. Specifically, it consists of cyan and yellow variants of GFP on opposite ends of a calmodulin (CaM)-M13 (derived from myosin light chain kinase) linker. In a low  $\text{Ca}^{2+}$  environment, violet light excites the cyan fluorescent protein (CFP) domain and cameleon emission is cyan. In high  $\text{Ca}^{2+}$ , however, CaM binds  $\text{Ca}^{2+}$  ions and  $\text{Ca}^{2+}$ -bound CaM is subsequently bound by M13. This induces a conformational change which either brings CFP into closer apposition with yellow fluorescent protein (YFP)—or alters their relative orientation to each other to one more favorable for FRET, whereby cyan emission becomes devoted to exciting YFP and cameleon now emits yellow light. A population of cameleon molecules, therefore, can be followed in a time-course for changes in yellow/cyan (Y/C) ratio as a read-out of changes in intracellular  $\text{Ca}^{2+}$ . Cameleon typically is expressed at concentrations of tens to hundreds of micromolar and can report on a dynamic range of  $\text{Ca}^{2+}$  concentrations from about  $10^{-7}$  to  $10^{-4}$  M. The elegance of cameleon lies in its *ratiometric* read-out—unlike the individual

yellow and cyan intensities, the Y/C ratio is subject to less noise and motion artifact because these factors cancel-out (within certain limits) (Miyawaki et al, 1997; Miyawaki et al, 1999).

Kerr et al (2000) first investigated practical use of cameleon in *C. elegans* in the large muscular organ of the pharynx—and, using reduction- and gain-of-function alleles in *egl-19*, found that most of the differences in mutant alleles of this Ca<sup>2+</sup> channel subunit manifested themselves in the *duration* of individual Ca<sup>2+</sup> transients. Mutations in the  $\alpha 2$  Ca<sup>2+</sup> channel subunit gene, *unc-36*, on the other hand, increased the slopes (without changing duration) of Ca<sup>2+</sup> transients, suggesting a normal role for  $\alpha 2$ 's in negative regulation of the main pore-forming  $\alpha 1$  subunit. Kerr et al concluded their study with a brief demonstration that *C. elegans* neurons could, in principle, be followed for meaningful ratiometric changes in cameleon by expressing the sensor pan-neuronally and inducing a transient by direct electrical stimulation. Since then, Kerr and others have successfully utilized cameleon in more specific subsets of worm neurons such as the AVM and ALM mechanosensory neurons (Suzuki et al, submitted) and the polymodal ASH nociceptive sensory neuron (Hilliard et al, submitted).

The aim of my graduate work has been to explore the physiology underlying *C. elegans* egg-laying behavior and, in so doing, to expand our understanding beyond the limits inherent to a solely genetic approach. It was my hope that using cameleon would also help to resolve some long-standing discrepancies and differences of

opinion about the precise nature and location of the effects of known genetic perturbations on egg-laying behavior.



This chapter was originally prepared as a manuscript of the same title which was recently submitted for publication: Shyn SI, Kerr R, Schafer WR. 2003. Serotonin and G<sub>o</sub> modulate functional states of neurons and muscles controlling *C. elegans* egg-laying behavior. (*submitted*). It has been reformatted to conform to the layout of the other chapters in this dissertation. A supplemental section (co-submitted with the manuscript) is retained as a separate addendum at the end of this chapter. The dissertation author was the primary researcher and author, with computer and statistical expertise contributed by Rex Kerr, the manuscript's second author.

## CHAPTER II. SEROTONIN AND G<sub>o</sub> MODULATE FUNCTIONAL STATES OF NEURONS AND MUSCLES CONTROLLING *C. ELEGANS* EGG-LAYING BEHAVIOR

### ABSTRACT

From nematodes to humans, animals of varying complexity employ modulators like the neurotransmitter, serotonin, to transition between alternative behavioral patterns and states. For example, in the nematode, *C. elegans*, serotonin has been shown to control a switch between active and inactive phases of egg-laying behavior. We have used the genetically-encoded calcium indicator, cameleon, to investigate the cellular basis of the modulation of egg-laying behavior by serotonin. We found that in wild-type vulval muscles, calcium transients occur in a sporadic and clustered pattern. Serotonin treatment altered this pattern to produce a sustained train of Ca<sup>2+</sup> events. This effect was independent of the egg-laying motoneurons, indicating that it was a consequence of direct modulation of the vulval muscles by serotonin. In contrast, when we used cameleon to record from the egg-laying motoneurons, we found that serotonin silenced the spontaneous activity observed in drug-free conditions. Mutations in the G<sub>o</sub>α-subunit gene, *goa-1*, also altered the pattern of Ca<sup>2+</sup> transients in both vulval muscles and egg-laying neurons. Specifically, *goa-1* mutations increased the frequency of vulval muscle calcium transients, either in the presence or absence of neuronal input, and prevented the silencing of motoneuron

activity by serotonin. These data indicate that serotonin stimulates egg-laying by directly modulating the functional state of the vulval muscles. In addition, serotonin also inhibits the activity of the motoneurons that release it, providing a feedback regulatory effect that may contribute to serotonergic adaptation.

## INTRODUCTION

Understanding behavior at the molecular and cellular level is a fundamental challenge in neurobiology. In principle, this problem is most tractable in animals with simple, well-characterized nervous systems and facile molecular genetics. In particular, the soil nematode, *Caenorhabditis elegans*, is an accessible model system for relating behavioral patterns at the level of the whole organism to the functional properties of identified neurons and muscle cells. One behavior that has been well-studied at the genetic and cellular level is egg-laying. Eight radially-oriented vulval muscles (4 vm1's and 4 vm2's) are responsible for opening a ventral slit through which the worm expels its eggs; 8 uterine muscles may additionally assist in egg-laying (though they are not essential for oviposition). All 16 egg-laying muscles are electrically-coupled through gap junctions, with the 4 vm2 vulval muscles receiving synaptic input from two classes of motoneurons: the 2 HSNs and VCs 4 and 5 (White et al, 1986).

Previous work has demonstrated that serotonin, which is released by the HSNs, plays an important role in stimulating egg-laying in *C. elegans*. Serotonin-deficient mutants are egg-laying defective, and exogenous serotonin can rescue the egg-laying

defects of animals lacking HSN neurons (Trent et al, 1983). More detailed studies of the temporal pattern of egg-laying events have suggested that serotonin acts in a modulatory fashion to facilitate a switch from an inactive state, during which egg-laying is infrequent, to an active state in which eggs are laid in bursts (Waggoner et al, 1998). Conversely, long-term exposure to high concentrations of serotonin has an adaptive, inhibitory effect on egg-laying (Schafer and Kenyon, 1995). Several other neurotransmitters and neuromodulators have also been shown to influence egg-laying, including: acetylcholine, dopamine, and FMRFamide-related neuropeptides (Trent et al, 1983; Weinshenker et al, 1995; Schafer and Kenyon, 1995; Schinkmann and Li, 1992; Waggoner et al, 2000b). In addition, multiple G-proteins have been shown to be expressed in the egg-laying muscles and/or motorneurons, and mutant alleles of several G-protein  $\alpha$ -subunit genes exhibit abnormal egg-laying behavior (Mendel et al, 1995; Segalat et al, 1995; Brundage et al, 1996; Jansen et al, 1999; Waggoner et al, 2000b). Different G-proteins have been shown to genetically interact with each other, as well as with RGS (Regulator of G-protein signalling) proteins to alter baseline or, sometimes, experience-dependent egg-laying (Lackner et al, 1999; Miller et al, 1999; Dong et al, 2000).

Despite the extensive genetic analyses of egg-laying performed to date, the functional activity of individual muscles and neurons in the egg-laying circuit (and the relationship of cell physiology to egg-laying phenotypes) has been more difficult to examine. For example, it has not been conclusively determined whether serotonin acts directly on the vulval muscles or acts indirectly through modulation of the egg-laying

motorneurons. Likewise, the specific effects of serotonin on vulval muscle activity that facilitate increased egg-laying have not been characterized. To address these questions, we have used the calcium-sensitive protein, cameleon, to optically image the activity of muscles and neurons in intact behaving animals. Cameleon is a GFP-based calcium indicator that uses fluorescence resonance energy transfer (FRET) to measure intracellular calcium transients that accompany depolarization in excitable cells. Since cameleon is genetically encoded, it can be specifically targeted to individual muscle and neuronal cells to allow non-invasive imaging of depolarization-induced calcium transients during normal behavior (Miyawaki et al, 1997, 1999).

## RESULTS

To monitor the activity of individual vulval muscles *in vivo*, we obtained a transgenic line (gift from Timothy Yu, Bargmann lab) that expresses cameleon under the control of the *myo-3* promoter (Okkema et al, 1993). Animals were immobilized on agarose pads containing Dent's saline, and fluorescent images were collected (generally, for 1 minute) and analyzed as described in *Supplemental Materials and Methods* (see also Kerr et al, 2000). A typical focal plane of image capture allowed the simultaneous monitoring of two vulval muscles as depicted in Figure 2-1. Figure 2-1A shows vulval muscles in a relaxed state while Figure 2-1B shows the same muscles at the height of contraction during an egg-laying event. During periods of muscle contraction, the yellow fluorescent protein (YFP) / cyan fluorescent protein (CFP) ratio transiently increased, and this ratio change was typically accompanied by

an increase in YFP emission intensity and a reciprocal decrease in CFP intensity (Figure 2-1C). Furthermore, the ratio change correlated temporally with small vulval muscle contractions (though video capture of actual egg-laying events proved quite rare under our recording conditions—i.e., about 1 in 500 recordings). Thus, cameleon appeared to be a reliable indicator of vulval muscle calcium transients in intact behaving animals.

Using cameleon, we recorded simultaneously from pairs of vm1 or vm2 muscle cells to investigate their patterns of activity *in vivo*. We found no significant differences between the frequency of calcium events in the vm1 and vm2 muscles; the vm1's averaged 6.82 events/min (n=12) while vm2's averaged 6.16 events/min (n=9) (no statistical difference). The activities of individual vulval muscle cells, imaged simultaneously in individual animals, show significant temporal correlation. For example, 23.2% of events in a pair of simultaneously imaged muscles were correlated within a window of 100 msec (about 3 frames of video capture at our recording rate), significantly higher than would be expected by chance (sample traces from a correlated muscle pair are shown in Figure 2-1D.) Baseline vulval muscle calcium transients were sporadic and temporally clustered (Figure 2-2A). To gain more information about the temporal pattern of vulval muscle calcium transients, we generated long recordings (~8 minutes) and analyzed the timing of active and inactive periods. We found that periods of high activity typically lasted 3-4 seconds and contained multiple small calcium events separated by an average of 1 sec. Inactive

periods lasted an average of 30 seconds, and occasionally persisted over 1-2 minutes in duration.

We next investigated whether the egg-laying motoneurons were required for this sporadic pattern of vulval muscle calcium transients. To address this question, we ablated all six VC neurons in an *egl-1(n986)* mutant background (in which the HSN neurons undergo inappropriate programmed cell death), and then imaged vulval muscle calcium transients. We observed that in the absence of neuronal input from the HSNs and VCs, the vulval muscles still exhibited calcium transients, although there was a downward trend in frequency (not significant with our limited numbers of ablated worms) (Figure 2-2, Table 2-1). These results indicated that spontaneous vulval muscle activity and the spontaneous pattern of transients persist in the absence of neuronal input. This is consistent with behavioral predictions that the egg-laying motoneurons play a modulatory role to facilitate increases in the frequency and/or strength of egg-laying contractions.

How might the egg-laying neurons modulate vulval muscle activity?

Behavioral data strongly implicated serotonin, a neuromodulator released from the HSN egg-laying motoneurons, in the control of egg-laying behavior. Specifically, serotonin both increased the overall rate of egg-laying and changed the temporal pattern of egg-laying from one in which clusters of egg-laying events were separated by long inactive phases to one in which egg-laying modeled as a simple Poisson process (Waggoner et al, 1998). To determine serotonin's effect on the vulval

muscles, we recorded muscle calcium transients in the presence of exogenous serotonin (1.3 mM). As shown in Table 2-1, application of exogenous 5HT led to a significant increase in the frequency of  $\text{Ca}^{2+}$  events, from a baseline of  $5.63 \text{ min}^{-1}$  to a rate of  $35.01 \text{ min}^{-1}$  ( $P < 0.001$ , Kolmogorov-Smirnov test). Moreover, serotonin treatment led to a dramatic change in the distribution of events, as the clustered pattern of transients in untreated worms gave way to a more continuous train of  $\text{Ca}^{2+}$  events (approximately 0.5-2 Hz) (Figure 2-2). Inter-muscle correlation of activity increased from a fraction of 0.232 (baseline) to 0.547 under 1.3 mM 5HT, and 31 of 35 muscle/trace pairs exhibited a level of correlation achieving a significance level  $P < 0.05$  (overall  $P = 1.99 \times 10^{-36}$ , Fisher exact test). Thus, exogenous serotonin appeared to modulate the functional state of the vulval muscles, switching them from an inactive state of sporadic calcium activity to an active state of continual calcium activity.

In principle, serotonin could exert its effects directly on the vulval muscles, or it could act indirectly by altering the activity of the egg-laying motorneurons. To resolve this issue, we ablated the egg-laying motorneurons (as above) and assayed, once again, the effect of serotonin on vulval muscle calcium transients. We found that ablated animals exhibited a continuous train of calcium transients on serotonin essentially identical to that exhibited by unablated wild-type animals (Figure 2-2). The ability of serotonin to increase the frequency of calcium events was not markedly affected by the absence of the egg-laying motorneurons (Table 2-1). Thus, serotonin



appeared to stimulate the activity of the vulval muscles by directly modulating their functional state.

To investigate the molecular requirements for serotonergic modulation of the vulval muscles, we tested the effects of mutations in genes known to affect egg-laying behavioral responses on serotonin's ability to induce the changes in vulval muscle calcium transients detailed above. Previous behavioral studies indicated that reduction-of-function mutations in the L-type  $\text{Ca}^{2+}$  channel gene, *egl-19*, strongly interfere with the ability of serotonin to stimulate egg-laying (Waggoner et al, 1998). When we imaged calcium transients in one such allele, *egl-19(n582)*, we observed very little activity compared to wild-type (Table 2-1). In the presence of serotonin, we observed no significant increase in the frequency of calcium transients. This suggests that the EGL-19 calcium channel is necessary for the generation of serotonin-evoked calcium transients in the vulval muscles. We also investigated another potential source of the calcium transients evoked by serotonin: the ryanodine receptor, UNC-68. In contrast to the results with *egl-19*, *unc-68* null mutants showed a normal pattern of calcium transients in the absence of drug and responded as robustly as wild-type animals to exogenous serotonin. Together, these results suggest a key role for the EGL-19 voltage-gated calcium channel in vulval muscle calcium influx during egg-laying.

We next explored the effects of G-protein signaling mutants on vulval muscle activity and its modulation by serotonin. Of the 20 G-protein  $\alpha$ -subunits in the *C.*

*C. elegans* genome, five are known to be expressed in the vulval muscles: *goa-1*, *gsa-1*, *gpa-7*, *gpa-14* and *gpa-16*. Viable loss-of-function alleles exist for *goa-1*, *gpa-7* and *gpa-14*; we, therefore, assayed the effects of these mutations on vulval muscle calcium transients in the presence and absence of serotonin. Mutations in *gpa-7* and *gpa-14* had no significant effect on baseline vulval muscle activity or its enhancement by 5HT (Table 2-1). *goa-1(n1134)* worms, however, displayed a higher level of baseline activity than wild-type (20.10 versus 5.63 events/min, respectively,  $P < 0.001$  by Kolmogorov-Smirnov) (Figure 2-2 & Table 2-1). To determine whether these effects were due to muscle-intrinsic action of GOA-1, we imaged animals in which the egg-laying motoneurons were ablated in the *goa-1(n1134)* mutant background. We observed that these ablated mutant animals showed elevated calcium activity compared with neuronally-ablated wild-type animals (10.69 versus 1.08 events/min, respectively,  $P < 0.01$  by Kolmogorov-Smirnov), and that this activity displayed a trend toward less activity than in unablated *goa-1* mutant animals (Figure 2-2 & Table 2-1). Together, these data indicated that GOA-1 negatively regulates vulval muscle activity, at least in part through cell-intrinsic action within the muscle cells.

We next investigated the effect of *goa-1* on the response of the vulval muscles to serotonin. *goa-1(n1134)* animals exhibited an already-elevated frequency of vulval muscle  $\text{Ca}^{2+}$  events in the absence of 5HT, and treatment with exogenous serotonin did not increase this vulval muscle activity further. However, when ablated *goa-1* animals were imaged in the presence of serotonin, they showed a robust increase in the frequency of calcium events (27.04 events/min) relative to the baseline of ablated

*n1134* (10.69 events/min) ( $P < 0.001$  by Kolmogorov-Smirnov). Thus, GOA-1 apparently is not required for vulval muscle serotonin response; rather the higher baseline of ablated *n1134* (relative to ablated wild-type) suggests that GOA-1 acts independently and antagonistically to the serotonin response pathway in the vulval muscles to inhibit the frequency of calcium transients.

Although our analysis of motoneuron-ablated animals demonstrated a direct action of serotonin and GOA-1 on the vulval muscle, an assortment of previous behavioral studies also implied possible actions of both serotonin and  $G_o$  in controlling the activity of the egg-laying motoneurons. We therefore investigated the effects of serotonin and *goa-1* on the neurons in the egg-laying motor circuit. To monitor egg-laying motoneuron activity in behaving animals, we generated a transgenic line (*cat-1::iYC2.1*) expressing cameleon in the HSN and VC4/5 neurons, and imaged spontaneous neuronal calcium transients under the same conditions used for vulval muscle imaging. Using this approach, we were able to record from both classes of motoneurons, but the HSNs gave us the most robust recordings. We observed spontaneous and aperiodic calcium transients in approximately 25% of all one minute recordings from N2 HSNs, with an overall mean of 1.04 events/min (Figure 2-3).

We next used cameleon-based imaging to assess the effects of exogenous serotonin and *goa-1* on motoneuron activity. In the presence of exogenous serotonin (1.3 mM) we unexpectedly observed a complete silencing of HSN activity: Out of 29 one-minute wild-type HSN recordings, none showed any detectable activity. This

difference was highly significant ( $P=0.018$  compared with [no drug], chi-square before Bonferroni correction), and suggested that in addition to stimulating the vulval muscles, serotonin acts as an inhibitory modulator of the motoneurons from which it is released. Mutations in *goa-1* did not significantly change the baseline activity of the HSNs in the absence of serotonin—out of 27 HSN recordings made from *goa-1(n1134)*, 33% exhibited activity, with an overall mean of 1.89 events/min (sample trace in Figure 2-3B). However, the HSNs from *goa-1(n1134)* appeared strongly resistant to serotonin-induced silencing of neuronal activity, as 28% ( $n=25$ ) of one-minute traces on 5HT showed activity ( $P=0.0081$  compared to wildtype on serotonin, chi-square before Bonferroni correction), averaging 0.84 events/min. Thus, GOA-1 appears to play two distinct roles in the egg-laying circuitry: In the vulval muscles it functions antagonistically to serotonin to inhibit muscle activity, while in the HSNs it appears necessary for serotonin silencing of neuronal activity. Together with its negative regulatory effect on vulval muscle calcium dynamics, this finding provides a cellular explanation for the well-characterized egg-laying-constitutive phenotype of *goa-1* mutants, and is consistent with genetic evidence suggesting a role for GOA-1 in inhibiting the activity of ventral cord motoneurons controlling locomotion (Mendel et al, 1995; Segalat et al, 1995; Nurrish et al, 1999).

## DISCUSSION

Our results provide a straightforward cellular basis for the effects of serotonin on egg-laying behavior. Previous behavioral studies (Waggoner et al, 1998;

Weinshenker et al, 1995) predicted a modulatory role for serotonin, in which serotonin release from the HSNs potentiates egg-laying events by altering the functional state of the vulval muscles and/or egg-laying motoneurons. Our results here demonstrate that the stimulatory effect of serotonin results at least in part from direct modulation of vulval muscle calcium dynamics, which leads to a marked increase in the frequency of calcium transients. The sensitivity of this effect to mutations in the L-type calcium channel gene, *egl-19*, suggests that serotonin exerts this effect by bringing the threshold for activation of vulval muscle voltage-dependent  $\text{Ca}^{2+}$  channels closer to the resting potential of the cell. Serotonin also affected the activity of the HSN motoneuron, except, in this case, the action of serotonin was inhibitory. Since the HSNs are themselves serotonergic, this inhibition could serve as a feedback mechanism by which serotonin could terminate its own release from the HSNs and thus maintain a clustered pattern of egg-laying. The inhibitory action of serotonin on the egg-laying motoneurons also suggests a possible mechanism for serotonergic adaptation. It is known that long-term exposure to high concentrations of serotonin has an inhibitory effect on egg-laying. Our results here suggest that this inhibition could result from prolonged inhibition of HSN activity combined with a desensitization of serotonin's stimulatory effect on the vulval muscles.

More generally, our studies establish the feasibility of using *in vivo* optical imaging with a genetically encoded sensor to monitor neuronal activity patterns in an intact behaving nematode. Future application of these methods in other neurons

should enable us to test and corroborate a wide range of cellular-level predictions about the neural basis for behavioral phenotypes.

## MATERIALS AND METHODS

### General Methods and Strains

Nematodes were grown and assayed at 22° C on standard Nematode Growth Medium (NGM) seeded with *E. coli* strain OP50 as a food source.

### Construction of *cat-1::iYC2.1*

An ~800 bp derivative of *nde-box::YC2.3* (18x *nde-box* vulval muscle enhancer from *ceh-24* and pSAK-10 backbone originally from A. Fire lab; *YC2.3* from Roger Tsien) with HindIII, NcoI sticky ends was transplanted to a pPD95.75 backbone containing *iYC2.1* (introns added for worm-optimized expression, gift of Jami Dantzker) and then cut again—this time with HindIII, NotI to replace most of the ~800 bp derivative (a short piece from NotI – NcoI was left in the backbone) with a *cat-1* promoter sequence derived from a *cat-1::gfp* plasmid (gift of Antonio Colavita). The *cat-1* promoter was transferred in two pieces: (1) a 2100 bp HindIII – NsiI restriction fragment from the *gfp* plasmid, and (2) a 214 bp PCR product with NsiI, NotI sticky ends generated from the *gfp* plasmid with PCR primers 5'-CGTGCCTTTCCTTTGAAGTTATTATGCAT-3' and 5'-ATGCGGCCGCACCTCCTTCTTCCAAGTTTTATTGAATG-3'. The final *cat-1::iYC2.1* construct was microinjected into N2 worms at 25 ng/μl according

to the protocol in Mello and Fire (1995). There was no co-injection marker since transformed worms could be readily identified by fluorescent neurons in the head, midbody, and tail. The extrachromosomal array line used in this study was designated *ljEx65*.

### **Laser ablation of VC neurons**

VC neurons 1-6 were ablated in late third-stage / early fourth-stage larvae of *egl-1(n986); nls106(lin-11b::gfp)* worms (Reddien et al, 2001). Expression of GFP in the developing VC cells was used to identify them prior to the ablation process; cell killing was verified the next day by scoring for the absence of GFP-expressing neurons and neuronal processes.

### **ACKNOWLEDGEMENTS**

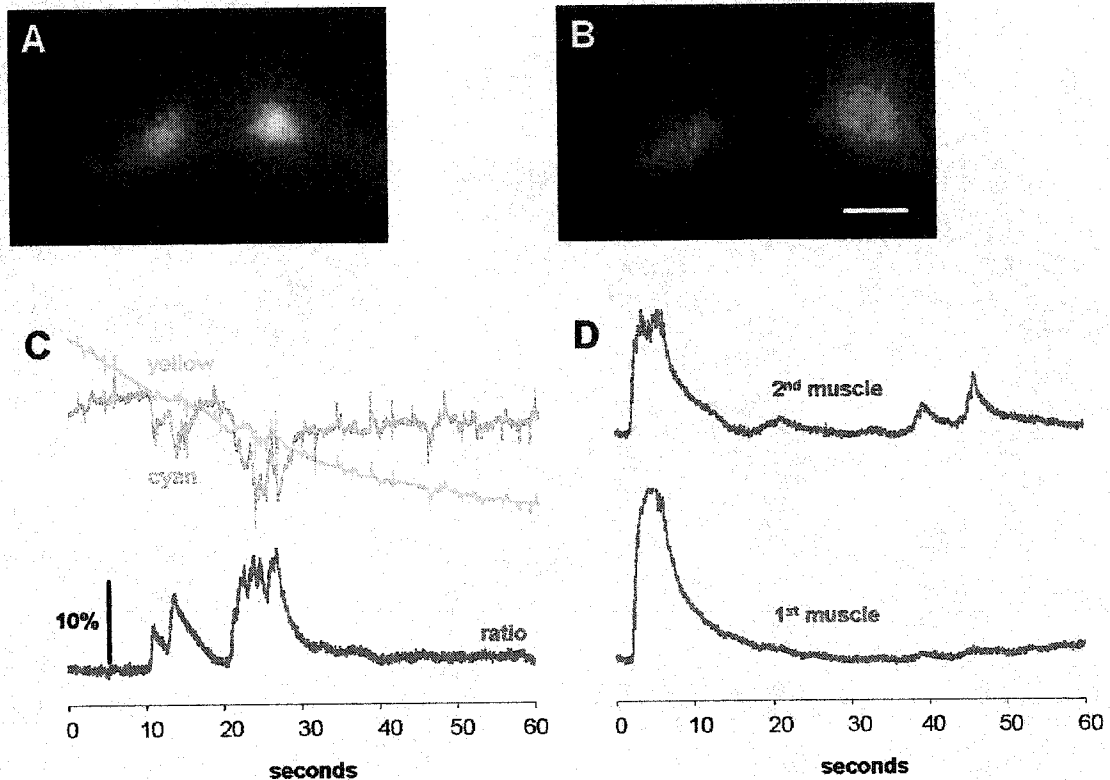
We are grateful to Timothy Yu and Jami Dantzker (Bargmann lab) for their generous gift of the *kyEx302[myo-3::YC2.0]* line and iYC2.1 plasmid DNA, to Antonio Colavita (Tessier-Lavigne lab) for *cat-1* promoter plasmid DNA, to Rene Garcia for *r1158*, and to the *Caenorhabditis* Genetics Center for all other strains. This work was supported by grants from NIH (DA16445), the Human Frontiers Science Program, and the Klingenstein Foundation. S.I.S. was partially supported by NIH/NIGMS Training Grant PHSGM07198 (Medical Scientist Training Program, UCSD).

**Table 2-1. Muscle Ca<sup>2+</sup> events/min.** Listed in bold are mean event frequencies (events/min),  $\pm$  SEM, (n) = number of animals/recordings used in calculation of mean frequency of events. One of two recordings in a pair was selected at random for data analysis, unless one of the pair was inactive or compromised by artifact or excessive noise—in which case, that recording was discarded and its partner utilized.

\*significant Kolmogorov-Smirnov score v. N2 no drug. ^significant Kolmogorov-Smirnov score v. same strain/ablation status, no drug. ^significant Kolmogorov-Smirnov score v. N2 ablated, no drug. One symbol denotes P<0.05, two symbols P<0.01, three symbols P<0.001. Bonferroni correction was employed in cases where there were multiple comparisons.

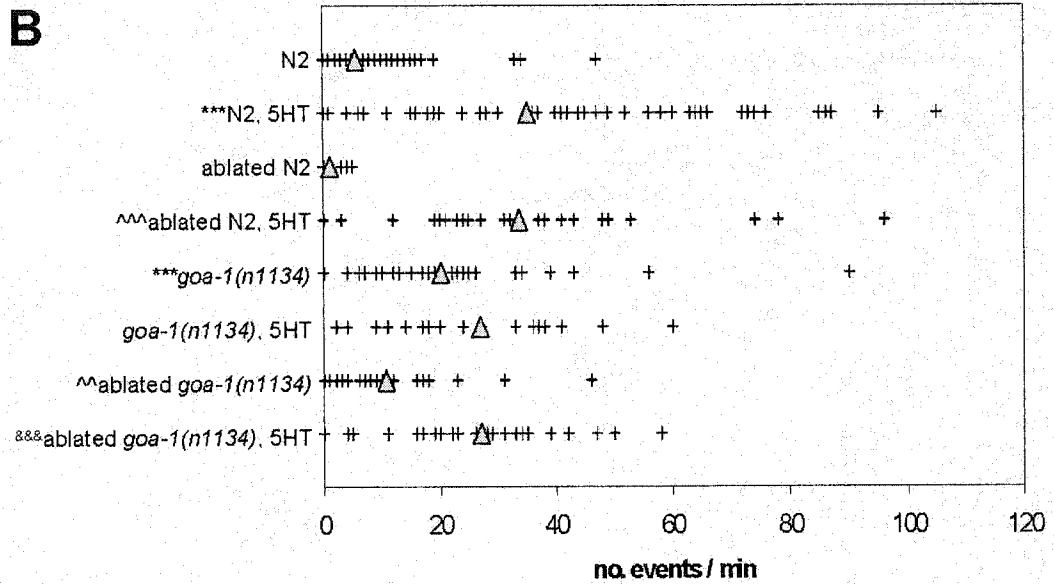
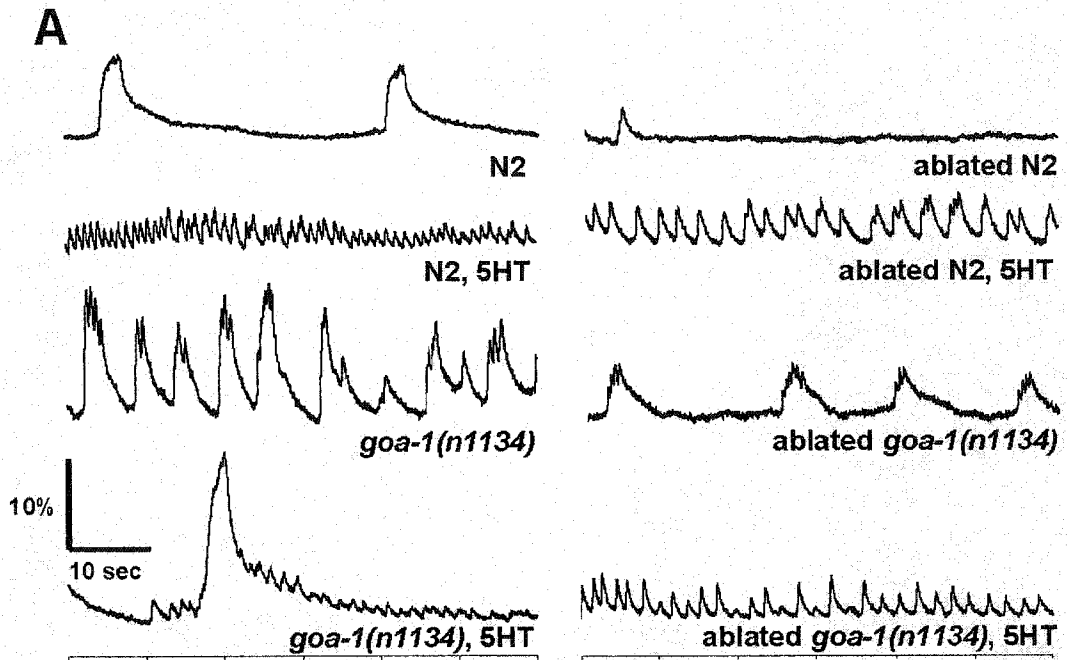
	Frequency of events (events/min)			
	intact nervous system		HSN(-), VC 1-6(-)	
	no drug 1.3 mM 5HT		no drug 1.3 mM 5HT	
N2	<b>5.63</b> $\pm 0.76$ (109)	<b>***35.01</b> $\pm 3.32$ (73)	<b>1.08</b> $\pm 0.53$ (12)	<b>^^^33.53</b> $\pm 4.22$ (28)
N2 (long recordings)	<b>6.54</b> $\pm 1.43$ (21)			
vm1 only	<b>6.82</b> $\pm 2.05$ (12)			
vm2 only	<b>6.16</b> $\pm 2.03$ (9)			
<i>egl-19(n582)</i>	<b>***0.35</b> $\pm 0.22$ (26)	<b>0.71</b> $\pm 0.49$ (17)		
<i>goa-1(n1134)</i>	<b>***20.10</b> $\pm 3.48$ (30)	<b>26.80</b> $\pm 3.93$ (20)	<b>^10.69</b> $\pm 2.05$ (26)	<b>^^&amp;&amp;27.04</b> $\pm 2.79$ (28)
<i>gpa-7(pk610)</i>	<b>10.57</b> $\pm 3.07$ (28)	<b>^^&amp;&amp;29.65</b> $\pm 3.11$ (37)		
<i>gpa-14(pk347)</i>	<b>4.05</b> $\pm 1.17$ (37)	<b>^^&amp;&amp;30.17</b> $\pm 4.45$ (36)		
<i>unc-68(r1158)</i>	<b>9.55</b> $\pm 2.27$ (40)	<b>^^&amp;&amp;40.52</b> $\pm 6.19$ (25)		





**Figure 2-1.  $\text{Ca}^{2+}$ -imaging of *C. elegans* vulval muscle with cameleon.** (A) Pseudocolor ratio image of vulval muscles at rest. (B) The same vulval muscles during contraction. Note the red pseudocolor shift. A to B spans an approximately 35% change in Y/C ratio. Scale bar is 10  $\mu\text{m}$ . (C) Sample one-minute ratio trace (red) from a separate pair of vulval muscles, N2 [no drug], corrected for photobleaching. Component yellow and cyan intensity curves (prior to photobleaching correction) are shown above. Note reciprocal deflections of yellow and cyan. Vertical scalebar represents 10% Y/C ratio increase. (D) Sample ratio traces from two vulval muscles in a simultaneously imaged pair. In this instance, 35.3% of the  $\text{Ca}^{2+}$  events were temporally correlated (using a defined correlation window of 100 msec). Drawn to scale with (C).

**Figure 2-2. Sample vulval muscle ratio traces & selected distributions of event frequency.** (A) Sample 1-minute ratio traces for N2 (wild-type) and *goa-1(n1134)*, on/off 1.3 mM serotonin (5HT), intact / neuronally ablated (HSN<sup>-</sup>, VC1-6<sup>-</sup>). N2 traces displayed a sporadic and clustered pattern of Ca<sup>2+</sup> events both with/without the egg-laying motoneurons. On 5HT, the sporadic pattern of Ca<sup>2+</sup> transients gave way to a more sustained train of events, with an approximate frequency of 0.5-2.0 Hz. This 5HT-induced change could be produced independent of the presence of the HSNs or VCs. A reduction-of-function allele of *goa-1*, *n1134*, results in higher baseline Ca<sup>2+</sup> activity, consistent with its hyperactive egg-laying behavior. *n1134* continued to exhibit elevated muscle Ca<sup>2+</sup> activity relative to N2 when both groups of worms were neuronally ablated, indicating that GOA-1 negatively regulates vulval muscle activity, at least in part through cell-intrinsic action within the muscles. Laser ablation of *n1134* also helped to establish that *goa-1* worms can still respond to 5HT with an increase in muscle Ca<sup>2+</sup> activity. (B) Scatter-plot distributions of events/min. Means are indicated by filled triangles, and individual data-points (each representing a one-minute trace) by crosses. This data is also presented in Table 2-1. \*significant Kolmogorov-Smirnov score v. N2 [no drug]. &significant Kolmogorov-Smirnov score v. same strain / ablation status, [no drug]. †significant Kolmogorov-Smirnov score v. N2 ablated, [no drug]. One symbol denotes P<0.05, two symbols P<0.01, three symbols P<0.001.



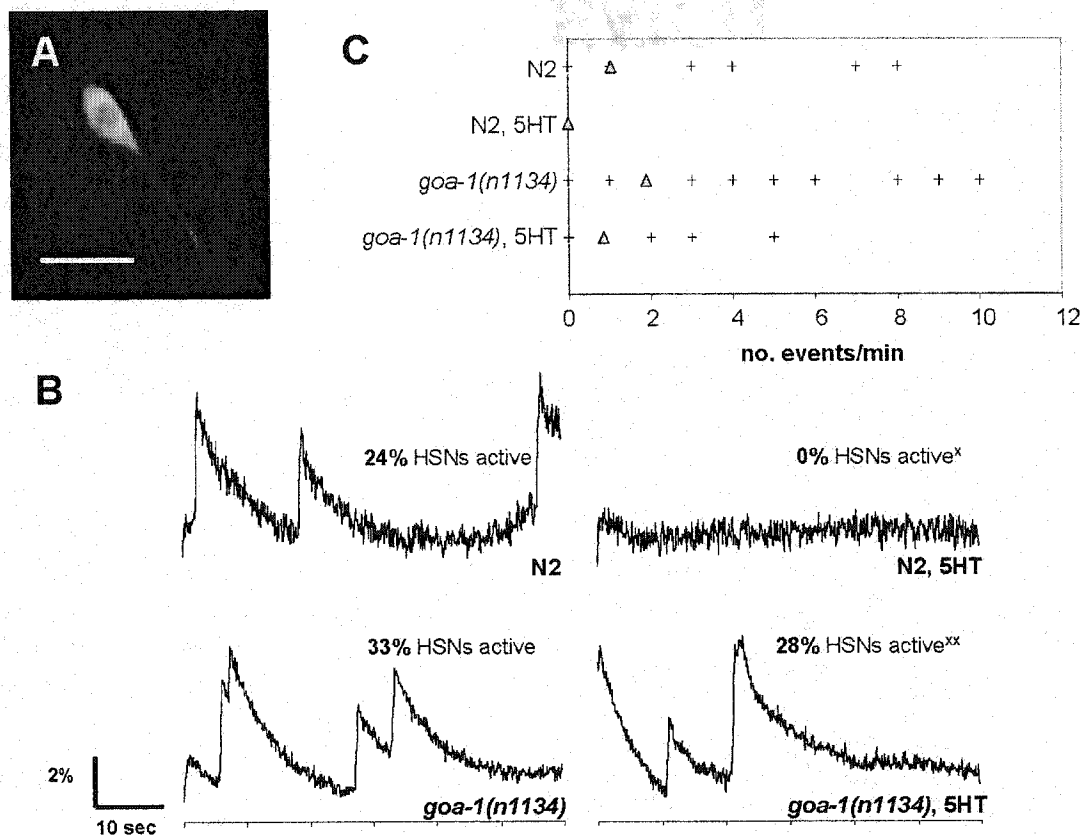


**Figure 2-3. HSN neuronal imaging with *cat-1::iY2C2.1* and neuronal silencing by serotonin.** (A) Sample field of view showing an HSN motorneuron with *cat-1::iY2C2.1*. Axons were variably fluorescent. VCs 4/5 also express *cat-1::iY2C2.1*, but are in a different focal plane. Scale bar is 10  $\mu$ m. (B) Representative HSN traces are shown for N2 and *goa-1(n1134)*, on/off 1.3 mM 5HT, with % total traces with activity as noted. Although N2 and *goa-1(n1134)* HSNs were indistinguishable in the baseline condition, on 1.3 mM 5HT, only N2 HSNs were silenced.  $P=0.018$  (N2 v. N2 5HT),  $P=0.0081$  (N2 5HT v. *n1134* 5HT), chi-square (active/inactive) before Bonferroni correction.  $n=25$  (N2 HSN), 27 (*n1134* HSN), 29 (N2 HSN, 5HT), 25 (*n1134* HSN, 5HT).

## **SUPPLEMENTAL MATERIALS AND METHODS**

### **Optical imaging of calcium transients**

Optical recordings were made from first-day adult hermaphrodite worms immobilized with cyanoacrylate glue on 2% agarose pads dissolved in Dent's saline (140 mM NaCl, 6 mM KCl, 3 mM CaCl<sub>2</sub>, 1 mM MgCl<sub>2</sub>, 5 mM HEPES, pH 7.4) (Avery et al, 1995). Gluing was dorsal-side only for vulval muscle studies, but required ventrally, too, in neuronal imaging—to more completely eliminate motion artifact. For drug experiments, serotonin (5-hydroxytryptamine, creatinine sulfate complex, Sigma) was added to the 2% agarose solutions along with a small volume of concentrated NaOH to correct for acidification caused by mM quantities of 5HT. We utilized a W-VIEW beam splitter (Hamamatsu Photonics) to facilitate simultaneous monitoring of cyan and yellow intensities with a single CCD camera (Hamamatsu Orca ER II). In later experiments, this was substituted with a Dual-View Micro Imager (Optical Insights) and Hamamatsu Orca ER CCD camera. Images were acquired with Metavue 4.6 (Universal Imaging) for 1 minute at approximately 32-40 Hz (10.8 Hz for neuronal recordings; 20.8 Hz for long N2 vulval muscle recordings) with 4x4 binning (8x8 for long N2 recordings). Filter/dichroic pairs were: excitation, 420/40; excitation dichroic 455; CFP emission, 480/30; emission dichroic 505; YFP emission, 535/30 (Chroma). Total yellow intensity (Y) of a given muscle was divided by its total cyan intensity (C) to obtain a Y/C ratio that could be used to follow changes in intracellular Ca<sup>2+</sup>.

### **Automated extraction of fluorescence intensity values from image series**

Image stack analysis for this study was performed much as in Kerr et al (2000), but a menu-driven Javascript program (Jmalyze) replaced the command line Windows 95 program of the earlier study. A single measurement box/ellipse was defined for each vulval muscle (or neuron), and total yellow and cyan intensities within that region calculated by summing the 12-bit values for each contained pixel prior to ratioing.

### **Image data processing**

XY-coordinates and total intensity values recorded by Jmalyze to log files were then cut and pasted into templates created in Microsoft Excel to facilitate the evaluation of each ratio trace. Each trace was examined for the presence or absence of  $\text{Ca}^{2+}$  activity and also for possible motion or tracking artifacts or problems with excessive noise.

When enough traces were collected for a given strain and treatment condition, batches of collected imaging data were then processed through MATLAB scripts to normalize baselines and correct for photobleaching--and to identify peaks corresponding to  $\text{Ca}^{2+}$  transients.

### **Peak-finding**

Peak identification was sometimes hampered by excessive noise, and so, while most peak data was retained for calculation of timing and parameters, traces with greater than 10% underdetection of peaks identifiable by eye were discarded. Traces with a few false positives could be manually adjusted in MATLAB to discard individual peak-finds deemed unreasonable by eye. Peak identification for vulval muscle and neuronal traces was performed with different MATLAB scripts. In the former case,

priority was placed on accurately detecting peaks and avoiding false-positives in the baseline or in noise. A best linear least squares fit was performed for every point in the trace with a nested set of 12 windows of exponentially increasing length (ranging in scale from 5 to 227 frames; each scale larger than the previous by approximately  $\sqrt{2}$ ) centered around the same point. The largest windows were used to estimate linearity of a trace by comparing the goodness of a linear least squares fit for their lengths to the expected goodness of fit given the measured noise. When the probability,  $p_1$ , that the error in fit was due to noise dropped below 0.0001, the trace segment in question was declared “nonlinear at scale K.” The largest scale (K) where there was still linearity would then set the scale for further analysis at 5 scales below (K-5)—or the shortest scale, by default, if all scales were nonlinear. A peak was defined as at least 3 consecutive data points where the slope of the fit at that scale was at least  $2.0\% \text{ sec}^{-1}$  (unless the smallest scale was being used, in which case this was  $1.5\% \text{ sec}^{-1}$ ). A peak was extended to include the entire (unbroken) stretch of slopes meeting the given criterion. Failure to detect activity at the K-5<sup>th</sup> scale would prompt the script to increase the scale by one and repeat this process. Finally, nearby peaks (within 11 frames) were merged into a single peak if they overlapped or if the data points between them fit either peak with a probability,  $p_2$ , of at least  $10^{-6}$ . If neither peak accounted for the intervening data points with this stringency, the peaks were kept separate.

Neuronal peak-finding prioritized accurate start- and endpoint determination and began by introducing to traces a Gaussian blur of 3 frames width. A peak was

detected every time 5 out of 5 frames had a slope of at least  $1.0\% \text{ sec}^{-1}$ . To ensure limits were properly chosen, each peak was extended right and left until less stringent slope criteria were failed (still  $1.0\% \text{ sec}^{-1}$  to the left, but  $0\% \text{ sec}^{-1}$  to the right) on a smaller window of a single frame. Further peak refinement was effected by shrinking a peak to the smallest interval where the endpoints were within expected deviation of noise (1 standard deviation) from the maximum and minimum values detected in the interval defined in the previous step.

### **Statistical analysis of recording parameters**

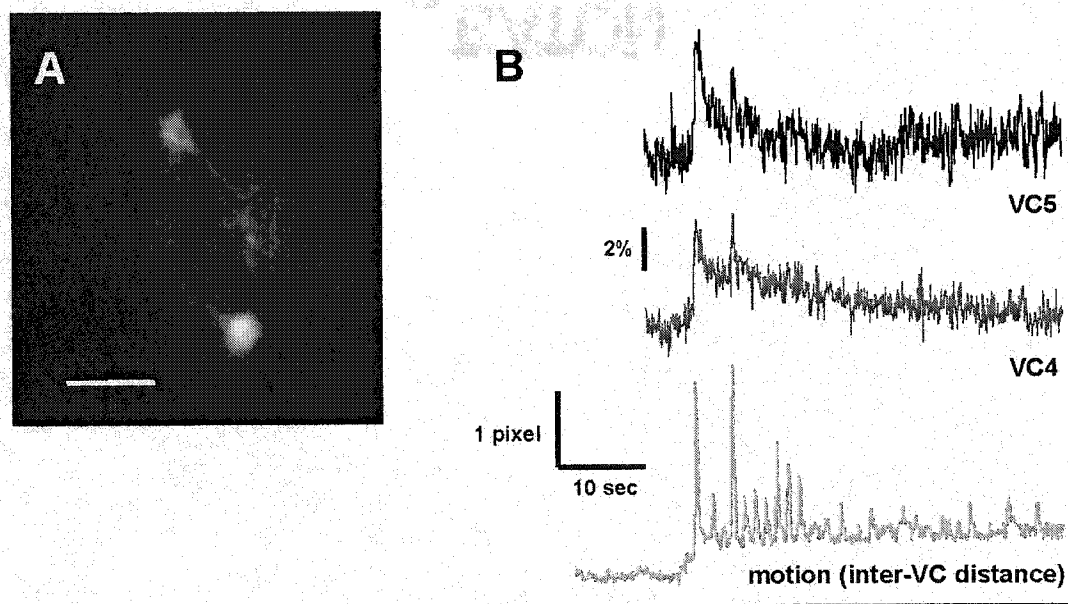
Statistical comparisons of mean event frequency (vulval muscle  $\text{Ca}^{2+}$  transients) were performed with the Kolmogorov-Smirnov test for goodness of fit (and Bonferroni correction for multiple comparisons, where appropriate). Statistical analysis for our correlation studies is described in the Supplemental Table 2-1 legend.



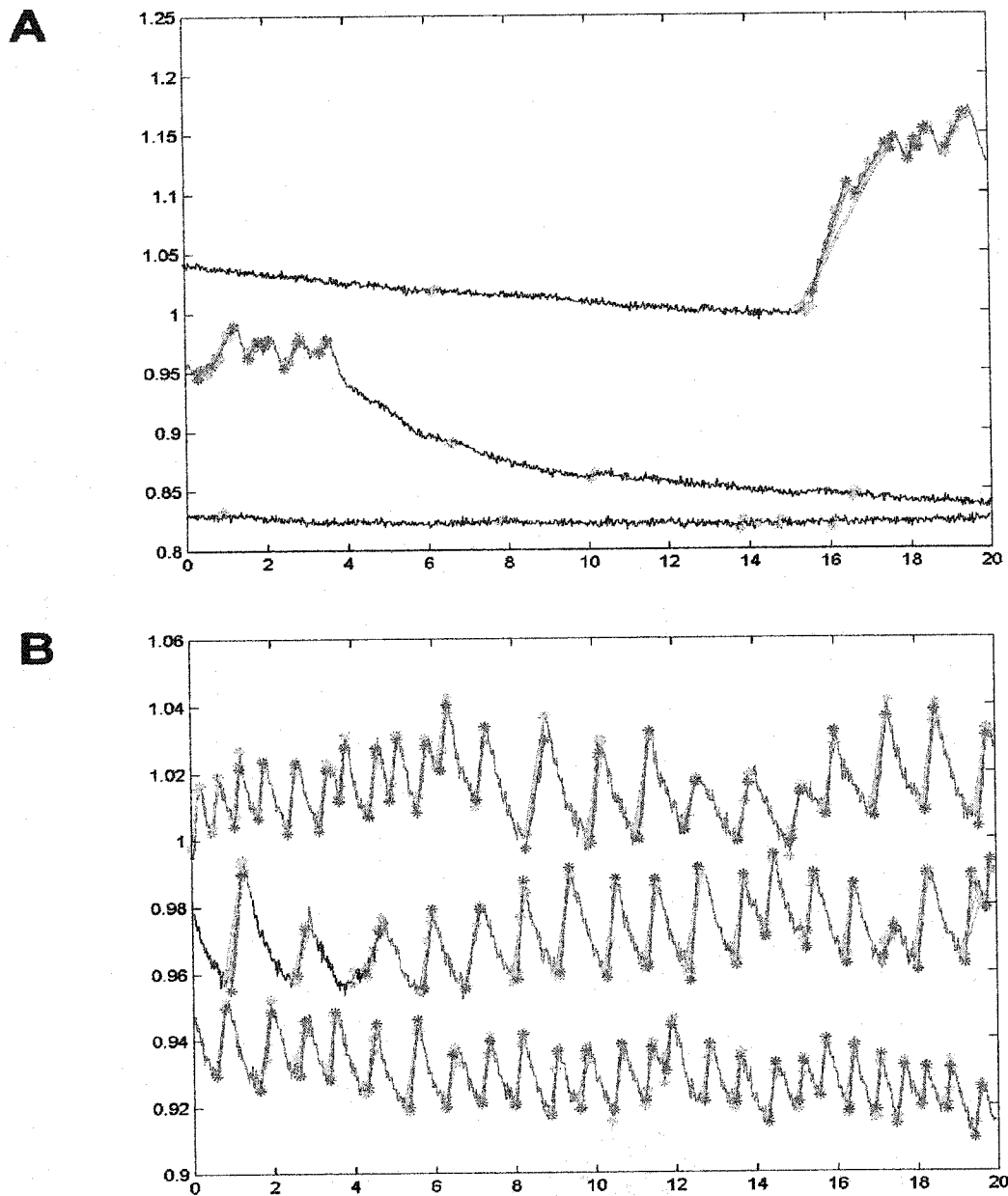
**Supplemental Table 2-1. Measures of inter-muscle correlation of activity.**

*Fraction events correlated* is a mean weighted by the number of events in each muscle/trace pair. P-values / quantiles were calculated for each pair after assigning random times to the same number of events in each trace to produce a distribution of correlation values arrived at by chance (Monte Carlo estimation, 500 trials). The number of traces assigned P-values <0.05 is listed in the second column. An overall probability of having x number of traces with P<0.05 out of y total number of traces (within a given data group) was calculated with the Fisher exact test. Chi-square analysis comparing vm1 v. vm2 for fraction of traces with significant correlations (P<0.05) did not reveal a significant baseline difference. Because the two vulval muscle types occupy different focal planes, we did not study correlation of activity in any vm1-vm2 muscle pairs. While the larger number of events in 5HT traces increased the possibility of correlation by chance, individual pair P-values were computed taking this into account. Chi-square analysis (for inter-group comparisons) indicated that the higher fraction of significantly correlated pairs (over the total number of muscle pairs imaged) with 5HT was significantly different from baseline—suggesting the possibility that 5HT enhances electrical coupling between vulval muscles by a mechanism beyond a simple increase in number of Ca<sup>2+</sup> events. <sup>xx</sup>P<0.01 (chi-square) for overall proportion of 5HT muscle pairs significantly correlated (31/35) v. overall proportion of no drug muscle pairs significantly correlated (23/38).

	<b>Fraction events correlated</b>	<b>no. trace pairs P&lt;0.05</b>	<b>total no. trace pairs</b>	<b>overall P</b>
<b>N2, no drug</b>	0.232	23	38	8.54 x 10 <sup>-21</sup>
<b>vm1</b>	0.204	7	12	
<b>vm2</b>	0.260	12	18	
<b>N2, 1.3 mM 5HT</b>	0.547	<sup>xx</sup> 31	35	1.99 x 10 <sup>-36</sup>
<b>vm1</b>	0.555	17	17	
<b>vm2</b>	0.551	8	12	



**Supplemental Figure 2-1. VC neuronal imaging with *cat-1::iY2C2.1*.** (A) Sample field of view showing a pair of VC motorneurons with *cat-1::iY2C2.1*. Axons were variably fluorescent. Scale bar is 10  $\mu$ m. (B) Ratio traces from simultaneously recorded VC4 and VC5 motorneurons demonstrating correlated activity and consequent vulval muscle twitching (as inferred by coincident increases in inter-VC4, 5 distance).



**Supplemental Figure 2-2. Peak-detection.** (A) One-minute N2 [no drug] vulval muscle ratio trace staggered as 3 segments across 20-second x-axis. Ratio trace is in black, with areas of higher activity in blue. Green represents detection of possible activity, with final peak-find calls along the rising phase of  $\text{Ca}^{2+}$  transients in red, delimited by asterisked endpoints. Y-axis represents fractional ratio changes (i.e., 0.05 = 5% increase in Y/C ratio). (B) One minute N2 [serotonin] vulval muscle ratio trace. Note that a more extended length of the ratio trace is denoted as a run of higher activity in blue.

## CHAPTER III. CHARACTERIZATION OF THE *ser-4(ok512)* SEROTONIN RECEPTOR GENE DELETION MUTANT

### ABSTRACT

SER-4 is the only known candidate 5HT receptor expressed in *C. elegans* vulval muscle. With the recent generation of a 1.3 Kb deletion allele in the *ser-4* gene, we had a unique opportunity to test existing hypotheses about serotonergic modulation of egg-laying and its purported ability to induce ‘active states’ in vulval muscle. This chapter expands on previous information about the expression pattern of *ser-4*, presents data on the nature of the molecular lesion in the *ser-4(ok512)* deletion allele, and outlines the efforts we made to characterize *ok512*’s behavior and vulval muscle physiology. To our surprise, there was no discernible phenotype in this worm. Possible explanations are discussed below.

### INTRODUCTION

Mammals carry 7 major classes of 5HT receptors, numbered 5HT<sub>1</sub> through 5HT<sub>7</sub>. Most of these classes appear to modulate cAMP—either through G<sub>i/o</sub> (5HT<sub>1</sub>) or G<sub>s</sub> (5HT<sub>4,6,7</sub>). The 5HT<sub>2</sub> class is believed to stimulate phospholipase C through G<sub>q</sub>, and, finally, 5HT<sub>3</sub> receptors are the lone ionotropic serotonin receptor class. (The 5HT<sub>5</sub> class is less well-studied; it has yet to be demonstrated to have endogenous expression in any organism.) (Hoyer et al, 2002)

The *C. elegans* genome contains over 1,000 representatives of the G-protein coupled receptor (GPCR) family (~5% of all genes in the worm genome). 10% of these have clear relationships to GPCRs in other organisms, but the remaining 90% are considered “orphan” receptors. Most of the GPCRs probably serve a chemosensory function, with much of the remainder activated by neurotransmitters (Bargmann, 1998). Several years ago, the Avery lab conducted a survey (Niacaris, 2001) to comprehensively identify all of the worm’s candidate 5HT receptors. Their list included open-reading frames (ORFs) for 11 metabotropic receptors—and two ionotropic receptors (not including MOD-1) with weak homology to the mammalian 5HT<sub>3</sub> class. The 11 GPCR candidates were identified by a BLAST (best local alignment search tool) search and the highest-scoring ORF for similarity to known vertebrate or invertebrate 5HT GPCRs was the gene, *ser-4* (ORF Y22D7AR.13 on Wormbase; formerly ORF Y119D3.a and referred to in previous literature as *5HT-Ce*, *ce5HT1*). While some of these 11 GPCRs have since been found to actually be activated by other biogenic amines (one, for example, is a tyramine/octopamine receptor), Niacaris (2001) mentions three that have been conclusively demonstrated to be serotonin-activated in heterologous expression systems: *ser-1* (Hamdan et al, 1999), M03F4.3 (an ORF designation), and *ser-4* (Olde and McCombie, 1997).

Niacaris (2001) successfully created *gfp* lines for 10 of the 11 GPCR candidates (most by overlap extension PCR), and, of these, only *ser-4::gfp* was reported to be expressed in the egg-laying system—specifically, in the vulval muscles. A few years earlier, Olde and McCombie (1997) had isolated *ser-4* cDNA from an

embryonic stage *C. elegans* cDNA library and found it to encode a predicted protein of 445 amino acids. Its highest amino acid homology was to the *Drosophila* 5HT-dro2a receptor (63% similarity), though it was also highly homologous to mammalian 5HT<sub>1</sub> receptors—especially in its transmembrane domain sequences. SER-4 was heterologously expressed in a mammalian kidney cell line, and a series of serotonergic agonists and antagonists tested for ability to compete-off radiolabeled [<sup>125</sup>I]LSD. The resulting pharmacologic profile for SER-4 was deemed typical for other characterized invertebrate 5HT receptors. (Notably, dopamine and octopamine were biologically inactive in the [<sup>125</sup>I]LSD competition studies.) Consistent with its 5HT<sub>1</sub> homology, in cell culture, SER-4 was able to attenuate forskolin-stimulated cAMP production by 60% upon activation by 5HT. Olde and McCombie also pointed out that SER-4's short C-terminus and basic residue (Arg) at position 434 are both hallmarks of a receptor that acts to inhibit adenylate cyclase.

Together with my advisor, I have examined the Avery lab's *ser-4::gfp* line to refine our knowledge of its exact expression pattern. Last Fall, when the *C. elegans* Knockout Consortium informed us of its isolation of a deletion allele in *ser-4* (a deletion I had requested), I obtained this mutant worm (*ser-4(ok512)*) and determined the exact breakpoints of the deletion to reveal the extent of the molecular lesion in the mutant SER-4 protein. This information, as well as data from experiments I have performed showing that *ok512* has no discernible behavioral or physiologic phenotype, is presented below.

## RESULTS

### ***ser-4* is expressed in the vm2 vulval muscles**

The Avery lab very kindly provided us with the array line, *adEx1616[ser-4::gfp]*, which fuses 4 Kb upstream regulatory sequence and approximately 28% of *ser-4*'s coding region to *gfp*. (Despite a 1.3 Kb cDNA clone, *ser-4*'s genomic region is characterized by unusually large introns for a worm gene—and spans approximately 10 Kb.) We confirmed the Avery lab's report of *ser-4* expression in the vulval muscles—and found, further, that this expression was specific to the vm2 vulval muscles (which, unlike the vm1s, receive most of the motor innervation to the egg-laying muscles). There was no HSN or VC expression of *ser-4::gfp*, but there was substantial head neuron expression as well as some signal in the tail region. Because this neuronal expression was faint, we elected to  $\gamma$ -irradiate *adEx1616* to integrate the *gfp* array into a chromosomal site (as outlined in Mello and Fire, 1995), and, in this way, obtained *ljIs3*. This integration succeeded in substantially increasing *gfp* signal intensity.

We were able to assign with confidence identities to the following *ser-4* expressing neurons: (in the head) AVFL,R, M1, RIM; (in the tail) PVT. Additionally, there was *gfp* expression in the excretory gland cell. With less confidence, we thought an additional neuronal pair in the head (anterior to the nerve ring and sending processes to the nose) might represent RIPL,R; in the tail, we made additional tentative assignments of DVA and DVC. The identification of signal in AVFL,R was of particular interest to us, since this neuron was implicated by a previous study in our

lab in the serotonin-mediated “velocity spike” behavior observed frequently just before egg-laying events. (Hardaker et al, 2001; see, also, “Locomotion and its modulation” section in Chapter I.)

At the time of writing, we learned that the Avery and Hobert labs had submitted a paper publishing a partial description of the *ser-4::gfp* expression pattern (Tsalik et al, in press). Their list of identified cells was: RIB, RIS, “a pharyngeal neuron,” “a pair of sublateral inter- or motoneurons,” a “pair of neurons in the retrovesicular ganglion,” PVT, and “DVA or DVC.” Our assignment of RIM probably corresponds to the same neuron Tsalik et al called RIB, and what we labeled the AVFs probably are the same neurons they identified within the retrovesicular ganglion (which the AVFs are a part of).

#### ***ser-4(ok512)* is an in-frame 1337 bp deletion**

Using a nested PCR primer set (sequences provided by the K.O. Consortium—see *Materials and Methods*) that produces a 3126 bp product in N2 (wild-type) worms, we were able to confirm that *ser-4(ok512)* was indeed deleted within this region by ~1.3 Kb. We decided to sequence this region to identify deletion breakpoints and assess the likelihood of residual protein function. The deletion endpoints (inclusive) are: 1,726,583 – 1,725,247 (following the numbering convention for the (+)-strand of Chromosome III used by Wormbase; *ser-4* is encoded on the (-)-strand). This juxtaposes 5’-...GGA AAA TTA TAT TTT TTT-3’ with 5’-CTA CAA AAA TTC AAA TGT ATA...-3’, and corresponds to a loss of 1337 bp. These breakpoints occur



in the introns flanking Exon 5 (there are 8 exons total) and, thus, eliminate it entirely (Figure 3-1A). Contained with Exon 5 is TM5, the entire 28-aa 5<sup>th</sup> transmembrane domain (of 7 putative transmembrane domains), along with 4 aa of extracellular loop 2 sequence (pre-TM5) and 53 aa of intracellular loop 3 (post-TM5). The loss of 86 amino acids corresponds to 19.3% of the original 445-aa protein (Figure 3-1B). Curiously, the positioning of the deletion endpoints allows the sequence to remain in-frame after the deletion. This leaves the fates of TM6 and TM7 uncertain since it is not possible to predict from sequence alone whether these transmembrane domains now insert into the membrane in an orientation opposite from normal or even insert at all. Issues of this sort are explored in a recent paper on membrane topology (Goder et al, 1999), and, indeed, consultations with Martin Spiess (an authority in this field) suggested yet another possibility: that of mixed populations of mis-inserted receptor protein.

There is significant potential for disruption of receptor function in *ok512*. The loss of so much sequence after TM5 would almost certainly disrupt the third intracellular loop of the receptor—which, in addition to the second loop (undisturbed in *ok512*)—is a domain implicated in G-protein-coupling within the 5HT<sub>1</sub> receptor family (Albert and Tiberi, 2001).

#### ***ser-4(ok512)* does not have a discernible phenotype**

*ser-4(ok512)* worms were not morphologically Egl. 6-hour video recordings of egg-laying on seeded regular NGM plates did not reveal lengthened long intervals in

*ser-4* relative to N2, either (Figure 3-2). Because a modulatory defect (as might be expected from deficient 5HT signalling) might not produce an overt phenotype on its own, we next examined egg-laying behavior in response to 5HT. Exogenous 5HT normally stimulates egg-laying in dose-dependent fashion in the inhibitory hypertonic salt solution, M9 (Trent et al, 1983). Figure 3-3 shows 5HT dose-response curves for N2 along with *ser-4(ok512)*. To our surprise, there was no difference in the response profiles.

We next tested 5HT egg-laying response on NGM plates with 7.5 mM 5HT—since occasionally there are differences in behavioral responses to drugs between liquid M9 and solid NGM assay conditions (Waggoner et al, 2000a). Inter-event interval peaks were at 96.4 and 94.2 seconds for *ser-4(ok512)* and N2, respectively—essentially identical (Figure 3-4).

At this point, despite the lack of any behavioral differences in egg-laying, we proceeded with  $Ca^{2+}$ -imaging using cameleon (see Chapter II). *ser-4(ok512)* vulval muscle  $Ca^{2+}$  physiology was remarkably like that of N2 (using the N2 data in Chapter II as reference). In the absence of drug, *ok512* averaged 6.92 events/min—and event frequency increased to 24.33 events/min on 1.3 mM 5HT (Table 3-1 and Figure 3-5). The change in *ok512* between the no drug and 5HT conditions was statistically significant ( $P=0.0132$ , Kolmogorov-Smirnov test). Ablation of the HSN and VC neurons in *ok512* (see Chapter II, *Materials and Methods*) did not appear to dampen 5HT response, either, ruling-out the possibility that the lack of a phenotype in intact animals was due to a second 5HT response system in the neurons (Table 3-1).

The lack of a behavioral or physiologic phenotype for egg-laying may be a reflection of SER-4's dispensability. Alternatively, the *ok512* lesion may not have sufficiently compromised SER-4 receptor function to significantly affect worms. Because of *ser-4::gfp* expression in the AVF neurons, we wondered if we might find a mutant phenotype (and, thus, demonstrate *ok512* is a significant lesion) in the examination of a second behavior: the characteristic 2-fold "velocity spike" in average locomotion rate which Hardaker et al (2001) found to precede egg-laying events. Hardaker et al documented that this phenomenon is 5HT-dependent—and that it can be disrupted by laser ablation of the AVF neurons, which receive serotonergic synaptic input from the HSN egg-laying motoneurons. (Loss of the HSNs also eliminates the "velocity spike" before egg-laying events.) Position data was acquired from the same video recordings used to obtain regular NGM tracking parameters in Figure 3-2, and used to generate data on velocity and its relation to egg-laying events as described in Hardaker et al (2001). As the averaged traces of normalized velocity show (Figure 3-6), once again, *ser-4(ok512)* was indistinguishable from N2.

#### **Overexpression constructs and the introduction of a putative gain-of-function mutation (W367R) do not produce hyperactive egg-laying**

Since we were still unable to distinguish between whether SER-4 serves a non-critical role in egg-laying and 5HT response—or if the *ok512* mutation does not eliminate SER-4 function—the next logical approach was to examine the consequences of overexpressing the wild-type receptor and, also, of introducing a

gain-of-function (GOF) construct. If there was a potentiation of 5HT response—or if the presence of SER-4 GOF mimicked 5HT treatment—this would have provided some evidence to support that SER-4 is an important 5HT receptor in egg-laying physiology and behavior.

A vulval muscle-specific enhancer (*nde-box*) was used to express cDNA encoding wild-type SER-4 and, separately, SER-4(W367R). The W367R amino acid substitution is a putative GOF mutation inspired by Pauwels et al (1999), in which recombinant human 5HT<sub>1B</sub> receptor was altered in a “BBXXB” motif (B=basic residue, X=non-basic residue) to generate constitutive receptor activity. This BBXXB motif is located in the C-terminal portion of the third intracellular loop, and altering the second X was hypothesized to unmask a G<sub>α</sub>-interaction point on the receptor. In Pauwels et al, “BBXXB” corresponded to Arg-Lys-Ala-Thr<sup>313</sup>-Lys, and the best enhancement of [<sup>35</sup>S]GTPγS binding appeared to occur with a Thr→Arg substitution. The resulting level of constitutive activity was found to be approximately 30% of the maximal level inducible by 5HT treatment (of Chinese Hamster Ovary cells expressing human 5HT<sub>1B</sub> receptor). The corresponding site in SER-4 was identified to be Arg-Lys-Ala-Trp<sup>367</sup>-Arg, and, hence, the tryptophan residue was altered to arginine.

*ljEx24* and *ljEx25* are 2 independently created extrachromosomal array lines of *nde-box::ser-4XS* (*XS* = overexpressing) and *ljEx52* is an array line of *nde-box::ser-4(W367R)*. *ljEx52* was also gamma-irradiated to create a chromosomally integrated line, *ljIs9* (subsequently backcrossed to N2 5x).

Surprisingly, in a liquid M9 + 5HT (5 mg/ml) behavioral assay, none of the overexpresser or putative GOF lines responded at even a wild-type level for number of eggs laid (Figure 3-7). Imaging of vulval muscle  $\text{Ca}^{2+}$  transients revealed, however, baseline levels of activity in *ljEx24*, *ljEx25*, and in the incomplete *ljEx52* and *ljIs9* datasets comparable with wild-type (compare Table 3-1 with Table 2-1). Imaging experiments have yet to be performed for these lines under 5HT treatment.

## DISCUSSION

Unfortunately, the data presented here do not allow an unambiguous determination of the reasons for the lack of a discernible behavioral or physiologic phenotype for *ser-4(ok512)*. One possibility is that the *ok512* lesion, despite its impressive span, might still permit significant residual function. While it might seem unlikely that a GPCR disrupted at its fifth transmembrane domain (and possibly downstream) could still function properly, there is a growing literature on GPCR heterodimerization, and perhaps SER-4 is only required for 5HT-binding in a receptor heterodimer pair, leaving its hypothetical GPCR partner responsible for then transducing ligand-binding into G-protein activation. The functional significance of GPCR dimerization—as well as the domains that mediate this process—are still not fully understood. But there is precedent for 5HT receptor heterodimerization (Xie et al, 1999), and the receptor domains critical for this process can vary for members of different GPCR subfamilies—sometimes involving cysteine-cysteine disulfide linkages in extracellular domains or even hydrophobic interactions between

transmembrane domains (Lee et al, 2000). The presence of a second serotonin receptor—even outside the context of receptor dimerization—may also be responsible for the lack of a *ser-4* phenotype. A second serotonin receptor would likely have to act in the vulval muscles, since ablation of the HSN and VC neurons did not compromise *ser-4* physiologic 5HT response in the vulval muscles. While none of the other candidate receptor *gfp* lines Niacaris (2001) examined expressed in the vulval muscles, *gfp* worms can give incomplete expression patterns if regulatory elements (sometimes in introns or very distal) are not all included. There was one candidate that a *gfp* line could not be created for because of technical difficulties in amplification from the genomic DNA (ORF C52B11.3). Additionally, the list of candidates may not be complete.

We also considered the possibility that SER-4 might actually be a receptor for another biogenic amine. Dopamine and octopamine, for example, are known to inhibit egg-laying behavior. Yet, as discussed in the introduction, neither neurotransmitter was found to be biologically active in the heterologous expression study of Olde and McCombie (1997). Further, if signalling through these inhibitory pathways had been amplified by overexpression of SER-4 (or the introduction of a GOF SER-4 receptor), we would have expected to see depressed vulval muscle  $Ca^{2+}$  activity in the baseline (no drug) condition. While there was not sufficient imaging data collected for the *XS* and putative *GOF* lines under 5HT treatment, the implication of the liquid M9 + 5HT behavioral assay—and the limited numbers for *ljIs9* worms imaged with 5HT—is that the depression of activity is induced by 5HT treatment.

The M9 assay results were completely unexpected and difficult to interpret. SER-4 might be an *inhibitory* 5HT receptor—while a second and, as yet, unaccounted 5HT receptor is responsible for the stimulatory effects of 5HT on egg-laying. Alternatively, perhaps flooding the vulval muscles with SER-4 overactivates 5HT signalling and results in desensitization. Or, returning to the receptor heterodimerization paradigm, perhaps SER-4 overexpression is having an unfavorable effect on receptor complex stoichiometry, and leading to the assembly of inactive homodimers (where heterodimers are, instead, necessary for signal transduction). A final possibility is that a flaw is present in the cDNA construct that was used to create these lines.

Returning to the central issue of the lack of a phenotype in *ok512*, one option would be to employ RNAi (RNA interference) to effect a “knock-down” phenotype. RNAi (reviewed in Grishok et al, 2002) is the use of double-stranded RNA to produce posttranscriptional gene silencing. Two popular approaches in the worm are RNAi by feeding and RNAi by soaking. Before the availability of *ser-4(ok512)*, however, both protocols were actually attempted (data not shown) and deemed unsuccessful because of a failure to extinguish *ser-4::gfp* in *ljIs3*. There was an expectation that this GFP signal should have been extinguished since the RNAi used was the length of the entire *ser-4* cDNA and since the *gfp* fusion contained 28% of *ser-4*'s coding sequence. (Of note, anti-*gfp* RNAi also failed to extinguish vulval muscle GFP signal.) Positive controls, meanwhile, like RNAi for *unc-22* (“twitcher” phenotype), successfully induced the expected phenotype. RNAi by a transgenic “loopback” construct (as

demonstrated in Tavernarakis et al, 2000) was under consideration last year—when we then received word of the generation of *ser-4(ok512)*. “Loopback” RNAi would certainly be a strategy worth considering again, now. Screening for further (and more convincing) deletion alleles in *ser-4* is also probably warranted.

Finally, if there are redundant 5HT signalling systems, the failure to observe a phenotype in *ok512*—or, in Chapter II, to identify a specific G $\alpha$  protein critical for vulval muscle 5HT response—might be a reflection of a requirement that two G-protein pathways need to be simultaneously disabled. Appendix A lists imaging data for some of the combinatorial possibilities that were created using *ser-4(ok512)* and available G $\alpha$  mutants.

## **MATERIALS AND METHODS**

### **Nested PCR Primers**

Primers for detection of *ser-4(ok512)* were designed by the *C. elegans* Knockout Consortium and were: 5'-AAT TAT CGG ATT TAG GGC CG-3' & 5'-ATG GAA CGG AGC ATT ATT CG-3' (outside); 5'-CAA CAC GCA ACG AAT GTA CC-3' & 5'-TGT GAA GTT TGG GAG GCT TT-3' (inside). These primers were used to follow the *ok512* deletion through 5 backcrosses to N2, prior to behavioral or physiologic characterization of this allele.

### **Creation of *ser-4XS* and GOF (W367R) lines**



*nde-box::ser-4* was created by first excising YC2.3 (cameleon) from a pre-existing *nde-box::YC2.3* plasmid (18x *nde-box* vulval muscle enhancer from *ceh-24* and pSAK-10 backbone originally from A. Fire lab; YC2.3 from Roger Tsien) with an EcoRI-EcoRI cut. The religated backbone was then cut with KpnI-SacI to allow the insertion of a 1.6 Kb KpnI-SacI fragment (carrying *ser-4* cDNA) liberated from pBICER (pBluescript with *ser-4* cDNA, gift of Bjorn Olde). W367R was introduced into *ser-4* cDNA with the following PCR primer pair: 5'-CGC TAG CCG TCG CTG ACT TGT TGG TC-3' & 5'-TGC TAG CGT TCT CCG CGC TTT CCG CTC-3' (underlined residue denotes critical nucleotide change), which amplified an 834 bp NheI-NheI fragment that could then be swapped into *ser-4* cDNA. Both the wild-type and W367R *nde-box::ser-4* constructs were injected into N2 worms at 100 ng/μl (along with *myo-2::YC2.1*, 80 ng/μl, as co-injection marker) by the micro-injection protocol of Mello and Fire (1995).

## ACKNOWLEDGEMENTS

The author wishes to thank the Avery and Hobert labs for sharing unpublished information on *ser-4::gfp* expression with us; Tim Niacaris (Avery lab), in particular, for sending us *adEx1616*; Martin Spiess for consultations on determinants of membrane protein topology and possible fates for TMs 6 and 7 in *ok512* SER-4 protein; Bjorn Olde for his generous gift of pBICER (*ser-4* cDNA); and the *C. elegans* Gene Knockout Project at Oklahoma Medical Research Foundation (member of the

International *C. elegans* Gene Knockout Consortium) for generating and providing *ser-4(ok512)*. DNA sequencing was performed by the DNA Sequencing Shared Resource, UCSD Cancer Center, which is funded in part by NCI Cancer Center Support Grant # 2 P30 CA23100-18.

**Table 3-1. Frequency of vulval muscle Ca<sup>2+</sup> events (events/min) in *ser-4* deletion mutant and in lines expected to have enhanced SER-4 function.** *ser-4(ok512)* worms did not appear under-active in the baseline condition, and still responded well to 5HT treatment. Imaging experiments of neuronally ablated *ser-4(ok512)* were discontinued when it became clear that 5HT response was still intact. Overexpression of wild-type SER-4 (*ser-4XS*) did not produce any noticeable hyperactivity. Data collection for *ser-4(W367R)* (putative GOF) was not completed at the time of writing, but, from the small sample numbers examined so far, the data do not suggest any enhancement of baseline vulval muscle Ca<sup>2+</sup> activity. In agreement with M9 behavioral assay results (Figure 3-6), however, *ljIs9* response to 5HT appears poor. (Statistical tests not performed on *ser-4(W367R)* data because of insufficient sample size.) Listed in bold are mean event frequencies  $\pm$  SEM, (n) = number of animals/recordings used in calculation of mean frequency of events. \*P<0.05, Kolmogorov-Smirnov test (*ok512*, no drug v. 1.3 mM 5HT).

	no drug	1.3 mM 5HT
<i>ser-4(ok512)</i>	<b>6.92</b> $\pm$ 1.24 (36)	<b>24.33*</b> $\pm$ 4.80 (33)
<i>ser-4(ok512)</i> HSN <sup>-</sup> , VC <sup>-</sup>		<b>32.00</b> $\pm$ 10.54 (5)
<i>nde-box::ser-4XS</i>		
<i>ljEx24</i>	<b>7.52</b> $\pm$ 1.43 (31)	
<i>ljEx25</i>	<b>8.41</b> $\pm$ 1.78 (41)	
<i>nde-box::ser-4(W367R)</i>		
<i>ljEx52</i>	<b>4.60</b> $\pm$ 1.51 (10)	
<i>ljIs9</i>	<b>6.67</b> $\pm$ 1.23 (6)	<b>0.57</b> $\pm$ 1.51 (7)

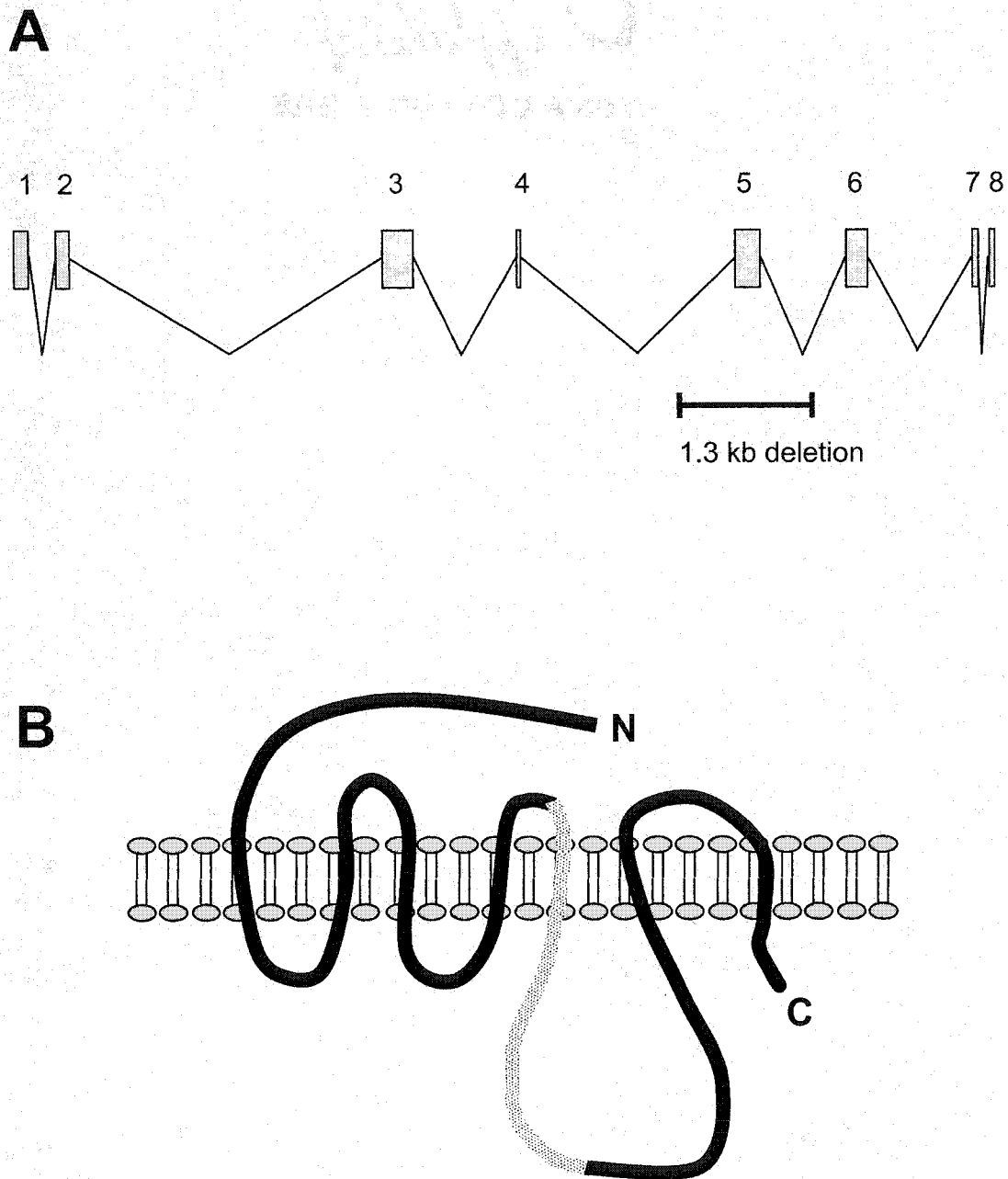


**Figure 3-1. Span of the *ok512* deletion and relation to SER-4 topology.** (A) *ser-4(ok512)* is an in-frame 1337 bp deletion eliminating Exon 5 (*ser-4* genomic region, 9910 bp). (B) 86 amino acids (including all of TM5) are eliminated in *ok512*. The effects on TM6 and TM7 topology remain unclear. (Note that wild-type SER-4 has a short C-terminal tail of only 20 aa, a feature common to 5HT<sub>1</sub> receptors.)

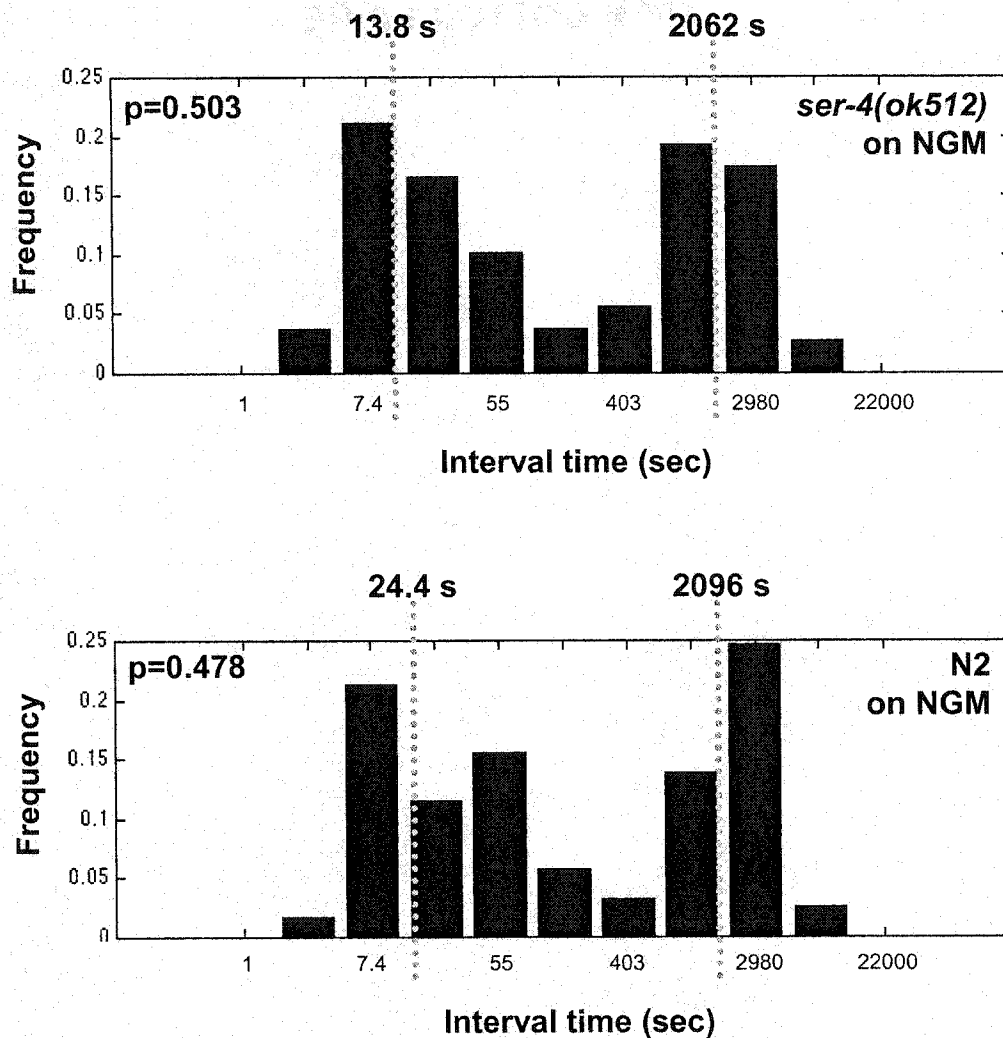


**Figure 3-2. Baseline egg-laying parameters for *ser-4(ok512)* do not reveal longer inactive phases.** Worms lay their eggs in clusters ('active' phases), spaced from each other by 'inactive' phases (Waggoner et al, 1998). The distribution of time intervals between egg-laying events can be described by linked Poisson processes creating a bimodal log distribution. The first peak represents 'short intervals' (intra-cluster events); the second peak 'long intervals' (inter-cluster events). P represents the probability of staying in the active phase after an egg-laying event. Worms deficient in 5HT signalling tend to have lengthened long intervals, but there appears to be no distinction here between *ser-4(ok512)* and N2. (See Figure 3-6 caption for numbers of worms, intervals.)

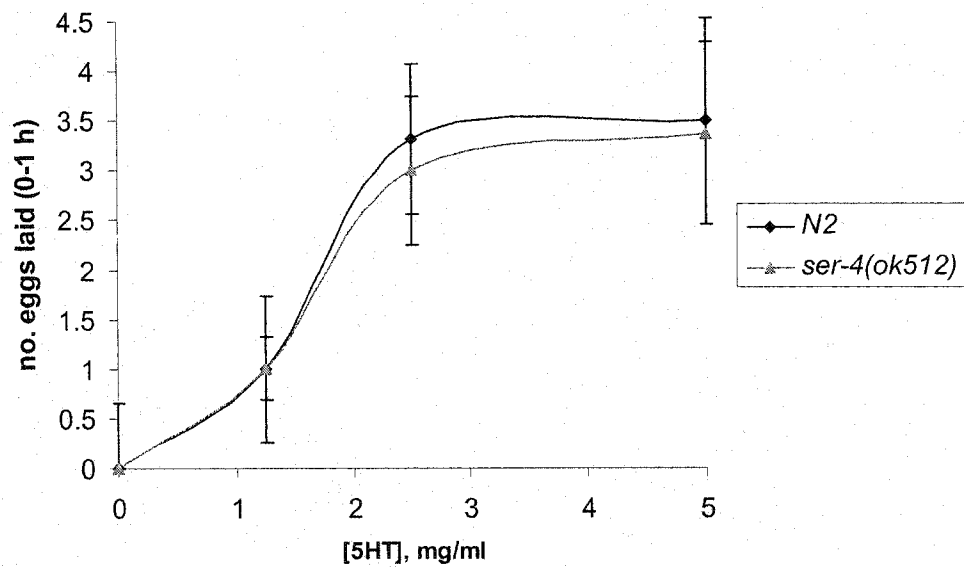


**Figure 3-3. 5HT dose-response curves in M9 buffer.** Worms were placed in individual microtiter wells containing 0, 1.25, 2.5, or 5 mg/ml 5HT (1 mg/ml = 2.5 mM), and allowed to lay eggs for 1 hour. *ser-4(ok512)*'s 5HT egg-laying response profile did not appear different from N2's.  $n=16$  for each data point. Error bars represent SEM.

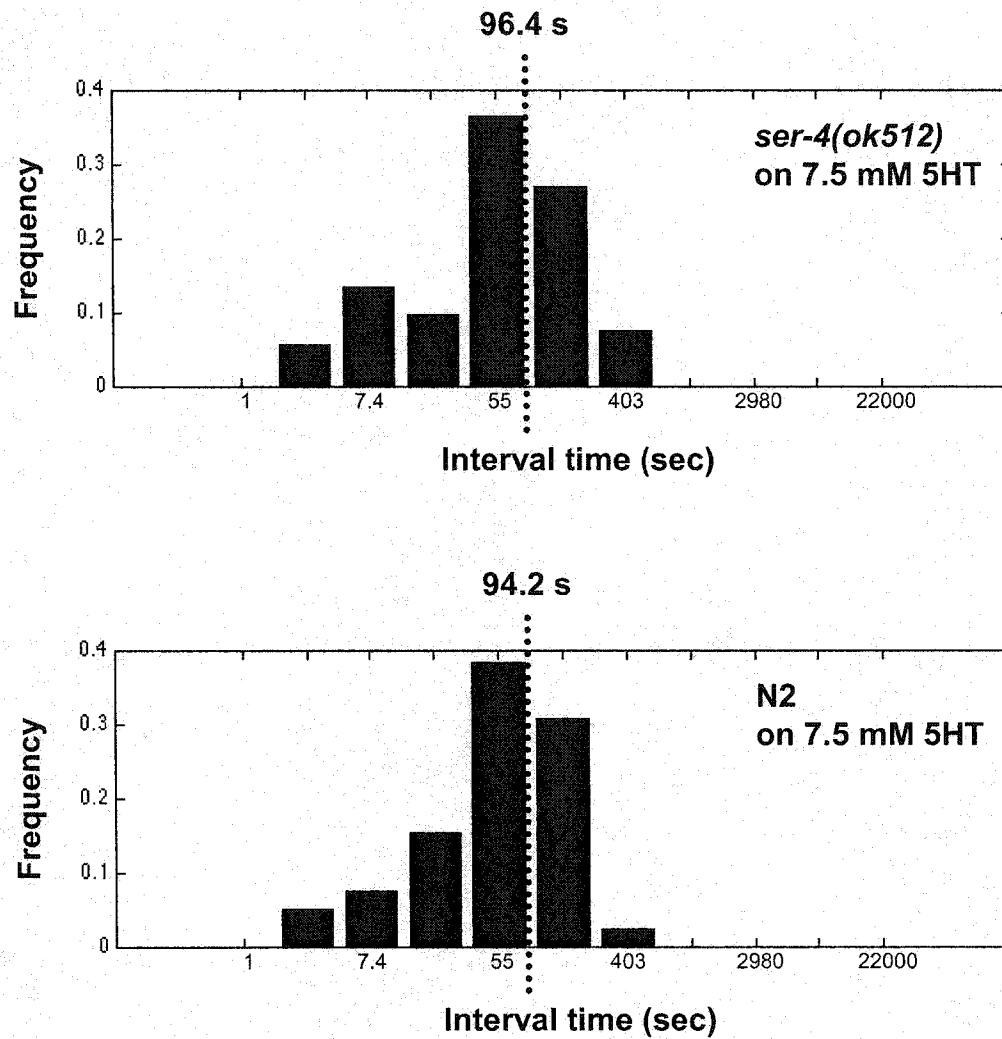


**Figure 3-4. 5HT egg-laying responses on NGM + 7.5 mM 5HT plates.** Worms were recorded for 20 minutes, and egg-laying times noted. A single exponential time-constant (dashed line) was estimated as described in Waggoner et al (2000b). The summary inter-event interval for *ser-4(ok512)* is not significantly different from that for N2. n=8 worms (52 intervals) for *ser-4(ok512)*, n=5 worms (39 intervals) for N2.

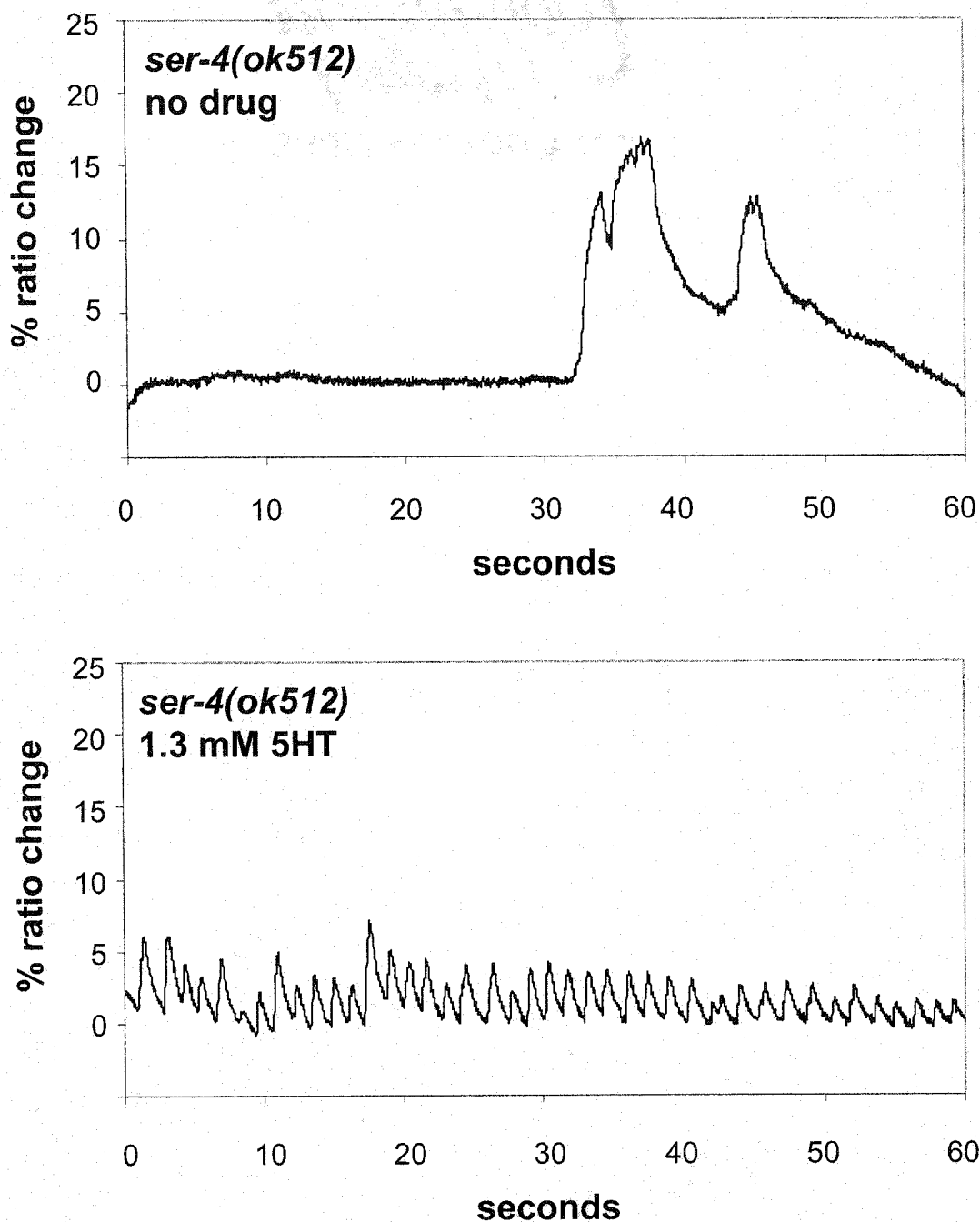


**Figure 3-5.** *ser-4(ok512)* vulval muscle  $\text{Ca}^{2+}$  traces. As with N2 (see Chapter II), *ser-4(ok512)* vulval muscles displayed a clustered pattern of  $\text{Ca}^{2+}$  transients in the absence of drug ( $6.92 \text{ events/min} \pm 1.24$ ) ( $n=36$  worms). On 1.3 mM 5HT, *ser-4(ok512)* vulval muscles displayed the characteristic pattern change to a more regular train of  $\text{Ca}^{2+}$  events ( $*24.33 \text{ events/min} \pm 4.80$ ) ( $n=33$  worms).  $*P=0.0132$  (5HT v. no drug), Kolmogorov-Smirnov test.



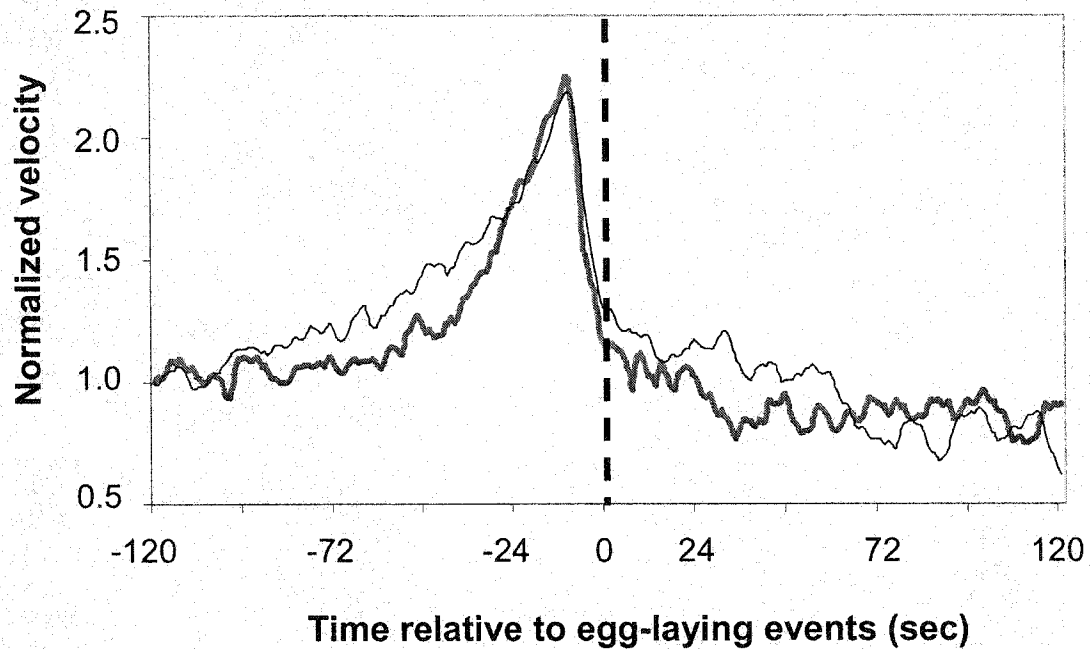


**Figure 3-6. Behavioral evaluation of *ser-4(ok512)* for “velocity spike” in locomotion before egg-laying events.** Plotted for *ser-4(ok512)* (in bold) and N2 (thin trace) is normalized velocity as a function of time, relative to egg-laying events (time zero). Just as Hardaker et al (2001) observed, average N2 velocity “spikes” approximately 15 seconds before an egg is laid. Apparently, so does *ser-4(ok512)* velocity. (*ok512*: 6 worms, 34.5 hours, 109 egg events. N2: 7 worms, 40.8 hours, 122 egg events.)

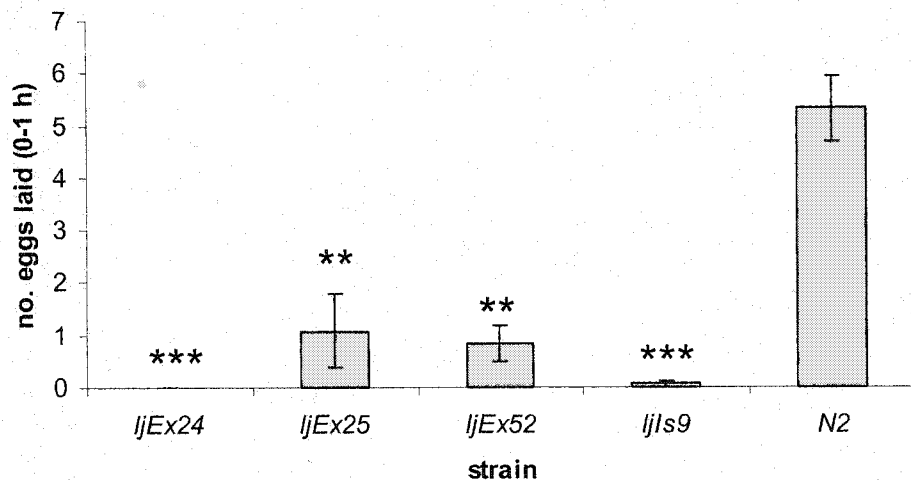


**Figure 3-7. *ser-4XS* and *ser-4(W367R)* do not respond to 5HT in an M9 behavioral assay.** Worms were incubated for 1 hour in M9 saline + 5 mg/ml 5HT (12.9 mM). *ljEx24* and *ljEx25* are independent array lines of *nde-box::ser-4XS*; *ljEx52* and *ljIs9* represent *nde-box::ser-4(W367R)* (array and integrated line, respectively). A third *ser-4XS* array line, along with 5 other independent integrants of *ser-4(W367R)*, displayed identical phenotypes (data not shown).  $P=4.3 \times 10^{-10}$ , Kruskal-Wallis test. \*\* $P < 0.01$ , \*\*\* $P < 0.001$ , post-hoc Dunn's test (single control).  $n=12$  worms for *ljEx24*, *ljEx25*, *ljEx52*;  $n=17$  worms for *ljIs9*;  $n=48$  worms for N2.

## APPENDIX A. OTHER CALCIUM-IMAGING RESULTS

This section summarizes vulval muscle  $\text{Ca}^{2+}$ -imaging work which was not included in the manuscript submitted for publication (Chapter II). Data is presented in Table A-1 and special remarks and commentary are provided below.

### Other $\text{Ca}^{2+}$ channels

The L-type voltage-gated  $\text{Ca}^{2+}$  channel  $\alpha_1$ -subunit, EGL-19, was found to be necessary for vulval muscle  $\text{Ca}^{2+}$  activity in Chapter II. There is no published literature to suggest that any other voltage-gated  $\text{Ca}^{2+}$  channels (VGCCs) are expressed in the egg-laying muscles, but mutants in the only other known VGCC genes, *unc-2* and *cca-1*, were examined with cameleon and found to respond well to 5HT.

The UNC-68 ryanodine receptor was not found to be important for baseline or 5HT-induced vulval muscle activity (Chapter II), and so we examined a hypomorph in the other known worm intracellular  $\text{Ca}^{2+}$  channel gene, *itr-1* ( $\text{IP}_3$  receptor). To date, there is no evidence *itr-1* is expressed in the vulval muscles, though a *gfp* expression study did locate *itr-1* expression in vulval epithelium (Gower et al, 2001). *itr-1(sa73)* worms appear to be good 5HT-responders when examined with cameleon in the vulval muscles.

*egl-30*

*egl-30(n686)*'s 5HT response is clearly compromised, but it is difficult to ascribe EGL-30 the role of 5HT's vulval muscle G-protein effector given that past studies have never detected vulval muscle expression for either *egl-30* or *egl-8*, the gene which encodes its downstream phospholipase C effector (Lackner et al, 1999; Miller et al, 1999). The *n686* mutation is only a hypomorph (true nulls are lethal—Brundage et al, 1996), and so it is difficult to unambiguously interpret the trend toward a residual 5HT response. Ablation of the egg-laying neurons in the *n686* background and testing on/off 5HT did not help to further clarify our understanding. (It should be noted that the neuronally ablated *n686* Ca<sup>2+</sup> event frequency mean presented below was skewed by one unusually active worm recording.)

### Mini-genes

Recognizing that null mutations in two of the known G<sub>α</sub> subunits expressed in the vulval muscles (among other tissues) are developmentally lethal, I employed the “mini-gene” approach of Gilchrist et al (1999) in the hope of creating a tissue-specific loss-of-function for *gsa-1* (G<sub>s</sub>) and *gpa-16* (distantly G<sub>i/o</sub>-like G<sub>α</sub> subunit gene). Under the control of the vulval muscle-specific *nde-box* enhancer, I expressed short nucleotide stretches for the C-terminal 11 amino acids of *gsa-1* or *gpa-16*, which, if successful, might have been expected to disrupt endogenous G-protein function in dominant-negative fashion. *ljEx60* and *61* [*nde-box::mini-gsa-1*] and *ljEx71* [*nde-box::mini-gpa-16*] did not seem to produce a 5HT-resistance phenotype, however, and it was not clear whether this was because GSA-1 and GPA-16 function are not critical

to vulval muscle 5HT response or if the plasmids carrying these mini-genes were improperly constructed. I have recently made *nde-box* mini-gene constructs, also, for  $G_o$  (*goa-1*) and  $G_q$  (*egl-30*), and, while these have not yet been imaged, there was no visually discernible behavioral phenotype. (Neuronal disruption of GOA-1 and EGL-30 function may additionally be necessary, however, to re-capitulate the known egg-laying phenotypes in mutants for these G-proteins.) Before proceeding further with these mini-gene lines, it may be prudent to generate better positive-controls demonstrating that mini-genes can, in principle, be utilized in worms as effectively as they were in mammalian cell culture with the study of Gilchrist et al (1999). A pan-neuronal *mini-goa-1* or *mini-egl-30* might be created to examine whether or not the resulting transgenic worms display the well-characterized locomotion phenotypes of *goa-1* or *egl-30* mutants. They could also be crossed into the lines I have already generated with vulval muscle *mini-goa-1* or *mini-egl-30* to address any uncertainties about the additive effects of different tissue contributions.

### **Vulval muscle-expression of Pertussis toxin**

Another approach to disrupting GPA-16 function was through the use of *nde-box*-expressed Pertussis toxin (PTX). PTX disables G-proteins of the  $G_{i/o}$  class by ADP-ribosylation of a cysteine residue 4 amino acids from the C-terminus of the target  $G\alpha$  protein (Avigan et al, 1992). Vulval muscle  $G_{i/o}$ -like G proteins were of particular interest because of SER-4's 5HT<sub>1</sub>-like homology (Chapter III). As it turns out, among the possible  $G_{i/o}$ -like G proteins in vulval muscle (GOA-1, GPA-7, and

GPA-16), only GOA-1 and GPA-16 carry the critical cysteine residue at their C-terminus (C-G-L-Y). There were fewer concerns here (than in my mini-gene series) about the proper construction of my DNA vector, since I used a subclone for the catalytic subunit of PTX derived from the same plasmid Darby et al (2001) used for heat-shock-induced PTX expression in *C. elegans*. (Darby et al successfully recapitulated the *goa-1* locomotion phenotype using this plasmid.) While the expectation would have been that vulval muscle PTX would have disabled both GOA-1 and GPA-16, this was not necessarily an undesired outcome since it would, at least, address the possible confound of functional redundancy. A look at *ljEx57*'s numbers in Table A-1 suggests a modest elevation of baseline vulval muscle  $Ca^{2+}$  activity (consistent with conclusions drawn in Chapter II about an inhibitory role for GOA-1 in vulval muscle)—and a still intact ability to respond to 5HT.

This result calls into question whether SER-4 is truly  $G_{i/o}$ -coupled or, alternatively, whether SER-4 (assuming it does act through GOA-1 and/or GPA-16) serves a stimulatory role with respect to egg-laying.

### **Double mutant combinations**

I also considered the possibility that the inability to unambiguously identify a vulval muscle 5HT effector G-protein (and, perhaps, even, the lack of a SER-4 phenotype) might stem from the existence of redundant signalling pathways. To that end, double mutant combinations were generated between different G-proteins and also between *ser-4(ok512)* and individual G-protein mutants—and analyzed with

cameleon. Not all combinatorial possibilities were explored (including combinations with muscle-specific mini-genes), but the ones examined and reported in Table A-1 did not uncover any synthetic 5HT-response phenotypes.

### **Levamisole experiments**

A subset of the data in Table A-1 examines vulval muscle  $\text{Ca}^{2+}$  responses to the cholinergic agonist, levamisole. The egg-laying system is believed to carry at least two types of nicotinic receptors (nAChRs)—one sensitive to levamisole and the other(s), not. (Kim et al, 2001). The levamisole receptor is believed to be present both neuronally and in the vulval muscles. Levamisole, like 5HT, appears to increase the frequency of vulval muscle  $\text{Ca}^{2+}$  events in N2. Despite this similarity, the morphology of levamisole-produced events retains a more “clustered” appearance than that of 5HT-stimulated event trains (Figure A-1A). Occasionally, however, levamisole and 5HT traces can be indistinguishable (data not shown).

*unc-38* (nAChR  $\alpha$ -subunit) mutants are levamisole-resistant, and tissue-specific rescue strains provided by Rene Garcia (formerly of the Sternberg lab) allowed us to explore an unresolved question about the differential contributions of neuronal v. muscle levamisole receptors to egg-laying behavior. Kim et al (2001) have previously shown that a muscle-specific rescue of *unc-29* (encoding a non- $\alpha$  subunit of the levamisole receptor) in an *unc-29* mutant background is sufficient, under some conditions, to restore levamisole-induced stimulation of egg-laying. Table A-1 seems

to suggest a larger contribution by muscle UNC-38 (compared to neuronal UNC-38) in egg-laying response to levamisole.

### **5-carboxamidotryptamine (5-CT)**

The vulval muscle 5HT effect described in Chapter II was not extensively examined from a pharmacologic perspective (with a series of serotonin analogs and antagonists) since the generation of the *ser-4(ok512)* deletion carried with it the (now-unfulfilled) prospect that we would have the unambiguous identification of the 5HT receptor responsible for the phenomenon we observed. In limited studies of the analog, 5-carboxamidotryptamine (5-CT) (not included in Table A-1), however, I was able to obtain vulval muscle  $Ca^{2+}$  traces much like those observed in experiments with 5HT (Figure A-1B). This would seem to suggest that the event trains described previously are indeed serotonergic in origin and not the product of non-specific cross-reactivity to a receptor for another biogenic amine.

## **MATERIALS AND METHODS**

### **Generation of mini-gene lines**

Primers for mini-gene inserts were as follows: 5'-C AAAA ATG GGA CAA CGC ATT CAT CTA CGA CAG TAC GAG CTT CTA TAA AT G-3' and 5'-AATTC AT TTA TAG AAG CTC GTA CTG TCG TAG ATG AAT GCG TTG TCC CAT TTTT GAGCT-3' for *mini-gsa-1*; 5'-C AAAA ATG GGA CTA CAG CAT AAT CTG AAG



GAG TAC AAC TTG GTG TAA AT G-3' and 5'-AATTC AT TTA CAC CAA GTT GTA CTC CTT CAG ATT ATG CTG TAG TCC CAT TTTT GAGCT-3' for *mini-egl-30*; 5'-C AAAA ATG GGA ATT GCC AAT AAT CTT CGT GGA TGC GGC TTG TAT TAA AT G-3' and 5'-AATTC AT TTA ATA CAA GCC GCA TCC ACG AAG ATT ATT GGC AAT TCC CAT TTTT GAGCT-3' for *mini-goal-1*; and 5'-C AAAA ATG GGA ATT CGA GAT AAC CTC CGC ACG TGC GGG CTC TAC TAA AT G-3' AND 5'-AATTC AT TTA GTA GAG CCC GCA CGT GCG GAG GTT ATC TCG AAT TCC CAT TTTT GAGCT -3' for *mini-gpa-16*. Oligos were designed to have hanging SacI, EcoRI sticky-ends, and ligated to each other in 1X NEB Buffer 3 by heating in a thermocycler to 95° C for 10 minutes, and then cooling gradually to RT on the thermocycler heating block. Inserts were then ligated into pre-cut *nde-box::YC3.3* (*YC3.3* eliminated by SacI, EcoRI-cuts). After confirmation of correct sequence, constructs were injected into worms (*myo-2::YC2.1*, co-injection marker) as described in Mello et al (1995) to obtain transgenic lines.

### **Generation of *nde-box::PTX***

Using PCR primers: 5'-CG GAG CTC AAAA ATG GAC GAT CCT CCC GCC AC-3' and 5'-CG GAA TTC AT CTA GAA CGA ATA CGC GAT GC-3', an ~700 bp product was amplified from pCBD14 (PTX catalytic subunit gene in pPD49.78 Fire lab backbone, gift of Creg Darby) and inserted into pCRII TA vector (Invitrogen). SacI, EcoRI cuts were then used to liberate *ptx* and swap-out *YC3.3* from *nde-*

*box::YC3.3. nde-box::ptx* was then injected into worms (*myo-2::YC2.1* co-injection marker) to obtain multiple transgenic lines, including *ljEx57*.

#### **ACKNOWLEDGEMENTS**

The author wishes to thank Rene Garcia for *sy576* and partial rescue worms; Ken Miller for generously sending *ce94*, *ce179*, and *mdl1756* worms prior to publication; Jim Thomas for *n693 sa373* and *n500 n1211* worms; Jane Mendel for *syIs18*; and Creg Darby for pCBD14.

**Table A-1. Other vulval muscle Ca<sup>2+</sup>-imaging data** (next 4 pages). Numbers represent mean  $\pm$  SEM, followed by sample size (no. worms) in parentheses. \*levamisole – 25  $\mu$ M, 5HT – 1.3 mM, unless otherwise noted. Additional notes: The 15° C N2, 5HT numbers are included as a control for *cha-1(y226)* which is a temperature-sensitive allele (hypomorph at lower temperatures, lethal at higher temperatures). The *kin-2(ce179)* is a LOF in a PKA regulatory subunit, implying a “GOF” in the now uninhibited catalytic subunit.

	Frequency of events (events/min)		
	<u>no drug</u>	<u>levamisole</u>	<u>5HT</u>
<i>acy-1(pk450)</i> adenylate cyclase	5.87 $\pm$ 1.58 (39)		16.24 $\pm$ 3.17 (46)
<i>acy-1(md1756)</i> GOF	8.89 $\pm$ 1.47 (27)		
<i>cca-1(ad1650)</i> T-type Ca <sup>2+</sup> channel $\alpha_1$ -subunit	5.20 $\pm$ 1.04 (30)		37.18 $\pm$ 8.34 (17)
<i>cha-1(y226)</i> choline acetyl- transferase	7.04 $\pm$ 1.41 (48)		15.86 $\pm$ 3.73 (35)
<i>egl-1(n986)</i> BH3-containing cell death activator (HSN <sup>1</sup> )	7.61 $\pm$ 1.49 (31)	24.53 $\pm$ 3.00 (30)	26.19 $\pm$ 3.81 (26)
<i>egl-2(n693 sa373)</i> LOF (revertant) EAG K <sup>+</sup> channel	7.83 $\pm$ 1.49 (36)		49.26 $\pm$ 4.93 (23)
<i>egl-19(ad695)</i> GOF L-type Ca <sup>2+</sup> channel $\alpha_1$ -subunit	21.57 $\pm$ 3.83 (21)		
<i>egl-19(n582); syEx</i> [ <i>myo-3::egl-19(+)</i> ] muscle rescue	6.47 $\pm$ 1.61 (32)		21.69 $\pm$ 5.44 (26)

<i>egl-19(n2368)</i> <b>GOF</b>	23.53 ± 5.87 (28)	
<i>egl-30(n686)</i> G <sub>q</sub> α	0.8 ± 0.6 (25)	9.44 ± 2.29 (41)
ablated	9.20 ± 7.24 (10)	14.31 ± 4.66 (16)
<i>egl-30(n686)</i> <i>ser-4(ok512)</i> double mutant		16.26 ± 3.48 (34)
<i>goa-1(syIs18)</i> <b>GOF</b> G <sub>o</sub> α, ablated	14.73 ± 4.83 (15)	
<i>goa-1(n1134)</i> <i>egl-30(n686)</i> double mutant	3.44 ± 0.92 (39)	9.71 ± 2.13 (45)
<i>goa-1(n1134)</i> <i>gpa-7(pk610)</i> double mutant		21.31 ± 3.96 (29)
<i>goa-1(n1134)</i> <i>ser-4(ok512)</i> double mutant	16.00 ± 3.14 (19)	17.47 ± 3.14 (36)
<i>goa-1(n1134)</i> <i>tph-1(mg280)</i> double mutant	16.55 ± 1.89 (22)	
<i>gpa-14(pk347)</i> <i>ser-4(ok512)</i> double mutant		23.50 ± 3.73 (32)
<i>gsa-1(ce94)</i> <b>GOF</b> G <sub>s</sub> α	14.26 ± 1.84 (38)	
<i>itr-1(sa73)</i> IP <sub>3</sub> receptor	7.05 ± 1.28 (43)	23.10 ± 3.97 (20)
<i>kin-2(ce179)</i> PKA regulatory subunit	6.95 ± 1.47 (37)	

<i>ljEx57[nde-box:: ptx]</i> pertussis toxin	13.83 ± 2.01 (24)	36.22 ± 4.74 (27)
<i>ljEx60[nde-box:: mini-gsa-1]</i> G <sub>s</sub> “mini-gene”		18.86 ± 4.40 (21)
<i>ljEx61[nde-box:: mini-gsa-1]</i> G <sub>s</sub> “mini-gene”	7.00 ± 1.71 (24)	19.31 ± 7.51 (13)
<i>ljEx71[nde-box:: mini-gpa-16]</i> novel G <sub>α</sub> “mini-gene”	2.39 ± 1.05 (18)	23.35 ± 3.90 (20)
<i>mod-5(n3314)</i> serotonin re-uptake transporter	5.88 ± 1.44 (32)	
N2 wildtype		11.06 ± 2.17 (32) (2.5 μM levamisole)
		21.14 ± 4.36 (27)
		39.75 ± 18.38 (4) (400 μM levamisole, 1.3 mM 5HT – drug combination)
		43.04 ± 4.65 (27) (0.13 mM 5HT)
		29.81 ± 5.15 (21) (raised at 15° C)
		29.17 ± 4.80 (35) (12.9 mM 5HT)
ablated	13.07 ± 3.63 (15)	
<i>ser-4(ok512)</i>		32.00 ± 10.55 (5)

ablated

<b><i>tpa-1(k501)</i></b> PKC homolog	10.17 ± 1.53 (29)		35.68 ± 4.48 (28)
<b><i>tph-1(mg280)</i></b> tryptophan hydroxylase	7.00 ± 1.09 (23)	34.73 ± 4.85 (26)	24.89 ± 4.35 (19)
<b><i>unc-2(mu74)</i></b> N,P/Q-type Ca <sup>2+</sup> channel α <sub>1</sub> -subunit	10.29 ± 3.20 (34)		27.80 ± 4.23 (25)
<b><i>unc-38(sy576)</i></b> levamisole nAChR, α-subunit	9.50 ± 1.87 (48)		16.46 ± 3.50 (26)
<b><i>unc-38(sy576); syEx</i></b> <b><i>[myo-3::unc-38(+)]</i></b> muscle rescue	5.87 ± 1.19 (38)	21.50 ± 4.79 (36)	
<b><i>unc-38(sy576); syEx</i></b> <b><i>[unc-119::unc-38(+)]</i></b> neuronal rescue	5.19 ± 1.83 (42)	12.34 ± 3.17 (29)	
<b><i>unc-68(r1158)</i></b> ryanodine receptor		10.89 ± 1.69 (35)	
<b><i>unc-103(n500 n1211)</i></b> LOF (revertant) ERG K <sup>+</sup> channel	8.98 ± 1.37 (46)		23.04 ± 4.45 (24)

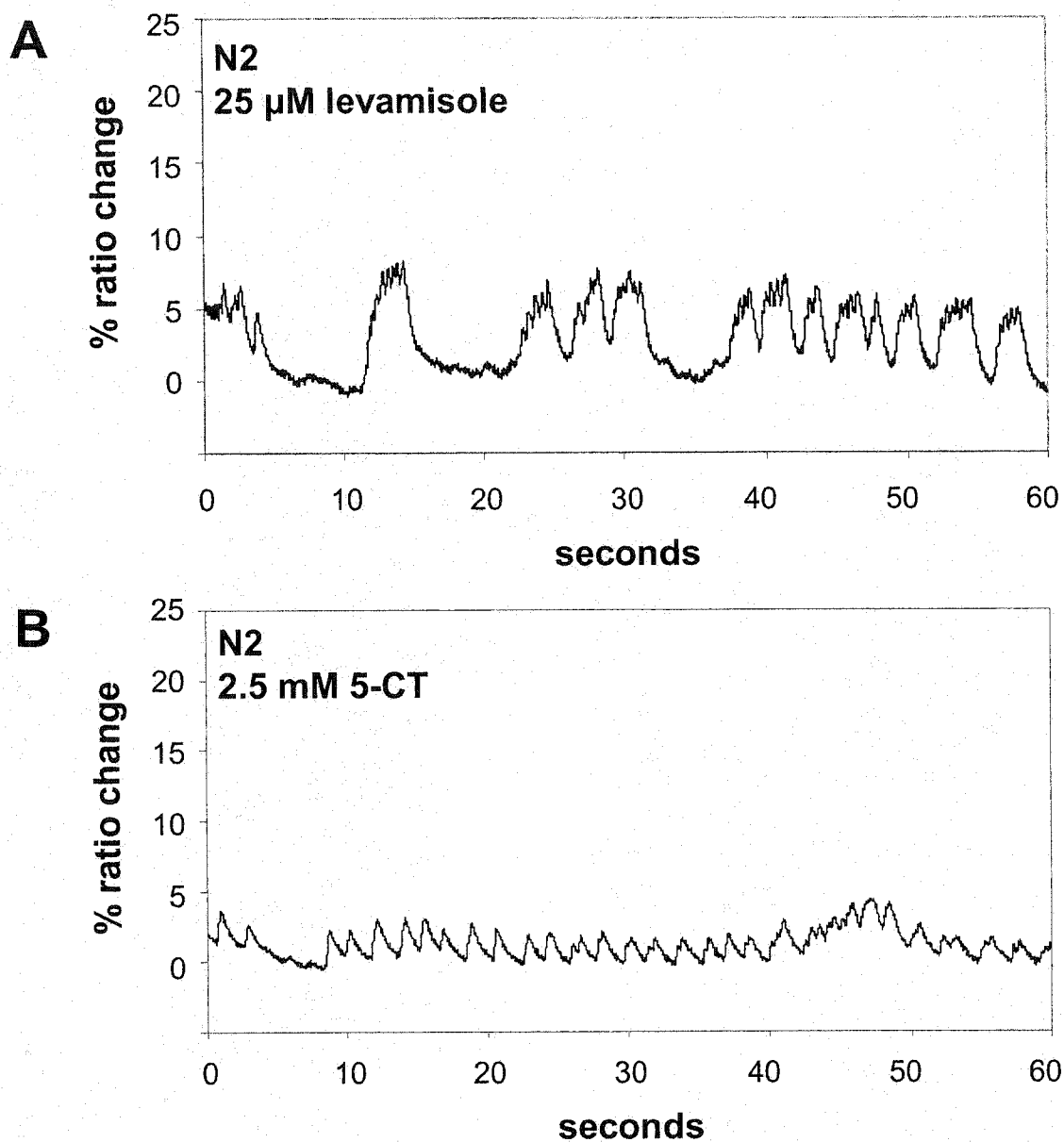


**Figure A-1. Sample levamisole and 5-CT Ca<sup>2+</sup> traces.** (A) Levamisole was observed to increase the frequency of vulval muscle Ca<sup>2+</sup> events while generally retaining a more “clustered” pattern of events. (Sometimes, however, a levamisole trace can look identical to a 5HT event train.) (B) 5-carboxamidotryptamine (5-CT), a serotonin analog, can produce a 5HT-like pattern of Ca<sup>2+</sup> activity.

## APPENDIX B. MICROARRAY STUDIES OF *mod-5(n3314)* AND FLUOXETINE

This section is a record of work performed from Summer 2000 – Summer 2002. It is not organized as a formal chapter because this project was discontinued (on the strong recommendation of my Thesis Committee). Additionally, there were flaws and shortcomings which are discussed below. This Appendix is presented anyway, however, because the issues this experiment series sought to address include questions of great scientific and medical interest—and a future effort could benefit from some of the lessons learned here. The *mod-5(n3314)* mutant, central to the studies described below, was generously provided to us by Rajesh Ranganathan (Horvitz lab, MIT) prior to his 2001 publication. Rajesh Ranganathan (and, later, his successor, Eric Miska) and I entered into a formal collaboration to perform the experiments in this Appendix. All of the work to determine ideal growth conditions and to raise worms for RNA was performed by the author; hybridization of samples to worm gene chips was performed by Kyle Duke (Kim lab, Stanford); and analysis of the data was then performed in parallel by the author and Eric Miska. Correspondence with Eric Miska indicated that both he and I reached the same limited conclusions, with most of the data we generated largely uninformative. The narrative below presents the author's own data analysis—which was made possible by significant computer assistance from Rex Kerr as well as advice from John Wang (Kim lab).



## BACKGROUND

Re-uptake blockers are a class of antidepressants proposed to achieve their clinical effects in people by inhibiting presynaptic norepinephrine and/or serotonin re-uptake transporters, which normally function to terminate transmitter signalling at synapses. It has never adequately been explained, however, why therapeutic relief of depression takes weeks when this particular action of re-uptake blockers occurs within hours of drug administration (Schafer, 1999).

A requirement for some form of adaptation at synapses is a frequently cited possibility, but recent work has also highlighted that there are a myriad of non-classical targets for re-uptake blockers, such as EAG-like K<sup>+</sup>-channels (blocked by imipramine) (Weinshenker et al, 1999) and novel membrane-spanning proteins typified by NRF-6 and NDG-4, identified as non-serotonergic fluoxetine (PROZAC) targets in a screen conducted in worms (Choy et al, 1999).

With the identification of MOD-5 as the *C. elegans* serotonin re-uptake transporter (SERT)—and the isolation of mutant alleles in the gene encoding MOD-5 (Ranganathan et al, 2001), a new approach to tackling this long-standing question became available.

In recent years, scientists have begun to examine gene expression changes on a *genomic* scale utilizing DNA microarray / gene chip technology (Schena et al, 1995; reviewed in Duggan et al, 1999). Gene chips are glass slides printed with thousands of spots, each corresponding to a PCR product, cDNA, or oligonucleotide from an individual gene. Because of the high resolution of special inkjet printers used to spot

this DNA, a representation for an entire genome can be fit within the space of one or two standard glass microscope slides. Two mRNA populations that are being compared to each other can be reverse-transcribed to cDNA, and, in the process, allowed to incorporate fluorescent nucleotides. One population can be tagged, for example, with red Cy3; the other, with green Cy5. Co-hybridization of these competing populations to their target spots then yields an array of fluorescent signals of varying red/green (R/G) relative intensity—which, when merged, can be coded on a pseudocolor scale to reflect in which of the two populations of fluorescently-labeled cDNA each of the thousands of genes being monitored is more enriched. Further, the pseudocolor scale provides a quantitative measure of the magnitude of a particular transcript's relative enrichment.

Beginning a few years ago, Stuart Kim's laboratory (Stanford University) opened-up its gene chip facility for use by the rest of the *C. elegans* community. The Kim lab offered the advantage of having available “full worm genome chips”—17,815 genes (or 94% of the worm genome), each represented by a PCR product. We, therefore, made arrangements to have our samples hybridized at Stanford in April 2001. Specific comparisons were made between RNA from N2 and *mod-5(n3314)* worms (*n3314* is a 1.6 kb deletion in the *mod-5* genomic locus), each on/off fluoxetine. We hoped to understand what baseline transcriptional differences exist between the two genotypes, how similar the effects of chronic fluoxetine in N2 are to the effects of a complete absence of MOD-5 in *n3314* worms, and to identify which

gene expression changes induced by fluoxetine are MOD-5-dependent and which are MOD-5-independent (see Figure B-1).

### **CHOICE OF FLUOXETINE DOSE**

The choice of an appropriate fluoxetine concentration for growing worms was determined with a series of tests summarized in Figure B-2. As a frame of reference, the concentration employed by Choy et al (1999) to identify non-serotonergic fluoxetine targets was 1 mg/ml (~2.89 mM) in liquid M9—while Sawin et al (2000) used 75 µg/ml in solid NGM agar plates in their studies of modulation of worm locomotion. Choy et al previously observed that 1 mg/ml is a largely fatal dose of fluoxetine (25-50% mortality within 1 hour). We also found significant mortality at this concentration in HGM plates (High Growth Medium, see *Materials and Methods*). Additionally, lawns of *E. coli* (OP50), which are normally “seeded” onto plates as a food source for worms, failed to grow until fluoxetine concentration was reduced to 100 µg/ml or lower. Using staged worms, we determined that sub-lethal doses of fluoxetine retarded the developmental growth rates of worms in dose-dependent fashion—with no discernible effect at 10 µg/ml and minor or transient developmental delay at 20 µg/ml (Figure B-2A). A 5HT dose-response test in M9 (Figure B-2B) and corresponding time-course (Figure B-2C) did not reveal statistically significant differences in worms grown for 3 days on fluoxetine concentrations less than 40 µg/ml. This left us in a working range of concentrations where there was no demonstrable phenotype for chronic fluoxetine treatment. In spite of this shortcoming,

we elected to use 20 µg/ml fluoxetine as our drug concentration for our gene chip experiments, since it seemed the highest possible dose for worms without causing deleterious (and presumably non-specific) effects.

Worms were raised for RNA as discussed in *Materials and Methods*.

## CO-HYBRIDIZATIONS

As discussed above and in Figure B-1, there were three *physical co-hybridizations* of particular interest to us: N2 v. *n3314*; N2 v. N2 fluoxetine; and *n3314* v. *n3314* fluoxetine. (A fourth physical co-hybridization that was performed was N2 v. *n3314* fluoxetine, which, in place of *n3314* v. *n3314* fluoxetine, would have made this a true “Type II” set-up—where all groups could be linked to a common control group. The N2 v. *n3314* fluoxetine comparison itself, however, was of no interest to us.)

## RESULTS

Microarray data was normalized as described in *Materials and Methods*, and downloaded in  $\log_2$  ratio format from the Stanford Microarray Database (SMD). Log transformation of microarray data allows symmetry in magnitude of gene expression changes: +2, 0 (no change), and -2 in  $\log_{10}$ , for example—instead of 100, 1 (no change), and 0.01 without log transformation. Where the former would rightly give an arithmetic mean of 0, the latter would yield a highly unrepresentative average of 33.7.

Figure B-3 displays a schematized spreadsheet of our microarray data, which was arranged by genes (rows) along what we called the “intra-experimental” axis, and by experiment / co-hybridization type (columns) along an “inter-experimental” axis. Mean  $\log_2$  R/G ratio and “local” standard deviation (SD) were calculated from the 3 independent repetitions performed for each experiment type (e.g., N2 v. N2 fluoxetine). A “global” SD, tallied by the Kim lab from the ~500 chip experiments that had passed through their lab previously, provided a second available measure of a particular gene’s variability. Because our limited number of repetitions (3) could artificially underestimate a gene’s SD, we followed the advice of the Kim lab and used the higher of the two SDs for each gene in the calculation of its ANOVA test statistic—which we used to call significant differences in mean  $\log_2$  R/G ratio along the inter-experimental axis. In this way, we identified 80 genes (from the over 17,000 arrayed genes) with an ANOVA score with  $P < 0.05$ . (By comparison, the less stringent standard of calculating ANOVA test statistics with local SDs only netted approximately 670 genes with  $P < 0.05$ .)

Within a given experiment type (column), however, it was also important to call which genes had significantly elevated or depressed expression relative to the bulk of genes presumably unaffected by the treatment variable being examined on that chip. As a first approximation, we utilized a test statistic we refer to as  $\delta_{\text{simple}}$  (or ‘simple’ delta), defined in Figure B-4. The larger the absolute value of  $\delta_{\text{simple}}$ , the more likely we presumed a gene’s up- or down-regulation was significant. Plotted in Figure B-4 are the numbers of genes meeting threshold values of  $\delta_{\text{simple}}$  for each of the 3 types of

chip experiment we performed. Notably, a  $\delta_{\text{simple}}$  absolute value of 2 was enough to exclude 96-98% of the ~17,000 genes we monitored.

A refinement of this technique, however, involved the use of a ‘modified’ delta statistic,  $\delta_{\text{modified}}$  or  $d_i$ .  $\delta_{\text{modified}}$  is almost identical to  $\delta_{\text{simple}}$ , but uses an additional term,  $s_o$ , in the denominator to create a more uniform variance of  $\log_2$  R/G ratios over a range of signal intensities (see Figure B-5). This adjustment was made possible by using an Excel add-in known as SAM (Significance Analysis of Microarrays)—which had the added benefit of a function to generate random permutations of the microarray data, enabling calculation of an estimated false positive rate for whatever  $\delta_{\text{modified}}$  cut-offs the user might select (Tusher et al, 2001). Thus, rather than apply a uniform  $\delta_{\text{modified}}$  threshold for all experiment types (e.g.,  $\delta_{\text{modified}} = 2$ ), the authors recommended, instead, a uniform standard for the false positive rate (and whatever individual adjustments of  $\delta_{\text{modified}}$  threshold this might entail). While we found the SAM method to be aesthetically and intellectually more satisfying than the use of a uniform  $\delta_{\text{simple}}$  threshold, 2 of the 3 experiment types we ran (N2N2f and N2m5) generated skewed results—leading to SAM calling only ‘red’ genes (or N2f and m5, respectively). It seemed implausible to us that the biology of fluoxetine treatment or the *mod-5(n3314)* genotype would not lead to statistically significant *down*-regulation of any genes, as well.

Examination of population distributions of  $\log_2$  R/G ratios (data not shown) revealed significant variability in the shapes or skews of different repetitions of the same experiment type. A possible contribution to this problem may have been

something we observed on visual inspection of many of the hybridized chips: There were often broad, systematic color sweeps where red/green bias changed along the length or width of the arrays. John Wang (Kim lab) examined these problems when we raised this issue and concluded that many of our repetitions should probably have been thrown-out and repeated on the basis of these systematic errors which contributed to significant “non-randomness” in the distribution of reds, greens, and yellows (yellows representing no relative difference in gene expression between two co-hybridized samples). As a matter of practice, many labs apparently must routinely throw-out ~60% of their hybridizations over these kinds of problems.

For this reason, the utility of the gene lists generated by our data analysis is probably even further limited. (Gene lists for those spots which met  $\delta_{\text{simple}}$  or SAM thresholds for significance are, therefore, not presented in this report.)

Apart from the issue of determining statistically significant changes, another important component of microarray data analysis is clustering. Cluster analysis is the decomposition and categorization of the data collected on many individual genes into more tractable, “bigger picture” trends to make sense (if possible) of the biology. DNA microarrays are still a relatively new technology, and methods for analyzing and clustering the data they generate are still in their infant stages. Examples of cluster analysis methods include: hierarchical; K-means; and self-organizing maps—and are reviewed in Sherlock (2000).

Using Michael Eisen's Cluster/Treeview software package (Eisen et al, 1998), we performed hierarchical clustering on the list of 80 genes with significant ANOVA scores (across the 3 experimental categories of N2m5, N2N2f, and m5m5f) discussed above. Figure B-6 displays the results of this analysis. To our disappointment, there did not seem to be a prominent cluster representing genes with similar expression changes in N2m5 and N2N2f (and m5m5f unaffected). Such a cluster would have had the potential for identifying key genes relevant to MOD-5-dependent mechanisms of fluoxetine action. Much of the list is of uncertain biological significance and difficult to interpret with the preponderance of "proteins of unknown function," obscure and seemingly irrelevant items, and signalling proteins present without the context of other proteins acting in the same pathway (to bolster the relevance of the pathways to which they belong). An exception to this occurs in the cluster of fluoxetine-activated genes (independent of genotype) which are not similarly upregulated by the *mod-5(n3314)* mutation (relative to N2). This cluster is a solid group of P450 proteins and glucuronide-conjugating enzymes which would be expected to help detoxify and solubilize a foreign agent (in this case, fluoxetine), and facilitate its excretion. That the induction of these genes is specific to the presence of drug, independent of *mod-5* genotype, and uninduced by the presence of the *mod-5(n3314)* mutation—is a logical finding and one that could readily have been predicted.

Expanding our hierarchical clustering to the list of ~670 genes with significant ANOVA scores (using the more permissive "local" SDs only), sizeable clusters of genes with parallel changes in N2m5 and N2N2f (and static in m5m5f) do appear



(data not shown), but are still difficult to interpret because of our incomplete knowledge of the functions of many of the gene products these ORFs encode. It should also be noted that there have been reports (Martie Chalfie, unpublished communication) that the gene annotations used by the Kim lab / SMD sometimes inappropriately make reference to a specific ORF when, in fact, the alpha-numeric designation is actually a reference to PCR primers which do not necessarily amplify the ORF of the same name.

Other cluster analysis methods were also employed (data not shown), but did not yield any additional insights.

A final issue we looked at was drug target validation by correlation analysis of microarray data—in similar fashion to the method employed by Marton et al (1998) in their study of cyclosporin A and FK506 drug action through putative calcineurin and immunophilin targets. Marton et al outlined a series of contingencies (summarized in Figure B-7) to two experimental questions: First, does a mutant (in the gene encoding a drug target of inhibition) display a global expression profile that resembles the profile for drug-treated wild-type? And, second, does the drug-treated mutant resemble drug-treated wild-type? These questions are answered by calculating a correlation coefficient,  $\rho$ , using a list of genes in which the log R/G ratio for each gene is significantly regulated (with a 95% confidence interval) for at least one of the two chip experiments being compared. We had at our disposal lists of called genes (within-chip, or intra-experimental axis) using either the  $\delta_{\text{simple}}$  threshold or SAM

analysis. While our inclination would have been to use the SAM-generated lists, because of the problems discussed above with excessive “redward” skew, we performed our correlation analyses, instead, with the  $\delta_{\text{simple}}$  threshold-generated lists.

As Figure B-7 shows, rho was an impressive 0.84 between N2 fluoxetine and *mod-5(n3314)* (both with respect to N2). This seemed to indicate that pharmacologic and genetic ablations of MOD-5 produced like global expression profiles, as might be expected if the principal action of fluoxetine is inhibition of MOD-5 function. Yet, when we next examined the correlation of significantly regulated genes in both genetic backgrounds with fluoxetine treatment (each normalized to their respective genetic background, untreated), we made the unexpected finding of another high correlation coefficient (0.77). This represented a fourth contingency (Figure B-7) which was not encountered in the Marton et al paper.

Rather than serve to validate or invalidate MOD-5 as a fluoxetine target, our analysis yielded an outcome which is difficult to interpret. It may be that using genes called by  $\delta_{\text{simple}}$  thresholds was not a sufficiently stringent criterion for identifying significantly regulated genes. Alternatively, the excellent correlations in both plots may suggest that the numbers of MOD-5-dependent and MOD-5-independent gene expression changes are both sizeable. An important consideration here, however, is how much of what we are seeing—in this particular analysis, but, also, in all of the other preceding analyses—is a “bulk” effect of gene expression changes in tissues that are largely irrelevant to the issues of our concern, but tissues which, nevertheless, are better represented because they possess greater mass than serotonergic neurons or the

excitable tissues which receive their input from serotonergic sources. In a microarray study of touch neuron development, for example, Zhang et al (2002) found that they were unable to confirm well-established controls or even identify differences in RNA from whole animals with/without touch neurons (which number 6 out of roughly 3,000 nuclei in an adult worm).

Methods have been developed in recent years to facilitate isolation of RNA from specific cells or tissues (rather than from whole worm) for global expression profiling. These include fluorescence-activated cell sorting (FACS) (Zhang et al, 2002) and “mRNA tagging” using tissue-specific promoters to drive the expression of epitope-tagged poly-A binding proteins which can then allow immuno-precipitation of mRNA from a specific tissue or subset of cells (Roy et al, 2002). In the context of this particular project, poly-A binding protein should probably be expressed from regulatory elements derived from *tph-1* (tryptophan hydroxylase) or *mod-5* (SERT) to facilitate isolation of RNA from pre-synaptic serotonergic neurons. With that said, there are reasons (Ji-Ying Sze and Rajesh Ranganathan, personal communication) why both of these pre-synaptic markers would pose difficulties, and so a different gene might actually be more ideal. Post-synaptic RNA might be isolated by a similar strategy, except with regulatory elements derived from genes for specific 5HT receptors. It should be noted that the “mRNA tagging” technique may have a significant lower bound for minimum tissue representation (as a % of whole worm)—in which case FACS may have to be the method of choice.

## DISCUSSION AND UNFINISHED WORK

There were several flaws and shortcomings in the way this work was carried-out. It begins with the lack of a chronic behavioral or physiologic phenotype for fluoxetine-treated worms with which we might have then validated microarray-identified candidate genes by RNAi or gene knock-out. Part of the problem is that the fluoxetine dose we used had to be sufficiently lowered to avoid the non-specific effect we noted on developmental rate. In retrospect, even 20  $\mu\text{g/ml}$  may have been too high—with closer to 10  $\mu\text{g/ml}$ , perhaps, a more ideal dose. Another issue in the search for a chronic worm phenotype is the short generation time of a worm: Worms give rise to progeny by the third day of life (at 22° C), precluding longer timepoints since staging is lost. Given that the clinical effects of antidepressants require 2-6 weeks to set-in in people, 3 days can seem an inadequate time to allow changes to manifest and from which to compare changes in worms with those in people with the relief of depression. One option might be to use worms which are conditional sterile, so that loss of developmental synchronization can be stayed for longer incubation times.

Additional areas for improvement of experiment design and execution are, of course, the isolation of more tissue-specific RNA—from serotonin-releasing as well as serotonin-responsive cells, if possible—and stricter standards for quality control of chip hybridizations, to avoid the systematic color sweeps which plagued many of our experiments.

Planning for a second wave of hybridizations (not yet implementing tissue-specific RNA isolation methods) had entailed further experiments to examine a time-series as well as a dose-response for fluoxetine treatment. Additionally, on the premise that the examination of expression profiles produced in response to multiple types and representatives of antidepressant drugs (e.g., paroxetine—a second SSRI, and imipramine—an older class tricyclic antidepressant) might reduce to “lowest terms” a drug signature unique to effective antidepressant action, we had hoped to chip worms grown on these other re-uptake blockers. We speculated that cross-comparisons of the different expression profiles might highlight a “core” group of genes, significantly regulated by all of the tested re-uptake blockers, that might otherwise be obscured by ‘genomic noise’ if examined in the context of experiments with only one drug. Finally, we were interested in how large a role endogenous 5HT might play in fluoxetine-induced gene expression profiles, and so we considered chip experiments with worms mutant in *tph-1*, the gene encoding tryptophan hydroxylase. Unfortunately, *tph-1* mutants develop more slowly than N2 worms, and we were not comfortable that we could adequately control for comparable fluoxetine treatment time while harvesting worms at an equivalent age.

With the exception of the *tph-1* experiments we briefly considered, RNA samples to explore these additional variables were collected and frozen—but never hybridized. This was because of logistical problems in finding a readily available alternative to the Kim lab for hybridizing our samples—and because of the judgment of my Thesis Committee that this project’s questions were not sufficiently focused.

Nevertheless, I remain convinced that experiments of this kind are important and will eventually be performed. It was 50 years ago that the serendipitous discovery of agents like the antipsychotic, chlorpromazine (originally intended as a sedative); the monoamine oxidase inhibitor, iproniazid (originally intended as an antibiotic for tuberculosis); and the re-uptake blocker, imipramine (originally intended as an antipsychotic) gave birth to modern-day biological psychiatry (Andreasen et al, 1995). Although the last half-century has seen landmark discoveries in neuroscience, the treatment of the major psychiatric disorders continues to rely, for its mainstay, on compounds which are essentially identical to their forerunners. With the molecular biology revolution of the last quarter-century, scientists have hoped to begin cracking the mysteries of mental illness with human genetics and linkage studies to identify disease loci and illuminate and make tractable relevant signalling pathways and molecules. The history of psychiatric genetics has, however, been fraught with disappointment and frustration as once-implicated loci have suffered from poor replicability or later contradictory studies (Risch and Bostein, 1996; Maier, 2003). It does not appear that a single-gene mutation or pedigree will be enough to provide that first insight. Rather, biological explanations will be multifactorial with the contributions of individual genes each very modest. DNA microarray technology may, thus, begin to empower and inform these studies by providing a more global perspective of gene expression changes and their dynamic interplay with environment. Here again, psychotropic medications can open the door to a new revolution in psychiatry. Examination of their effects on model organisms would be less prone to

the uncertainties in clinical definitions and heterogeneity of medical populations inherent to directly studying psychiatric diseases. Microarrays can mean better drug target validation and a more thorough understanding than has previously been possible for cataloging the many downstream changes in gene expression that contribute to therapeutic relief. Studies of this kind are already appearing in the published literature (Mirnics et al, 2000; Niculescu et al, 2000). What an organism like *C. elegans* could add is unparalleled cellular resolution in, for example, separating those effects of an antidepressant drug like fluoxetine which are pre-synaptic and those that are post-synaptic. Its ease of maintenance and of genetic manipulation makes the pieces that are missing from this report worth filling-in.

## **MATERIALS AND METHODS**

### **Media**

The solid agar medium we used is a variation on NGM we refer to as HGM (High Growth Medium). HGM facilitates the growth of denser worm populations—helping to reduce the number of plates (and amount of labor) needed to achieve target yields of RNA. HGM also tends to potentiate the effects of drugs at a given concentration, relative to the same drug concentration in NGM. HGM contains (per liter): 3 g NaCl, 15 g agarose, 20 g peptone, 4 ml cholesterol (5 mg/ml stock in EtOH), 1 ml CaCl<sub>2</sub> (1 M stock), 1 ml MgSO<sub>4</sub> (1 M stock), 25 ml K-PO<sub>4</sub> (pH 6), dH<sub>2</sub>O for a final volume of 1 L.

Fluoxetine was added to HGM (for drug plates) after the autoclaved media cooled to about 65° C.

### **Worm cultivation for RNA**

Worms were generally amplified as unsynchronized populations on regular HGM for 2 rounds before bleaching to stage eggs. Bleach solution consisted of 25% (v/v) bleach (5.25% sodium hypochlorite stock), 5% KOH (5 M stock) in dH<sub>2</sub>O. (I learned belatedly that tighter synchronization can be achieved by a 48-hour incubation of bleached eggs in S medium to allow different stage eggs to hatch and eventually arrest uniformly at the L1 larval stage.) Eggs were seeded to 100 or 150 mm HGM plates +/- fluoxetine at a density of 1.27 eggs/mm<sup>2</sup> (i.e., ~10,000 eggs per 100 mm plate), and then grown for 65 hours at 22° C. At the end of this period, RNA was isolated by a protocol adapted from Reinke et al (2000).

Specifically, worms were rinsed off each plate with several ml M9 saline, pooled (for those plates belonging to the same independent isolate), and then spun gently in a clinical centrifuge for ~1 min. (For a second wave of planned—but never hybridized experiments—allowing the worms to settle by gravity sufficed.) The supernatant was removed and replaced with fresh M9 and the preceding step repeated until there did not appear to be any clouding by bacteria. 4 ml TRIZOL (Invitrogen) were added for every ml packed worms—and the mixture was then vortexed vigorously for about 1 min. 2 cycles of flash-freezing in liquid N<sub>2</sub> and thawing were then performed, and then 2 more ml TRIZOL were added / ml starting packed worms and vortexed vigorously. 2 ml chloroform were added / ml starting packed worms,



hand-shaked for 15 seconds, then allowed to sit at RT for 3 min. Samples were centrifuged in RNase-free 16 ml Nalgene polypropylene centrifuge tubes at 12,000g for 15 min. Then the resulting aqueous phase was transferred to new Nalgene tubes, an equal volume of isopropanol added, and the mixtures allowed to sit at RT for 10 minutes. Samples were centrifuged again, this time at 10,000g for 30 minutes. Pellets were rinsed with 10 ml 75% EtOH for a 10-minute spin at 7,000-10,000g, and then re-suspended in RNase-free H<sub>2</sub>O (0.5-1.0 ml / ml starting packed worms).

Poly-A selection proceeded as follows: 1g oligo-dT cellulose (Ambion) was resuspended in 10 ml 1x NETS (100 mM NaCl, 10mM Tris-Cl pH 7.4, 10 mM EDTA, 0.2% SDS), and then washed 3x with 1x NETS by a succession of clinical centrifuge spins and resuspensions. 1 mg total RNA was diluted into 1 ml of 10 mM Tris-Cl pH 7.4, and then mixed with 1 ml dT suspension. The total 2 ml mix was then transferred to a 2 ml minicolumn (Biorad catalog no. 731-1550) sealed at the bottom. Minicolumns were rotated for 1 hour at RT, and then caps and lower twist-offs removed to allow drainage into collection tubes. After drainage, minicolumns were washed 5x with 700 µl 1x NETS. New collection tubes were introduced after washes to collect RNA eluted with 2 successive boluses of 700 µl elution buffer (10 mM Tris-Cl pH 7.4) pre-heated to 70° C. Collected eluate was then cleaned of residual cellulose with 2 chloroform extractions. RNA was then precipitated with 0.3 M NaOAc and 1 volume isopropanol at -20° C for 1 hour, followed by a 30 minute microfuge spin at 4° C. Pellets were washed with 75% EtOH, spun for 15 more minutes at 4° C, and then air-dried for 10-15 minutes prior to a final resuspension in 10-20 µl RNase-free water.

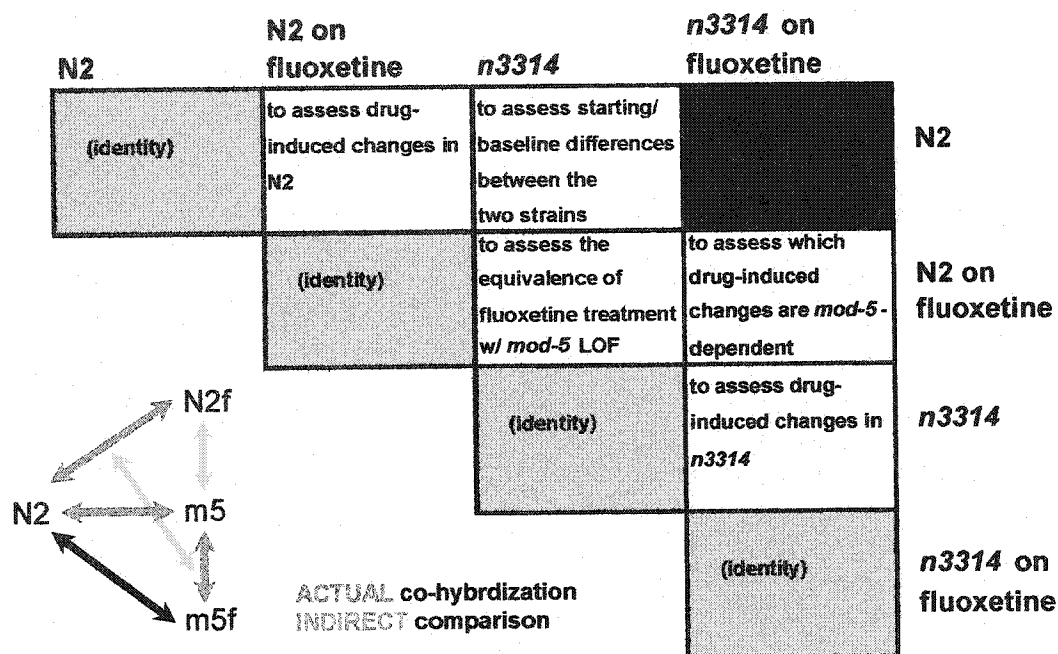
The target yield for one isolate was 15  $\mu$ g poly-A-selected RNA, and three independent isolates were collected for each of the 4 treatment groups (N2, N2 fluoxetine, *n3314*, *n3314* fluoxetine). (In retrospect, it may have been advisable to raise more independent isolates in those cases where a particular treatment group was involved in more than one category of co-hybridization.) Samples were stored at  $-80^{\circ}$  C until the April 2001 trip to the Kim lab.

### **Data normalization**

SMD data normalization proceeded by first selecting spots with intensities greater than a default threshold value above background. If this represented fewer than 10% of all spots on the print, this threshold was progressively lowered until at least 10% of the spots qualified. Once this was completed, the average natural log of [background-subtracted] red/green ratio was computed for the selected dataset of all qualifying spots. Raw intensity and background for red were then each divided by the anti-natural log of this number to produce normalized red intensity and background—which, in turn, were used for subsequent calculation of normalized red/green ratio.

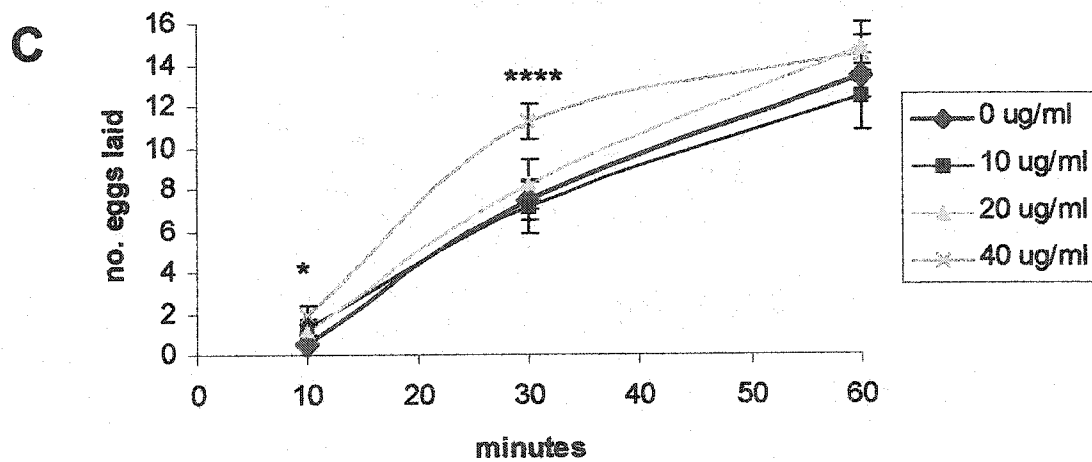
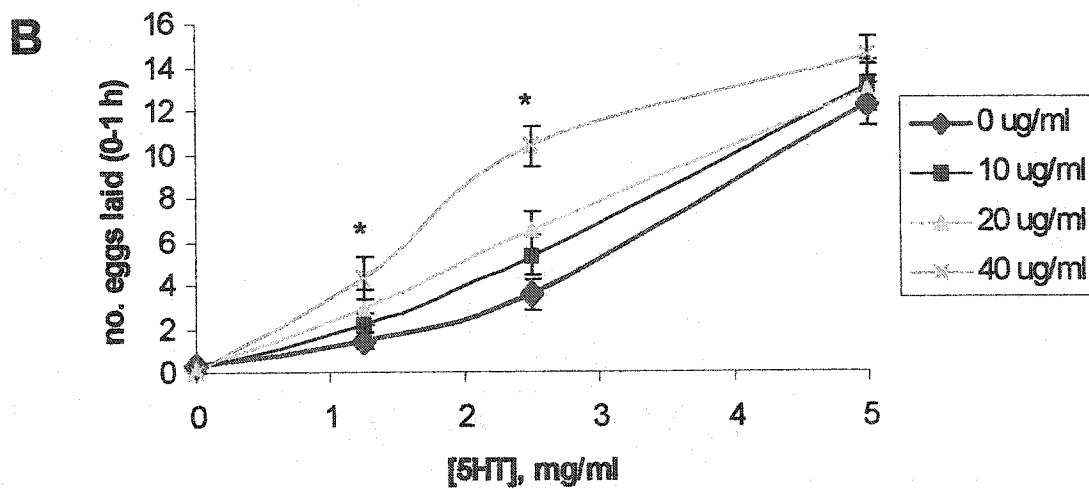
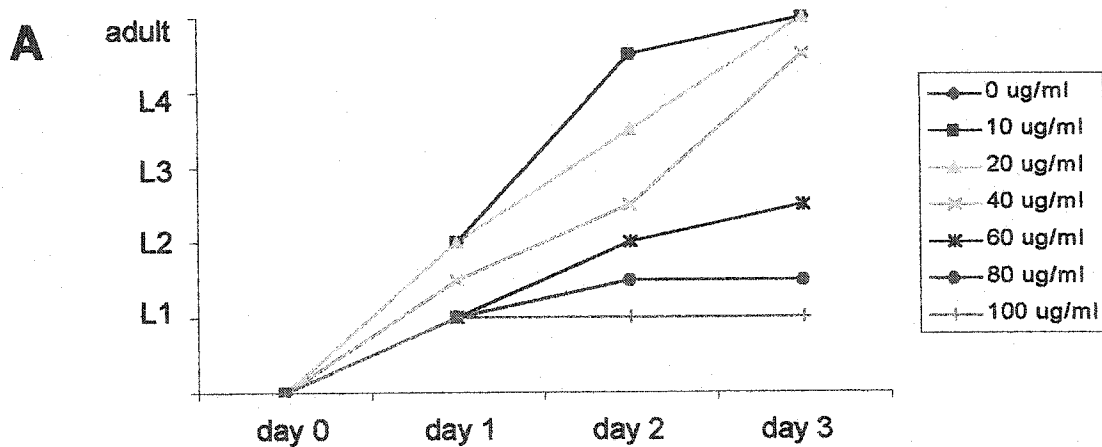
### **ACKNOWLEDGEMENTS**

We wish to thank Stuart Kim and John Wang for the generous use of their microarray facility, for RNA isolation protocols, and help with data analysis and software.



**Figure B-1. April 2001 experiment grid.** There were 4 treatment groups involved (N2, N2 fluoxetine, *mod-5(n3314)*, *mod-5(n3314)* fluoxetine) and 5 global comparisons we were interested in examining (indicated in the white squares). Three were actual co-hybridizations (N2 – N2 fluoxetine; N2 – *mod-5(n3314)*; and *mod-5(n3314)* – *mod-5(n3314)* fluoxetine), and the remaining two (N2 fluoxetine – *mod-5(n3314)*; N2 fluoxetine – *mod-5(n3314)* fluoxetine) indirect comparisons. (Note that the N2 fluoxetine – *mod-5(n3314)* fluoxetine is actually a comparison of N2N2f to m5m5f rather than N2f to m5f.) Abbreviations: m5 = *mod-5(n3314)*, f = fluoxetine-treated.

**Figure B-2. Determination of appropriate fluoxetine dose.** (A) Growth rates of fluoxetine-treated worms. This was a non-quantitative assessment (by eye) over whole plates of synchronized worms. Untreated (0  $\mu\text{g}/\text{ml}$ ) is masked from view by a perfectly overlapping curve for 10  $\mu\text{g}/\text{ml}$ . (B) Dose-response curves of egg-laying in M9 + 5HT by fluoxetine pre-treated worms. \* $P < 0.05$  for 0 v. 40  $\mu\text{g}/\text{ml}$  groups (Dunn's single control).  $n = 24$  for all 40  $\mu\text{g}/\text{ml}$  points;  $n = 36$  for all other data points. (C) Time-course of egg-laying by fluoxetine pre-treated worms in M9 + 5HT. \* $P < 0.05$  for 0 v. 40  $\mu\text{g}/\text{ml}$  groups (Dunn's single control), \*\*\*\* $P < 0.0001$ .  $n = 24$  for all data points.



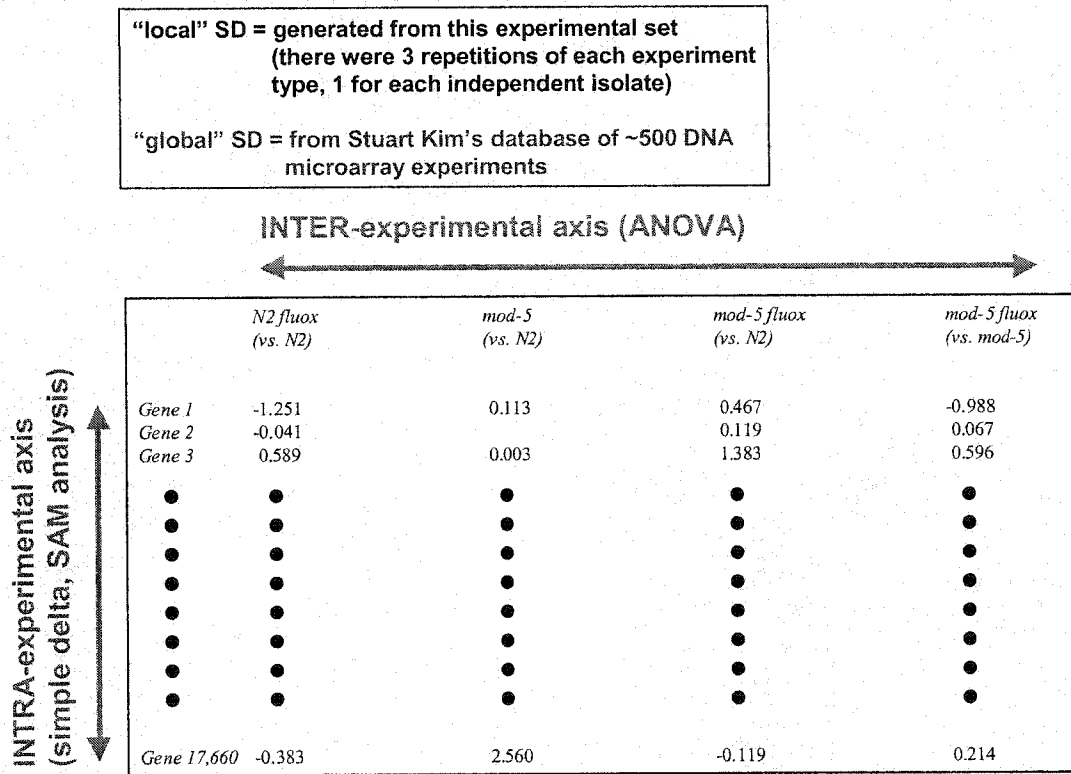


**Figure B-3. Axes of statistical analysis of microarray data.** Displayed above is a schematized spreadsheet of ~17,000 genes (rows) across 4 experimental categories / co-hybridization types (columns). Red:green (R/G) ratios were listed in  $\log_2$  format so that equal-fold changes in either direction could be represented by numbers of equal magnitude (but opposite sign). A test statistic for analysis of variance (ANOVA) was calculated for each gene along the inter-experimental axis (spanning columns), and used to call a statistically significant difference in  $\log_2$  R/G ratio across experiments for that gene. (For our purposes, we considered only the N2N2f, N2m5, and m5m5f categories for ANOVA.) Standard deviations (SD) were available for each gene in the form of either “local” SD (generated from the 3 independent repetitions of each experimental category) or “global” SD (from the Kim lab database of ~500 worm chip experiments performed through April 2001). On the recommendation of the Kim lab, the greater of the two SDs was used for a gene’s ANOVA test statistic calculation. Significance determination along the other axis (intra-experimental) was done in one of two ways—summarized in subsequent figures.

## “Simple delta” test statistic

$$d_{\text{simple}} = \frac{\log_2 R/G}{\max(\text{local, global SD})}$$

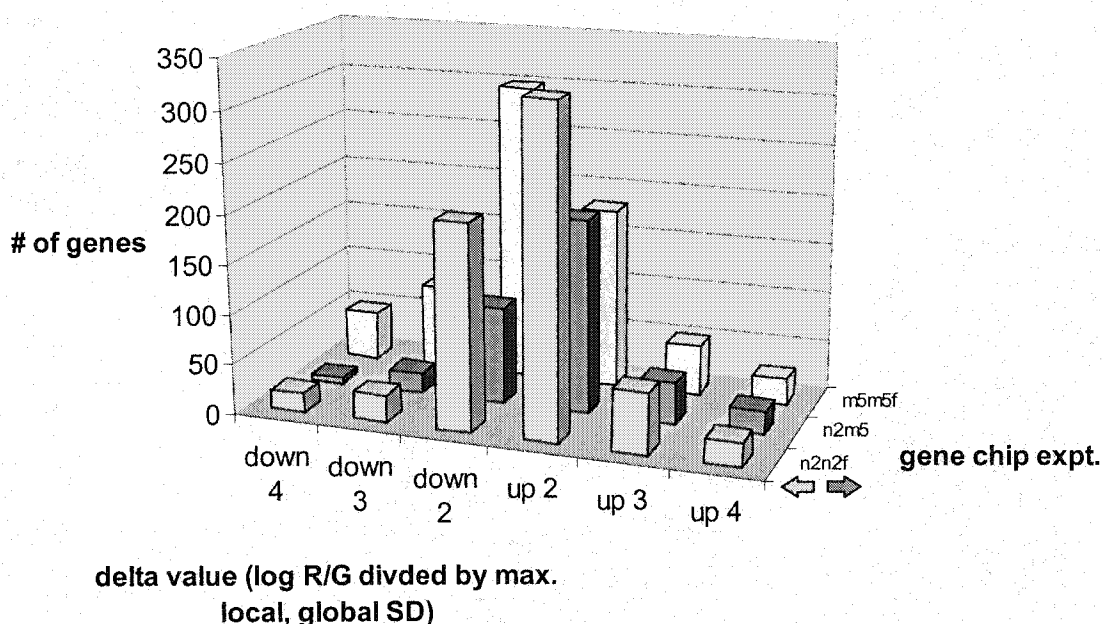


**Figure B-4. Calculation of “simple delta” for significance analysis along intra-experimental axis of microarray data.** One method for calling significance within a given experiment type was to calculate what we termed a “simple”  $\delta$  statistic, taking the  $\log_2 R/G$  ratio and dividing by the maximum SD (local or global). The graphic above gives a sense for how many genes met simple  $\delta$  thresholds of 2, 3, or 4 (absolute value)—for each of the 3 experiment types of interest to us (N2N2f, N2m5, m5m5f). Even for the most permissive  $\delta$  threshold of these ( $\delta=2$ ), only ~400-700 genes (2-4% of 17,000 genes) are called “significant.”

## SAM (“modified delta”) test statistic

$$d_{\text{modified}} = \frac{\log_2 R/G}{SD + s_0}$$

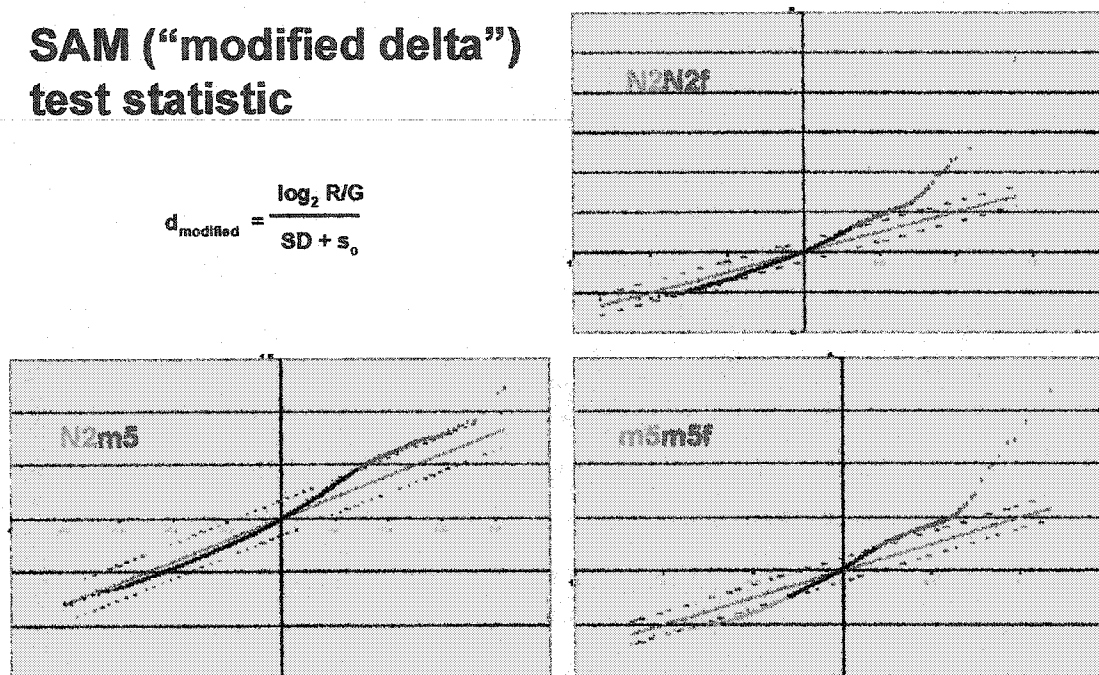


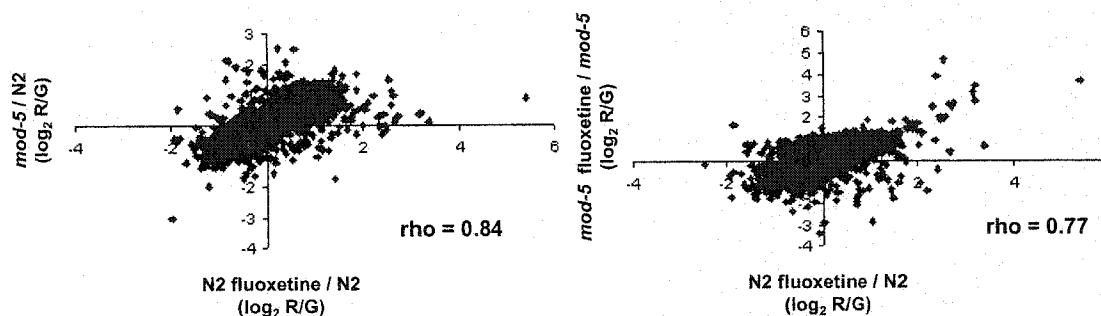
**Figure B-5. Calculation of a “modified delta” by Significance Analysis of Microarrays (SAM).** Tusher et al (2001) introduced SAM, a novel method for calling significance within a given chip. SAM employs a ‘modified’ delta statistic referred to as  $d_i$ —and identical to the ‘simple’ delta statistic we used (Figure B-4) save for the introduction of an  $s_0$  “fudge” factor in the denominator.  $s_0$  was introduced by Tusher et al to compensate for larger variances in  $\log R/G$  ratio at low signal intensities and smaller variances in  $\log R/G$  ratio at high signal intensities—thereby ensuring a more uniform variance across all signal intensities. Additionally, SAM creates plots of expected  $d_i$  (x-axis) v. observed  $d_i$  (y-axis) (shown above), where expected  $d_i$  is created by a user-set number of random permutations (in this case, 100). For the vast majority of genes, the difference between observed and expected  $d_i$ ’s is unremarkable (because both are of very small magnitude), but those genes with very large observed  $d_i$ ’s constitute “outliers” and lie outside of dotted boundaries set at specific limits for a user-decided acceptable false positive rate (in this case, 5%). Note that in the SAM plots above, there is an unexplained skew in the N2N2f and N2m5 curves—where the only called genes are red (upregulated in N2f and m5, respectively) and there are no called genes for green.



**Figure B-6. Hierarchical clustering of genes with significant changes in expression across inter-experimental axis** (next 2 pages). Most of the clusters are of uncertain biological significance and uninterpretable. (This may be due, in part, to the use of whole worm RNA rather than a more tissue-selective sampling.) The one exception is the drug-induced cluster (independent of genotype) of genes encoding P450 family proteins and glucuronide-conjugating enzymes. Logically, these genes would indeed be expected to be upregulated by fluoxetine treatment and not by genetic mutation of *mod-5*. The 80 genes listed in this figure were selected for cluster analysis because they achieved an ANOVA test statistic score (across the 3 listed categories) with  $P < 0.05$ . Hierarchical clustering was performed with Michael Eisen's Cluster and Treeview software (Eisen et al, 1998). The left colorbar reflects direction of gene expression according to the experiment category color legend atop each of the 3 columns. Gene annotations (Kim lab) were abbreviated in some instances to allow optimal page-fitting. There are reports (Martie Chalfie, unpublished communication) that although most of the annotations are correct, some may be in error because the alpha-numeric designations listed are actually references to PCR primers (and not necessarily to the ORFs of the same designation). This may mean that the actual gene is, in some cases, displaced by an ORF.

- 21048 G-protein coupled receptor, distant homology to SRG subfamily X 9892975 F09B9.1  
 20988 Transporter (ABC superfamily), strong similarity to human MDR proteins PG1A3 5 17664168 C47A10.1  
 26084 Member of the glutathione S-transferase protein family 5 12356497 K01D12.11  
 52561 Member of the ligand-gated ion channel protein family X 10207811 C39B10.2  
 23363 Member of the P450 heme-thiolate protein family 5 7347500 C03G6.15  
 53119 Protein of unknown function X 7747010 F49E1.1  
 51095 Protein of unknown function, has strong similarity to C. elegans T08H10.3 4 49066660 E03H12.7  
 34009 Member of an uncharacterized protein family 4 12733064 C3ZH11.10  
 34008 Member of an uncharacterized protein family 4 12731363 C3ZH11.9  
 27587 Member of the UDP-glucuronosyltransferase protein family 1 4054539 C10H11.3  
 21677 Member of the UDP-glucuronosyltransferase protein family 4 10060840 F01D4.2  
 26199 Member of the P450 heme-thiolate protein family 5 3904374 K07C6.3  
 28706 Member of the phospholipase A2 receptor protein family 4 3852768 F50D6.1  
 20865 Member of the alcohol/ribitol dehydrogenase-like protein family 2 14363613 C01G12.5  
 53615  
 25419 Putative NADH/NADPH oxidase 5 1007499 T10B5.8  
 29175 Member of an uncharacterized protein family 4 12673007 ZK896.5  
 23821 Member of the P450 heme-thiolate protein family 5 3993786 C49G7.8  
 26198 Member of the P450 heme-thiolate protein family 5 3907512 K07C6.2  
 26750 Member of an uncharacterized protein family 4 631142 K11H12.4  
 24311 Protein with similarity to NADH oxidases 5 6053962 F17A9.5  
 21103 Member of an uncharacterized protein family 5 9322445 E02C12.6  
 21089 Member of an uncharacterized protein family 5 13720890 F20E2.5  
 27480 Protein of unknown function, has moderate similarity to C. elegans Y39E4B.4 3 7678406 C02F5.8  
 23919 Casein kinase I subfamily, similarity to S. cerevisiae Yck1b & 2b 2 6569496 C56C10.6  
 20949 G-protein coupled receptor, distant homology to SRG subfamily Y 16226950 C31A11.5  
 26259 Protein of unknown function, putative paralogue of C. elegans Y43F4A.2 X 16836525 K09E3.1  
 50410 Protein of unknown function, has weak similarity to C. elegans Y63D3A.8 1 1064972  
 21039 Strong similarity to human enoyl-CoA hydratase/3-OM-acyl-CoA dehydrogenase 4 9824667 F01G10.3  
 53226 Member of the histone H2B protein family 5 8497707 his-8/F43F2.12  
 24896 Member of the peptidase protein family 5 16627559 Y70C5C.1  
 27926 Protein with strong similarity to mouse RSU-1 protein, RAS suppressor protein 3 2909244 C34C12.5  
 49902  
 50078 Protein with strong similarity to human Hs.6817, a putative oncogene 3 4708158 ZC395.7  
 24846 Protein of unknown function, has strong similarity to C. elegans Y7A9C.1 4 6938821 F42C5.4  
 53015 Weak similarity to worm ubx-2 (Ubiquitin monomer fused to ribosomal protein) 2 3325741 F14D2.11  
 53311 Moderate similarity to human sodium/bile acid cotransporters 4 2151627  
 43158 Protein with similarity to human and D. melanogaster organic cation transporters 5 17923449 C06H5.6  
 49497 Protein of unknown function, has moderate similarity to C. elegans C55C2.3 1 1943806  
 33298 Protein of unknown function, has strong similarity to C. elegans ZC139.6 2 2627672 F22E5.13

- 24994 Protein of unknown function, putative paralog of *C. elegans* T26E4.7 5 6579002 ZK1055.2
- 49434 Protein of unknown function, has weak similarity to *C. elegans* F10E9.2 4 13183315 Y30H8A.2
- 32022 Protein of unknown function, has weak similarity to *C. elegans* T13F3.6 5 7522006 C54F6.12
- 53348 Putative ortholog of fly Calo [Calossin, a calmodulin-binding protein] C44E4.1
- 33599 Zinc finger protein with similarity to nuclear hormone receptors 5445955 T05C3.1
- 50063 Protein with strong similarity to Rab-GAP protein 4 13185995 Y45F10A.6
- 32458 Member of uncharacterized protein family, similar to *E. histolytica* lysozymes 4 11213740 F50B3.3
- 49066 Protein of unknown function 2 1483593
- 51083 Member of the lipase protein family 4 1462660 K03H6.2
- 50990 Protein with strong similarity to human xeroderma pigmentosum repair complementing protein p125 4 1971742
- 28237 Pumilio-family RNA binding domains 2 12876878 vuf-6/F18A11.1
- 25110 Protein of unknown function, weak similarity to human KIAA0590 3 12895658 ZK520.1
- 33431 Member of uncharacterized protein family, similar to *E. histolytica* lysozymes 4 11211082 F50B3.2
- 25066 Similarity at C-term of *S. cerevisiae* mtDNA repair/recombination protein 2 1943131 ZK250.9/Y16E11A.2
- 50742 Protein of unknown function 2 7085273 T02G5.2
- 27823 Putative cytochrome P450 5 7664487 C12D5.7
- 53636 Weak similarity to *S. cerevisiae* MREG3 (of MREG trx regulatory complex) 4 12343842 ZK795.1
- 53766 Protein of unknown function 4 10228092 F56C4.1
- 24451 Polyubiquitin 3 5399610 ubq-1/UBI1/T23B5.4
- 49594 Protein with strong similarity to *C. elegans* W06E11.5 gene product 3 622429 W06E11.6/chic
- 51199 Protein with strong similarity to *C. elegans* F56D6.2 4 3864805
- 50298 Protein of unknown function, weak similarity to human B3GALT4 and B3GALT2 13709925 F40F7.3
- 52521 Member of an uncharacterized protein family 2 13567980 R06B9.4
- 53718 Protein of unknown function, has moderate similarity to *C. elegans* F14D2.9 5 17552290 F57G4.9
- 23811 Member of the polypeptide chain release factor protein family 4 465064 W03G1.4
- 23689 Protein of unknown function 2 5043506 C27A2.3
- 23431 Putative membrane transporter with similarity to human Na<sup>+</sup>/Ca<sup>2+</sup>. K<sup>+</sup> exchangers 9156507 C07A9.11
- 28999 Member of the nuclear hormone receptor/Zinc finger protein family 5 13278346 C50B6.8
- 51152 Protein of unknown function X 12056304 F17A2.4
- 29730 Protein of unknown function, strong similarity to human retinal epith. pigment protein 2 3888722 F53C3.12
- 31549 Protein of unknown function, has strong similarity to *C. elegans* R09E12.5 2 653338 K07E8.10
- 52272 Protein of unknown function, has moderate similarity to *C. elegans* F36H12.5 4 6185260 T13A10.1
- 30311 Protein of unknown function, has strong similarity to *C. elegans* F57G4.7 5 17550208 F57G4.5
- 24726 Member of the C2 domain protein family 3 6154100 F37A4.7
- 50223 Member of C-type lectin family, weak similarity to human neurocan chondroitin sulfate 5 2431417
- 29755 Protein of unknown function, putative paralog of *C. elegans* F57G4.6 5 17553767 F57G4.7
- 49366 Protein of unknown function X 17354735 F15G10.2
- 49587 Member of C-type lectin family, weak similarity to human neurocan chondroitin sulfate 5 2323452
- 24344 Putative coiled-coil protein, has weak similarity to mvosins 2 3640263 F19B10.4
- 29756 Protein of unknown function, putative paralog of *C. elegans* Y37H2A.I 5 17557197 F57G4.8



	looks like WT on drug?			
	1	2	3	4
mutant	yes	no	no	yes
mutant on drug	no	no	yes	yes

- 1 - gene product is confirmed target of drug inhibition
- 2 - gene product is essential for drug action, but not an exclusive target
- 3 - gene product is irrelevant to drug action
- 4 - (this situation was not encountered in the paper)

**Figure B-7. Correlation plots of called genes for drug target validation.** Taking those genes with  $\delta_{\text{simple}}$  scores  $\geq 2$ , we performed a correlation analysis and calculated a correlation coefficient,  $\rho$ , to determine how similar the *mod-5(n3314)* expression profile was to N2 on fluoxetine. We next sought to determine how similar the expression profile of mutant *n3314* worms on drug was to that of N2 worms on drug. By answering these questions and then considering a contingency table like the one above, we hoped to be able to perform a drug target validation much like one performed by Marton et al (1998). The results we obtained would seem to fit the 4<sup>th</sup> hypothesized situation best, but this is also, unfortunately, the least interpretable outcome. One possibility is that the sets of genes induced by fluoxetine which are MOD-5-dependent and -independent are both sizeable. Additionally, because we used whole worm RNA, our experiments may not have been sufficiently sensitive to detect MOD-5-dependent and -independent changes relevant to serotonergic neurons or their targets. The correlated genes above may, instead, represent 'bulk' effects for phenomena less relevant to neuronal function in the other tissues of the worm.

## REFERENCES

- Albert PR, Tiberi M. 2001. Receptor signaling and structure: insights from serotonin-1 receptors. *Trends Endocrinol & Metabolism*. 12:453-460.
- Andreasen NC, Black DW. 1995. *Introductory Textbook of Psychiatry*, Second Edition. Washington, DC: American Psychiatric Press, Inc.
- Avery L, Raizen D, Lockery S. 1995. Electrophysiological methods. In: *Caenorhabditis elegans: Modern Biological Analysis of an Organism*, Methods in Cell Biology, Volume 48 (H.F. Epstein and D.C. Shakes, eds.) San Diego: Academic Press.
- Avery L, Thomas JH. 1997. Feeding and defecation. In: *C. elegans II* (DL Riddle, T Blumenthal, BJ Meyer, JR Priess, eds.). New York: Cold Spring Harbor Laboratory Press.
- Avigan J, Murtagh JJ Jr, Stevens LA, Angus CW, Moss J, Vaughan M. 1992. Pertussis toxin-catalyzed ADP-ribosylation of G(o) alpha with mutations at the carboxyl terminus. *Biochemistry*. 31:7736-7740
- Bargmann CI. 1998. Neurobiology of the *Caenorhabditis elegans* genome. *Science*. 282:1448-1453.
- Bargmann CI, Mori I. 1997. Chemotaxis and thermotaxis. In: *C. elegans II* (DL Riddle, T Blumenthal, BJ Meyer, JR Priess, eds.). New York: Cold Spring Harbor Laboratory Press.
- Brenner S. 1974. The genetics of *Caenorhabditis elegans*. *Genetics*. 77:71-94.
- Brownlee DJA, Fairweather, I. 1999. Exploring the neurotransmitter labyrinth in nematodes. *Trends Neurosci*. 22:16-24.
- Brundage L, Avery L, Katz A, Kim UJ, Mendel JE, Sternberg PW, Simon MI. 1996. Mutations in a *C. elegans* G<sub>q</sub>α gene disrupt movement, egg laying, and viability. *Neuron*. 16:999-1009.
- Chase DL, Patikoglou GA, Koelle MR. 2001. Two RGS proteins that inhibit G<sub>αo</sub> and G<sub>αq</sub> signaling in *C. elegans* neurons require a Gβ5-like subunit for function. *Current Biology*. 11:222-231

- Choy RKM, Thomas JH. 1999. Fluoxetine-resistant mutants in *C. elegans* define a novel family of transmembrane proteins. *Mol Cell*. 4:143-152.
- Christensen M, Estevez A, Yin X, Fox R, Morrison R, McDonnell M, Gleason C, Miller DM, Strange K. 2002. A primary culture system for functional analysis of *C. elegans* neurons and muscle cells. 33:503-514.
- Darby C, Falkow S. 2001. Mimicry of a G protein mutation by Pertussis toxin expression in transgenic *Caenorhabditis elegans*. *Infect Immun*. 69:6271-6275.
- Davis MW, Somerville D, Lee RY, Lockery S, Avery L, Fambrough DM. 1995. Mutations in the *Caenorhabditis elegans* Na,K-ATPase alpha-subunit gene, eat-6, disrupt excitable cell function. *J Neurosci*. 15:8408-18.
- Davis MW, Fleischhauer R, Dent JA, Joho RH, Avery L. 1999. A mutation in the *C. elegans* EXP-2 potassium channel that alters feeding behavior. *Science*. 286:2501-2504.
- Deutch AY and Roth RH. 1999. Neurotransmitters. In: *Fundamental Neuroscience* (M Zigmond, ed.). San Diego: Academic Press.
- Dong MQ, Chase D, Patikoglou GA, Koelle MR. 2000. Multiple RGS proteins alter neural G protein signaling to allow *C. elegans* to rapidly change behavior when fed. *Genes Dev*. 14:2003-2014.
- Driscoll M, Kaplan J. 1997. Mechanotransduction. In: *C. elegans II* (DL Riddle, T Blumenthal, BJ Meyer, JR Priess, eds.). New York: Cold Spring Harbor Laboratory Press.
- Duggan DJ, Bittner M, Chen Y, Meltzer P, Trent JM. 1999. Expression profiling using cDNA microarrays. *Nat Genet*. 21(1 Suppl):10-14.
- Eisen MB, Spellman PT, Brown PO, Botstein D. 1998. Cluster analysis and display of genome-wide expression patterns. *Proc Natl Acad Sci USA*. 95:14863-14868.
- Francis MM, Mellem JE, Maricq AV. 2002. Bridging the gap between genes and behavior: recent advances in the electrophysiological analysis of neural function in *Caenorhabditis elegans*. *Trends Neurosci*. 26:90-99.
- Franks CJ, Pemberton D, Vinogradova I, Cook A, Walker RJ, Holden-Dye L. 2002. Ionic basis of the resting membrane potential and action potential in the pharyngeal muscle of *Caenorhabditis elegans*. *J Neurophysiol*. 87:954-961

- Garriga G, Desai C, Horvitz HR. 1993. Cell interactions control the direction of outgrowth, branching and fasciculation of the HSN axons of *Caenorhabditis elegans*. *Development*. 117:1071-1087.
- Gilchrist A, Bunemann M, Li A, Hosey M, Hamm HE. 1999. A dominant-negative strategy for studying roles of G proteins *in vivo*. *J Biol Chem*. 274:6610-6616.
- Goder V, Bieri C, Spiess M. 1999. Glycosylation can influence topogenesis of membrane proteins and reveals dynamic reorientation of nascent polypeptides within the translocon. *J Cell Biol*. 147:257-265.
- Goodman MB, Hall DH, Avery L, Lockery SR. 1998. Active currents regulate sensitivity and dynamic range in *C. elegans* neurons. *Neuron*. 20:763-772.
- Gotta M, Ahringer J. 2001. Distinct roles for G $\alpha$  and G $\beta\gamma$  in regulating spindle position and orientation in *Caenorhabditis elegans* embryos. *Nature Cell Biology*. 3:297-300.
- Gower NJ, Temple GR, Schein JE, Marra M, Walker DS, Baylis HA. 2001. Dissection of the promoter region of the inositol 1,4,5-trisphosphate receptor gene, *itr-1*, in *C. elegans*: a molecular basis for cell-specific expression of IP3R isoforms. *J Mol Biol*. 306:145-157
- Grishok A, Mello CC. 2002. RNAi (Nematodes: *Caenorhabditis elegans*). *Adv Genet*. 46:339-360.
- Hajdu-Cronin YM, Chen WJ, Patikoglou G, Koelle MR, Sternberg PW. 1999. Antagonism between G(o)alpha and G(q)alpha in *Caenorhabditis elegans*: the RGS protein EAT-16 is necessary for G(o)alpha signaling and regulates G(q)alpha activity. *Genes Dev*. 13:1780-1793.
- Hamdan FF, Ungrin MD, Abramovitz M, Ribeiro P. 1999. Characterization of a novel serotonin receptor from *Caenorhabditis elegans*: cloning and expression of two splice variants. *J Neurochem*. 72:1372-1383.
- Hardaker LA, Singer E, Kerr R, Zhou G, Schafer WR. 2001. Serotonin modulates locomotory behavior and coordinates egg-laying and movement in *Caenorhabditis elegans*. *J Neurobiol*. 49:303-313.
- Hilliard MA, Apicella AJ, Kerr R, Suzuki H, Bazzicalupo P, Schafer WR. 2003. *In vivo* imaging of *C. elegans* nociceptor neurons reveals a role for novel G-protein subunits in chemosensory signaling and adaptation. (*submitted*).

- Hoyer D, Hannon JP, Martin GR. 2002. Molecular, pharmacological and functional diversity of 5-HT receptors. *Pharm Biochem and Behav.* 71:533-554.
- Jansen G, Thijssen KL, Werner P, van der Horst M, Hazendonk E, Plasterk RHA. 1999. The complete family of genes encoding G proteins of *Caenorhabditis elegans*. 21:414-419.
- Jansen G, Weinkove D, Plasterk RHA. 2002. The G-protein subunit *gpc-1* of the nematode *C.elegans* is involved in taste adaptation. *EMBO.* 21:986-994.
- Kerr, R, Lev-Ram V, Baird G, Vincent P, Tsien RY, Schafer WR. 2000. Optical imaging of calcium transients in neurons and pharyngeal muscle of *C. elegans*. *Neuron.* 26:583-594.
- Kim J, Poole DS, Waggoner LE, Kempf A, Ramirez DS, Treschow PA, Schafer WR. 2001. Genes affecting the activity of nicotinic receptors involved in *Caenorhabditis elegans* egg-laying behavior. *Genetics.* 157:1599-1610
- Korswagen HC, Park JH, Ohshima Y, Plasterk RHA. 1997. An activating mutation in a *Caenorhabditis elegans* G<sub>s</sub> protein induces neural degeneration. *Genes Dev.* 11:1493-1503.
- Lackner MR, Nurrish SJ, Kaplan JM. 1999. Facilitation of synaptic transmission by EGL-30 G<sub>q</sub>α and EGL-8 PLCβ: DAG binding to UNC-13 is required to stimulate acetylcholine release. *Neuron.* 24:335-346.
- Lee SP, Xie Z, Varghese G, Nguyen T, O'Dowd BF, George S. 2000. Oligomerization of dopamine and serotonin receptors. *Neuropsychopharmacology.* 23:S32-S40
- Lewis JA, Wu CH, Berg H, Levine JH. 1980. The genetics of levamisole resistance in *Caenorhabditis elegans*. *Genetics.* 95:905-928.
- Maier W. 2003. Psychiatric genetics: Overview on achievements, problems, perspectives. *Methods Mol Med.* 77:3-20.
- Marton MJ, DeRisi JL, Bennett HA, Iyer VR, Meyer MR, Roberts CJ, Stoughton R, Burchard J, Slade D, Dai H, Bassett DE Jr, Hartwell LH, Brown PO, Friend SH. 1998. Drug target validation and identification of secondary drug target effects using DNA microarrays. *Nat Med.* 4:1293-1301.
- Mello C, Fire A. 1995. DNA Transformation. In: *Caenorhabditis elegans: Modern Biological Analysis of an Organism.* Methods in Cell Biology. Volume 48 (HF Epstein and DC Shakes, eds). San Diego: Academic Press.



Mendel JE, Korswagen HC, Liu KS, Hajdu-Cronin YM, Simon MI, Plasterk RHA, Sternberg PW. 1995. Participation of the protein G<sub>o</sub> in multiple aspects of behavior in *C. elegans*. *Science*. 267:1652-1655.

Miller KG, Alfonso A, Nguyen M, Crowell JA, Johnson CD, Rand JB. 1996. A genetic selection for *Caenorhabditis elegans* synaptic transmission mutants. *Proc Natl Acad Sci USA*. 93:12593-12598

Miller KG, Emerson MD, Rand JB. 1999. G<sub>o</sub> $\alpha$  and diacylglycerol kinase negatively regulate the G<sub>o</sub> $\alpha$  pathway in *C. elegans*. *Neuron*. 24:323-333

Mirnics K, Middleton FA, Marquez A, Lewis DA, Levitt P. 2000. Molecular characterization of schizophrenia viewed by microarray analysis of gene expression in prefrontal cortex. *Neuron*. 28:53-67.

Miyawaki A, Llopis J, Heim R, McCaffery JM, Adams JA, Ikura M, Tsien RY. 1997. Fluorescent indicators for Ca<sup>2+</sup> based on green fluorescent proteins and calmodulin. *Nature*. 388:882-887.

Miyawaki A, Griesbeck O, Heim R, Tsien RY. 1999. Dynamic and quantitative Ca<sup>2+</sup> measurements using improved cameleons. *Proc Natl Acad Sci USA*. 96:2135-2140.

Nelson LS, Rosoff ML, Li C. 1998. Disruption of a neuropeptide gene, *flp-1*, causes multiple behavioral defects in *Caenorhabditis elegans*. *Science*. 281:1686-1690.

Niacaris TR. 2001. Serotonergic and G-protein mediated regulation of the *C. elegans* pharyngeal muscle action potential. PhD thesis. University of Texas, Southwestern. Dallas, TX.

Niculescu AB 3rd, Segal DS, Kuczynski R, Barrett T, Hauger RL, Kelsoe JR. 2000. Identifying a series of candidate genes for mania and psychosis: a convergent functional genomics approach. *Physiol Genomics*. 4:83-91.

Nurrish S, Segalat L, Kaplan JM. 1999. Serotonin inhibition of synaptic transmission: G<sub>o</sub> $\alpha$  decreases the abundance of UNC-13 at release sites. *Neuron*. 24:231-242.

Okkema PG, Harrison SW, Plunger V, Aryana A, and Fire A. 1993. Sequence requirements for myosin gene expression and regulation in *Caenorhabditis elegans*. *Genetics*. 135:385-404.

Olde B, McCombie WR. 1997. Molecular cloning and functional expression of a serotonin receptor from *Caenorhabditis elegans*. *J Mol Neurosci*. 8:53-62.

- Pauwels PJ, Gouble A, Wurch T. 1999. Activation of constitutive 5-hydroxytryptamine<sub>1B</sub> receptor by a series of mutations in the BBXXB motif: positioning of the third intracellular loop distal junction and its G<sub>o</sub>α protein interactions. *Biochem J.* 343:435-442.
- Raizen DM, Avery L. 1994. Electrical activity and behavior in the pharynx of *Caenorhabditis elegans*. *Neuron.* 12:483-495.
- Rand JB, Nonet ML. 1997. Neurotransmitter assignments for specific neurons. In: *C. elegans II* (DL Riddle, T Blumenthal, BJ Meyer, JR Priess, eds.). New York: Cold Spring Harbor Laboratory Press.
- Rand JB, Russell RL. 1984. Choline acetyltransferase-deficient mutants of the nematode *Caenorhabditis elegans*. *Genetics.* 106:227-248.
- Ranganathan R, Cannon SC, Horvitz HR. 2000. MOD-1 is a serotonin-gated chloride channel that modulates locomotory behaviour in *C. elegans*. *Nature* 408:470-475
- Ranganathan R, Sawin ER, Trent C, Horvitz HR. 2001. Mutations in the *Caenorhabditis elegans* serotonin reuptake transporter MOD-5 reveal serotonin-dependent and -independent activities of fluoxetine. *J Neurosci.* 21:5871-5884.
- Rankin CH. 2002. From gene to identified neuron to behavior in *Caenorhabditis elegans*. *Nat Rev Genetics.* 3:622-630.
- Reddien PW, Cameron S, Horvitz HR. 2001. Phagocytosis promotes programmed cell death in *C. elegans*. *Nature.* 412:198-202.
- Reinke V, Smith HE, Nance J, Wang J, Van Doren C, Begley R, Jones SJM, Davis EB, Scherer S, Ward S, Kim SK. 2000. A global profile of germline gene expression in *C. elegans*. *Mol Cell.* 6:605-616.
- Richmond JE, Jorgensen EM. 1999. One GABA and two acetylcholine receptors function at the *C. elegans* neuromuscular junction. *Nature Neurosci.* 2:791-797.
- Risch N, Botstein D. 1996. A manic depressive history. *Nat Genet.* 12:351-353.
- Robatzek M, Niacaris T, Steger K, Avery L, Thomas JH. 2001. *eat-11* encodes GPB-2, a Gβ<sub>5</sub> ortholog that interacts with G<sub>o</sub>α and G<sub>q</sub>α to regulate *C. elegans* behavior. *Current Biology.* 11:288-293.
- Roy PJ, Stuart JM, Lund J, Kim SK. 2002. Chromosomal clustering of muscle-expressed genes in *Caenorhabditis elegans*. *Nature.* 418:975-979.

- Sawin ER, Ranganathan R, Horvitz HR. 2000. *C. elegans* locomotory rate is modulated by the environment through a dopaminergic pathway and by experience through a serotonergic pathway. *Neuron*. 26:619-631.
- Schafer WR. 1999. How do antidepressants work? Prospects for genetic analysis of drug mechanisms. *Cell*. 98:551-554.
- Schafer WR, Kenyon CJ. 1995. A calcium-channel homologue required for adaptation to dopamine and serotonin in *Caenorhabditis elegans*. *Nature*. 375:73-78.
- Schena M, Shalon D, Davis RW, Brown PO. 1995. Quantitative monitoring of gene expression patterns with a complementary DNA microarray. *Science*. 270:467-470.
- Schinkmann K, Li C. 1992. Localization of FMRFamide-like peptides in *Caenorhabditis elegans*. 316:251-260.
- Segalat L, Elkes DA, Kaplan JM. 1995. Modulation of serotonin-controlled behaviors by G<sub>o</sub> in *Caenorhabditis elegans*. *Science*. 267:1648-1651.
- Sherlock G. 2000. Analysis of large-scale gene expression data. *Curr Opin Immunol*. 12:201-205.
- Suzuki H, Kerr R, Bianchi L, Slone D, Frøkjær-Jensen C, Xue J, Driscoll M, Schafer WR. 2003. In vivo functional analysis of *C. elegans* mechanosensory neurons distinguishes a specific role for the MEC-4 channel in the process of gentle touch sensation. (*submitted*).
- Swanson LW, Lufkin T, Colman DR. 1999. Organization of Nervous Systems. In: *Fundamental Neuroscience* (M Zigmond, ed.). San Diego: Academic Press.
- Tavernarakis N, Wang SL, Dorovkov M, Ryazanov A, Driscoll M. 2000. Heritable and inducible genetic interference by double-stranded RNA encoded by transgenes. *Nat Genet*. 24:180-183.
- Trent C, Tsung N, Horvitz HR. 1983. Egg-laying defective mutants of the nematode *Caenorhabditis elegans*. *Genetics*. 104:619-647.
- Tsalik EL, Niacaris T, Pau K, Avery L, Hobert O. 2003. LIM homeobox gene-dependent expression of biogenic amine receptors in restricted regions of the *C. elegans* nervous system. *Dev Biol*. *in press*.
- Tusher VG, Tibshirani R, Chu G. 2001. Significance analysis of microarrays applied to the ionizing radiation response. *Proc Natl Acad Sci USA*. 98:5116-5121.

van der Linden AM, Simmer F, Cuppen E, Plasterk RHA. 2001. The G-Protein  $\beta$ -subunit GPB-2 in *Caenorhabditis elegans* regulates the Go-Gq signaling network through interactions with the Regulator of G-Protein Signaling proteins EGL-10 and EAT-16. *Genetics*. 158:221-235.

Waggoner LE, Zhou GT, Schafer RW, Schafer WR. 1998. Control of alternative behavioral states by serotonin in *Caenorhabditis elegans*. *Neuron* 21, 203-214.

Waggoner LE, Dickinson KA, Poole DS, Schafer WR. 2000a. Long-term nicotine adaptation in *Caenorhabditis elegans* involves PKC-dependent changes in nicotinic receptor. *J Neurosci*. 20:8802-8811.

Waggoner LE, Hardaker LA, Golik S, Schafer WR. 2000b. Effect of a neuropeptide gene on behavioral states in *Caenorhabditis elegans* egg-laying. *Genetics*. 154:1181-1192.

Weinshenker D, Garriga G, Thomas JH. 1995. Genetic and pharmacologic analysis of neurotransmitters controlling egg-laying in *C. elegans*. *J neurosci*. 15:6975-6985.

Weinshenker D, Wei A, Salkoff L, Thomas JH. 1999. Block of an ether-a-go-go-like  $K^+$  channel by imipramine rescues *egl-2* excitation defects in *Caenorhabditis elegans*. *J Neurosci*. 19:9831-9840.

White JG, Southgate E, Thomas JN, Brenner S. 1986. The structure of the nervous system of the nematode *Caenorhabditis elegans*. *Philos Trans R Soc Lond. (Biol.)* B 314:1-340.

Xie Z, Lee SP, O'Dowd BF, George SR. 1999. Serotonin 5-HT<sub>1B</sub> and 5-HT<sub>1D</sub> receptors form homodimers when expressed alone and heterodimers when co-expressed. *FEBS Lett*. 456:63-67.

Zhang Y, Ma C, Delohery T, Nasipak B, Foat BC, Bounoutas A, Bussemaker HJ, Kim SK, Chalfie M. 2002. Identification of genes expressed in *C. elegans* touch receptor neurons. *Nature*. 418:331-335.

Zwaal RR, Ahringer J, van Luenen HG, Rushforth A, Anderson P, Plasterk RH. 1996. G proteins are required for spatial orientation of early cell cleavages in *C. elegans* embryos. *Cell*. 86:619-629.